Exploring the mammalian small heat shock protein family

A study of function, and the identification and characterization of new members

een wetenschappelijke proeve op het gebied van de
Natuurwetenschappen, Wiskunde en Informatica.

Proefschrift

ter verkrijging van de graad van doctor
aan de Katholieke Universiteit Nijmegen
op gezag van de Rector Magnificus, Prof. Dr. C.W.P.M. Blom,
volgens besluit van het College van Decanen
in het openbaar te verdedigen op
vrijdag 3 oktober 2003,
des namiddags om 3:30 uur precies
door

Pauline Verschuure

geboren op 10 juni 1974
te Delfzijl

Promotor
Prof. Dr. W.W. de Jong

Co-promotor
Dr. W.C. Boelens

Manuscriptcommissie
Prof. Dr. H.H. Kampinga (RUG)
Dr. G.N.P. van Muijen

ISBN 90-9017213-0

TABLE OF CONTENTS

1

General introduction

INTRODUCTION TO SMALL HEAT SHOCK PROTEINS

The multichaperone network

In order to be functional, proteins need to adopt a correct three-dimensional structure. The sequence of amino acids alone determines the protein conformation as was initially proposed by Anfinsen [1]. However, the nascent chain emerging from the ribosome is prone to misfolding and subsequent aggregation. The aggregation is enhanced by the fact that the intracellular environment is very crowded with an estimated concentration of approximately 300 mg/ml of protein and RNA [2]. To prevent both premature folding and aggregation, cells contain molecular chaperones. These chaperones enhance the efficiency of protein folding (rather than the specificity) and in this way help proteins to adopt a biologically active conformation. The functional, well-folded proteins are not infinitely stable and many kinds of physiological and non-physiological conditions may affect their conformation thereby reducing their activity. Also, these proteins may be refolded with the help of molecular chaperones.

Heat shock proteins, also named stress proteins, are induced by heat shock and other stressful circumstances, and have been identified as molecular chaperones. Heat shock proteins can roughly be divided into five families [3] based on their monomeric size as well as specific function: HSP100, HSP90, HSP70, HSP60 and the small heat shock proteins (sHSPs). The interaction of the chaperone with the unfolded substrates is transient, takes place through hydrophobic contacts, and is generally regulated by ATP and cofactors. However, sHSPs are not regulated by ATP, but - together with ATP-dependent chaperones such as HSP70 - there can be release and reactivation of the sHSP-bound substrate [4].

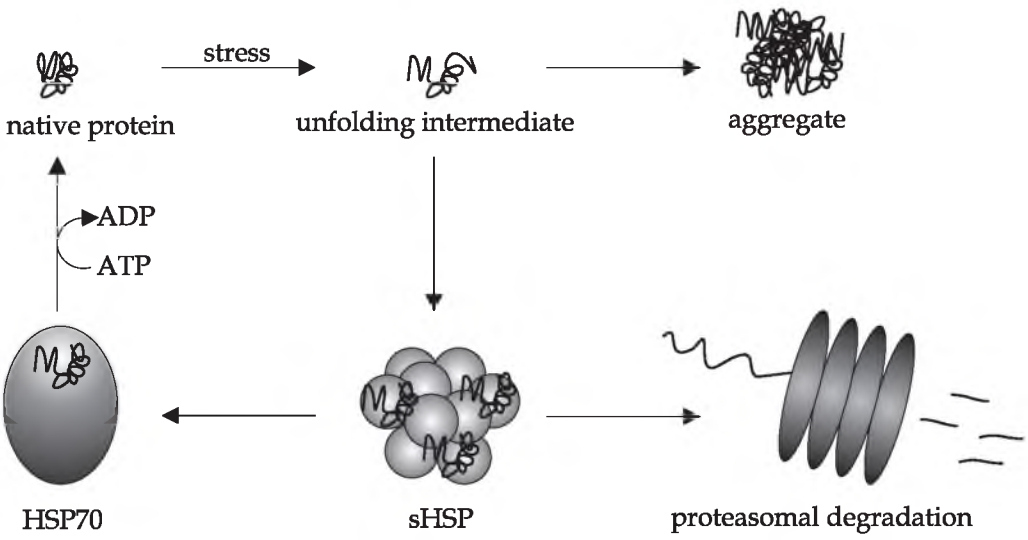

Figure 1. Model for the function of small heat shock proteins during stress
Unfolding of native proteins as a result of stress (e.g., heat shock) leads to the formation of aggregates. In the presence of small heat shock proteins, the unfolding protein intermediates can be bound in a soluble and refoldable state. In the presence of HSP70, ATP and co-factors, the bound protein can be released and refolded into its native state. Alternatively, bound proteins may also be directed to the proteasome for degradation. (Figure is adapted from [5])

This places sHSPs within a multichaperone network in which non-native proteins are bound by sHSPs during stress, which prevents irreversible aggregation of these non-native proteins and keeps them in a folding-competent state (reviewed in [5]). When physiological conditions are restored, non-native proteins may spontaneously dissociate, be refolded with help of ATP-dependent chaperones or directed to the proteasome for degradation (Fig. 1).

Small heat shock proteins

The sHSPs are a very diverse family amongst the heat shock proteins. They are characterized by the presence of the so-called α-crystallin domain, a stretch of approximately 100 aminoacids in the C-terminus of the proteins [6]. They further contain a variable N-terminal sequence and a short and variable C-terminal tail. sHSPs have a monomeric molecular mass ranging from 12 to 43 kDa, but they can form large oligomers of multiple subunits. The crystal structures of two small heat shock proteins have been resolved: HSP16.5 from the archaeal bacterium *Methanococcus jannaschii* [7] and wheat HSP16.9 [8]. The structures show that the primary building block of the oligomer is a dimer in which the α-crystallin domain forms a β-sandwich together with one of the β-strands from the dimer partner.

The *M. jannaschii* HSP16.5 complex is monodisperse and consists of exactly 24 subunits with a total molecular mass of 400 kDa, but many sHSPs have variable quaternary structures, which can change depending on a number of parameters such as temperature, pH, ionic strength and phosphorylation state of the protein. The dissociation into smaller complexes and the reassociation may be necessary for the chaperone function of sHSPs, since it has been shown that specifically the dimer binds non-native polypeptide chains [9]. The oligomeric complexes may be homomeric, as in the case of *M. jannaschii* HSP16.5, but probably most are heteromeric containing two or more different types of sHSPs. The dynamic regulation of sHSPs further includes alterations in amount, subcellular localization, and phosphorylation state, which all will be dicussed in more detail below for the mammalian sHSPs. Besides

Table 1. The ten known human small heat shock proteins

sHSP	Alternative name(s)	Main tissue expression	Reference(s)
HSPB1	HSP27, HSP25	heart, skeletal muscle	[16,17]
HSPB2	MKBP	heart, skeletal muscle	[19]
HSPB3	HSPL27	heart	[21]
HSPB4	αA-crystallin	eye lens	
HSPB5	αB-crystallin	eye lens, heart, skeletal muscle	
HSPB6	HSP20, p20	heart, skeletal muscle	[18]
HSPB7	cvHSP	heart, skeletal muscle	[22]
HSPB8	H11, E2IG1, HSP22	heart, skeletal muscle	[23-25]
HSPB9		testis	[27]
HSPB10	ODF1	testis	[13]

MKBP, myotonic dystrophy protein kinase binding protein; HSPL27, HSP27-like protein; cvHSP, cardiovascular heat shock protein; E2IG1, estrogen-induced gene 1; ODF1, outer dense fiber protein 1

the more general chaperone function, some sHSPs also have very specific functions not directly related to chaperoning, which is further supported by the fact that not all sHSPs studied so far exhibit chaperone properties [10].

DISCOVERY OF HUMAN SHSPS

Almost all organisms contain sHSPs, however some prokaryotes seem to be able to do without [11,12]. In human, so far 10 different sHSPs have been recognized (see Table 1, Fig. 2) using exhaustive database search procedures [13], and it thus seems unlikely that additional sHSPs still will be detected. Some sHSPs have been known for a long time (αA- and αB-crystallin, HSP27), while others have been discovered very recently. The lens-specific α-crystallin is composed of the closely-related αA- and αB-crystallin subunits. In lens, α-crystallin acts as a structural protein and is important for lens transparency, since a mutation found in αA-crystallin causes hereditary cataract [14]. While αA-crystallin is still considered to be more or less lens-specific, it has become apparent that αB-crystallin is also found outside the lens with high expression in heart and muscle [15]. HSP27 was identified as a gene upregulated by estrogen [16] and as an inhibitor of actin polymerization [17], but many more interesting functions have been assigned to HSP27 since then (see below).

Figure 2. Multiple alignment of the ten human small heat shock proteins.

Sequences of the ten known human small heat shock proteins were aligned using ClustalW and manually edited using GeneDoc. Residues in black are conserved in at least eight human small heat shock proteins, while residues in grey are conserved in five to seven members. The alignment is taken with permission from [13].

The more recently discovered sHSPs have been found in very different ways. HSP20 was originally obtained as a by-product of purification of HSP27 [18]. HSPB2 was identified as an interactor of Myotonic Dystrophy Protein Kinase in a yeast two-hybrid screen and activates this kinase [19]. The first reported sequence for HSPB3, HSPL27 [20], turned out to be a cloning artefact and was later corrected [21]. cvHSP was found as a gene that is selectively expressed in heart tissue and it was shown to interact with α-filamin [22]. HSPB8 was identified in several ways and for this reason it has various names (H11 kinase, E2IG1, HSP22, and HSPB8). As E2IG1, it was found to be a gene which is upregulated upon estrogen treatment [23], as HSP22 it was shown to bind pseudophosphorylated HSP27 [24], and as H11 kinase it was found to show some similarity to the large subunit of herpes simplex virus type 2 ribonucleotide reductase [25]. As HSPB8 it was found in a human genome search using a search profile based on the α-crystallin domain (Chapter 3). In this same search also HSPB9 was found (Chapter 3). HSPB9 is exclusively expressed at specific stages during spermatogenesis and is a cancer/testis associated gene (Chapter 6). HSPB10, known for some time as ODF1, but only recently identified as a member of the sHSPs family, is a structural component of the outer dense fibers in sperm [13].

EXPRESSION

Mammalian sHSPs are expressed in a wide variety of tissues and almost every tissue contains one or more sHSPs. Expression of sHSPs can be constitutive, is regulated during development and differentiation, and may be induced under pathological and stressful conditions. Regulation of expression is considered to be primarily at the level of transcription.

Constitutive expression

Most sHSPs (HSP27 [26], αB-crystallin [28], HSP20 [18], HSPB2 [19], HSPB8 [29]) have a very broad tissue distribution. High expression is almost always seen in heart and skeletal muscle, however, levels of expression vary considerably between analyzed tissues. HSPB3 [21,30] and cvHSP [22] seem to be exclusively expressed in heart and skeletal muscle. αA-crystallin is found in very high amounts in the eye lens, where it forms the lens-specific complex α-crystallin together with αB-crystallin. Low, but significant, αA-crystallin expression is also found outside the lens in spleen and thymus [31]. The most recent additions to the family of sHSPs, HSPB9 and HSPB10, are exclusively found in testis [13,27].

In rat muscle, two types of oligomeric complexes have been discovered: one large complex composed of HSP27, αB-crystallin and HSP20, and the other one, which is slightly smaller, composed of HSPB2 and HSPB3 [30]. The authors hypothesize that these complexes are two kinds of stress response systems of divergent sHSP members and that these systems work independently in muscle maintenance and differentiation. Whether or not cvHSP and HSPB8 belong to either one of these two complexes is not known (see also Chapter 4).

Expression during development and differentiation

Developmental regulation of sHSPs is common and has been described in many different organisms. The different sHSPs present at a certain developmental stage of a tissue probably reflect the particular need of that tissue at that specific moment. In mammals most developmental studies have

focussed on heart and muscle, since the expression of most sHSPs is very high in these tissues. In the rodent heart, HSP27, αB-crystallin, HSPB2 and HSPB8 are differentially regulated during development. HSP27, αB-crystallin and HSPB2 are present in the fetal heart, but while αB-crystallin levels remain constant [32], HSP27 decreases after birth [32,33]. In contrast, HSPB2 first increases in the neonatal heart and then rapidly decreases to below fetal levels [33]. HSPB8 expression is not detected in the fetal heart, but follows the same pattern after birth as HSPB2: first it increases and then decreases significantly with age [34].

The expression of other sHSPs has not been studied during heart development, but semiquantitative analysis of cvHSP mRNA levels showed its presence in human heart and lower levels in fetal heart [22], and HSPB3 ESTs have been found in both human adult and fetal heart [21]. In the developing porcine heart, both cvHSP and HSPB8 levels do not seem to change, while HSP20 and HSPB2 increase during aging (Chapter 5). The increase in expression of some sHSPs may be due to exercise. In rat hindlimb muscle, HSP27 and αB-crystallin increase dramatically after birth, while denervation of the muscle by transection of the sciatic nerve results in a decrease of sHSP levels [35]. HSP20, HSPB2, cvHSP and HSPB8 all increase in porcine skeletal muscle during aging (Chapter 5).

Besides the developmental regulation in tissues, many studies have also focussed on the expression of sHSPs during the differentiation of cells. During the *in vitro* differentiation of the mouse myoblast cell line C2C12, levels of αB-crystallin, HSPB2 and HSPB3 are upregulated, HSP27 remains constant, while HSP20 levels are reduced [30]. The *in vitro* differentiation of C2 cells, of which C2C12 is a subclone, showed similar results. Additionally, we found that – like HSP27 - HSPB8 levels remain constant during differentiation of C2 cells (Chapter 4). HSP27 and αB-crystallin expression is also regulated during the differentiation of numerous other cells, such as Ehrlich ascites cells, embryonal stem cells, osteoblasts, keratinocytes, neurons and epithelial cells (reviewed in [36]). For some cell types HSP27 is necessary for their differentiation [37,38]. HSP27 expression is regulated during mouse oocyte maturation and is important for preimplantation embryo development [39], which may be the reason why a HSP27 knock-out animal has not been reported yet.

Stress-induced expression

When cells are subjected to heat or another type of stress, sHSPs (but also other classes of heat shock proteins) are induced. The induced expression of sHSPs makes cells more resistant to a subsequent stress. However, differences in stress response are observed between types of stress and cell lines used, indicating that caution is needed in generalizing the results. The original categorization of sHSPs was based on their molecular weight and their ability to be induced upon heat shock. It has now become clear that not all sHSPs are heat-inducible. In both the undifferentiated and differentiated C2C12 cell line HSP27 and αB-crystallin are heat-inducible, while HSP20, HSPB2 and HSPB3 are not [30]. We could confirm this for HSP27, αB-crystallin and HSP20 in the C2 cell line and our results further show that HSPB8 is only slightly heat-inducible (Chapter 4). Even though αB-crystallin is inducible to a great extent after heat shock, its most closely related family member, αA-crystallin, is not.

Other stresses such as oxidative stress, exposure to heavy metals or amino acids analogues may also induce sHSP expression. Although αA-crystallin is not heat-

inducible, a very recent report shows that expression can be induced in lens epithelial cells by copper-ions [40]. Furthermore, depolymerization of microtubules induces the synthesis and accumulation of αB-crystallin, but not of HSP27 [41].

In contrast to increased expression, expression can also be reduced upon stress. For instance αB-crystallin expression is reduced in human trabecular meshwork cells subjected to mechanical stretch [42]. Also overexpression of Bcl-2 in cells has been reported to specifically reduce αB-crystallin levels [43].

Regulation of gene expression

The regulation of mammalian sHSP gene expression is considered to be primarily at the level of transcription. The promoters have not been extensively studied, except those for αA-, αB-crystallin and HSP27. Lens-specific expression of αA-crystallin only requires a small region of the promoter to which Pax-6, upstream transcription factor (USF), cyclic AMP (cAMP)-responsive element protein (CREB) and α-crystallin binding protein (α-cryBP1) can bind [44,45]. The lens-specific activity of the αB-crystallin promoter depends on two lens-specific regulatory regions (LSR1 and LSR2) while the upstream αB-crystallin enhancer, containing E-boxes and a myogenic response factor binding site, is required for promoter activity in all non-lens tissues [46,47]. The promoter of HSP27 contains a myocyte enhancer factor consensus site [48], possibly responsible for muscle expression, while the presence of an imperfect estrogen response element (ERE) may explain HSP27 upregulation after estrogen treatment [49].

Heat-induced expression of sHSPs is under the control of heat shock elements (HSE), to which the stress-related heat shock transcription factors (HSF) can bind. HSEs have been detected in promoters of those sHSPs which are inducible by heat (HSP27 and αB-crystallin). The absence of a HSE in the promoter region of αA-crystallin may explain why it is not heat-inducible. Since the HSPB2 gene is head-to-head with αB-crystallin, there is a possibility that they share promoter elements. However, αB-crystallin expression is found in eye lens and HSPB2 is not [50]. Furthermore, HSPB2 is not stress-inducible, while αB-crystallin is [30]. The αB-crystallin enhancer found in the intergenic region has been shown to be orientation-dependent and has a preferential effect on the αB-crystallin promoter, but also a minor effect on HSPB2 was found [51]. Besides heat shock also other environmental and physiological stresses can induce the activation of HSF and binding to HSE resulting in elevated expression of sHSPs (reviewed in [52]).

POST-TRANSLATIONAL MODIFICATIONS

Several post-translational modifications of human sHSPs have been described of which phosphorylation is best studied and will be described in more detail below. Several other modifications such as methylglyoxal modification [53] and S-thiolation of HSP27 [54], and O-linked N-acetylglucosamine modification of αB-crystallin [55] have been described, but not extensively studied.

Phosphorylation

Phosphorylation of serine residues has been described for several sHSPs. In most cases stress-activated kinases are responsible for this modification, but phosphorylation is also observed in non-stress situations. Human HSP27 can be phosphorylated at serines 15, 78 and 82, but mouse HSP25 only at serines 15 and 86 (corresponding with

human 82). MAPKAP kinase 2, MAPKAP kinase 3 and PKC are responsible for the phosphorylation of these serine residues without apparent selectivity [56-58]. Phosphorylation of HSP27 in response to stress is rapid and results in the dissociation of the large complex into smaller complexes. Treatment of human fibroblasts with either TNF or sodium arsenite induces HSP27 phosphorylation within five minutes. In the case of TNF, phosphorylation reaches a plateau after 10-30 minutes, after which it decreases. However, after arsenite treatment phosphorylation persists for at least four hours [59]. The degree of phosphorylation is not only regulated by kinases, but also by phosphatases. *In vivo* dephosphorylation of HSP27 has been shown to be catalyzed by protein phosphatase 2A [60].

In the eye lens, phosphorylated forms of both αA- and αB-crystallin have been found. αA-crystallin in lens is phosphorylated at serine 122, probably via a cAMP-dependent pathway or via its reported autokinase activity [61]. This autokinase activity was also described for αB-crystallin [61]. Human αB-crystallin is phosphorylated at serines 19, 45 and 59 in response to various types of stress. Enzymes responsible for phosphorylation at serines 45 and 59 have been identified as p44/42 MAP kinase and MAPKAP kinase 2, respectively. Like HSP27, phosphorylation of αB-crystallin also results in the dissociation of the large complex into smaller complexes [62]. Interestingly, other than in stress situations, αB-crystallin has also been found to be phosphorylated during the cell cycle. In mitotic cells, phosphorylation at serines 19 and 45 is enhanced, while phosphorylation at serine 59 is lower when compared to control cells [63]. Dephosphorylation of α-crystallin has only been tested *in vitro* and was shown to depend on the state of oligomerization [64].

HSP20 can be phosphorylated at several positions, but only serine 16 has been identified, which is phosphorylated by PKA during cyclic nucleotide-dependent relaxation of bovine carotid artery smooth muscle [65]. HSP20 phosphorylation is, like HSP27 and αB-crystallin phosphorylation, associated with the dissociation of large complexes into smaller ones [66]. The phosphorylation status of HSP27 may influence phosphorylation of HSP20, since it was shown that phosphorylated HSP27 inhibits HSP20 phosphorylation in an *in vitro* assay [67].

HSPB8 has been reported to be phosphorylated in melanoma cells [25] and can *in vitro* be phosphorylated at serine 14 and threonine 63 by PKC, and at serine 27 and threonine 87 by p44 MAP kinase [24]. Also autokinase activity has been reported for HSPB8 [25]. We showed that HSPB8 phosphorylation takes places in C2, but not in HeLa cells (Chapter 4).

For HSPB2/MKBP, HSPB3, HSPB7/cvHSP, HSPB9 and HSPB10/ODF1 it is not known whether they can be phosphorylated.

INTRACELLULAR LOCALIZATION

Even though most sHSPs are mainly cytosolic and soluble proteins, associations have been found with cytoskeleton (see also below), mitochondria and membranes. In muscle, a specific sarcomeric sHSP localization has been found. Besides the soluble cytoplasmic staining, HSP27 [68-70], αB-crystallin[69,71-73], HSPB2 [19,33,70] all localize at the Z bands either in unstressed cells or after stress. Also in other tissues than muscle, sHSPs can be associated with the cytoskeleton [74-76]. We have shown that, upon proteasomal inhibition, all sHSPs tested (αA- and αB-crystallin, HSP27, HSP20, HSPB2 and HSPB3) translocate to

the actin cytoskeleton (Chapter 2). HSP27 and HSP20 are cytoplasmic proteins, but can translocate to the nucleus after heat shock [33,69,73], where they may chaperone nuclear proteins. No stress-induced nuclear localization has been described for αB-crystallin, except in [77]. Despite the lack of nuclear translocation, αB-crystallin is insolubilized, like HSP27, a phenomenon observed in various cell types after various stresses ([69,73,77], Chapter 2).

Besides cytoplasmic and cytoskeletal localizations, other cellular localizations have been described. HSPB2 associates with mitochondria [78], and it has been reported that also a small fraction of HSP27 co-localizes with mitochondria [79], although others found no mitochondrial localization for HSP27 [80]. Also localization at membranes has been described. αB-crystallin binds membranes [81] and modulates membrane fluidity [82], and also HSPB8 is associated with plasma membranes [29]. HSP27 has been observed to translocate to membranes after stress [83]. sHSPs may preserve membrane structure and integrity during the initial stages of stress conditions [82].

The two testis-specific sHSPs, HSPB9 and HSPB10, show specific localizations. In non-stress conditions HSPB9 is found in the nucleus of developing sperm cells (Chapter 6), while HSPB10 is part of the outer dense fibers in sperm tails [13].

FUNCTIONS OF SHSPS

Not much is known about the actual functions of sHSPs, but members of the sHSP family have been implicated to play a role in eye lens transparency [84], human diseases [85], and various developmental processes. Furthermore, involvement of sHSPs in cellular processes such as resistance to apoptosis, cytoskeletal modulation, thermotolerance, protection against oxidative stress, and cell growth [34,86] has been demonstrated (see below). Most of these functions relate to the general protection of other proteins, but there is increasing evidence that sHSPs are also involved in other functions than chaperoning. Besides the more specific functions for the sHSP family in general, also specific functions for a particular sHSP have been described, such as inhibition of translation during heat shock by HSP27 [87], promotion of ubiquitination by αB-crystallin [88] and maintaining the passive elastic structures and elastic recoil of the sperm tail by outer dense fibers, of which HSPB10 is a component [13].

Since many sHSPs are expressed in the same tissue, it could be argued that not all of them would be needed. Indeed mice lacking αA-crystallin are viable and fertile, but cataract is induced [84], and mice in which αB-crystallin and HSPB2 are knocked out also survive, but have problems with maintaining muscle cell integrity in some skeletal muscles [89].

Protection against stress

sHSPs can protect cells against damage caused by heat and a wide variety of other stresses. Increased expression of sHSPs makes cells more thermoresistant. The overexpression may be artificial (after transfection of cells) or physiological (as a results of a previous stress). Cells treated with a minor stress before a more severe stress, thus inducing sHSPs, survive better than cells without the pre-treatment. Thermoresistance has been observed for HSP27 [90], αA-[91] and αB-crystallin [92,93], HSP20 [93] and HSPB2 [78]. The mechanism by which sHSPs can provide thermotolerance to cells is not known despite extensive research on the subject. It

is thought that their *in vitro* chaperone-like activity is involved in the protection against heat shock or other types of stress that cause *in vivo* protein denaturation. However, the *in vivo* chaperone-like activity does not seem to be directly linked to cell survival [93]. Also the ability of α-crystallin to stabilize membranes could be involved in the cellular protection since membranes are known to be among the most sensitive targets of heat-stress damage in cells [82].

sHSPs (at least HSP27 and αB-crystallin) can also modulate intracellular redox state. They can protect against oxidative stress, which can be induced by exposure of cells to peroxides, glutathione-depriving drugs, toxins, or inflammatory cytokines. During oxidative stress, reactive oxygen species (ROS) are produced at high concentration and can be cytotoxic. HSP27 can modulate ROS levels, probably by upregulating glutathione levels and keeping it in its reduced state. HSP27 can probably do this by activating enzymes in the ROS-glutathione pathway, as has been shown for the activity of glucose-6-phosphate dehydrogenase, glutathione reductase and glutathione transferase [94].

Protection against apoptosis

There are two types of cell death induced by stress, necrosis and apoptosis, and the intensity of the stress will determine the way in which cells will die. In the case of a moderate stress, apoptosis is induced. Apoptosis is the process of programmed cell death which requires ATP and in which proteolytic cleavage by caspases is characteristic. The two major pathways which lead to activation of caspases are the death receptor and the mitochondrial pathway. Stress induced apoptosis usually occurs through the activation of the latter pathway. Chaperone proteins control specific steps of the apoptotic pathway (Fig. 3; reviewed in [36,95]). For instance, HSP70 and HSP90 negatively regulate apoptosis at several levels [96]. In contrast, HSP60 and HSP10 act as pro-apoptotic chaperones [97,98], but more recently also anti-apoptotic properties have become apparent [99].

Recently, it has become clear that some sHSPs (HSP27, αA- and αB-crystallin) also have the ability to reduce or delay apoptotic processes. In this respect, HSP27 is best studied. It interferes with the release of cytochrome c from the mitochondria. This may be due to an upstream effect of HSP27 protection of F-actin, since F-actin depolymerization induces cytochrome c release from mitochondria, and this phenomenon is inhibited by HSP27 expression [79]. HSP27 can also directly interact with cytochrome c, once it is released from the mitochondria [100]. It is thought that HSP27 prevents apoptosome formation in this way. However the mechanism remains unclear since it was found that only a small fraction of cytochrome c interacts with HSP27. HSP27 has also been found to interact with Daxx, a mediator of Fas-induced apoptosis, preventing interaction of Daxx with Fas and Ask1, and thereby blocking apoptosis [101]. Furthermore, also a direct interaction of HSP27 with pro-caspase 3 has been documented [102] and it is thought that by this binding it prevents the proteolytic activation of pro-caspase 3. HSP27 can protect against TNFα-induced apoptosis by lowering basal levels and the burst of intracellular ROS generated by the binding of TNFα to its receptor [103].

In contrast to HSP27, which seems to influence the apoptotic execution machinery at different levels, αB-crystallin has, so far, only been shown to affect the pathway at the level of pro-caspase 3 activation [43,104]. Mutants of αB-crystallin (R120G and a C-terminal deletion mutant) provide diminished

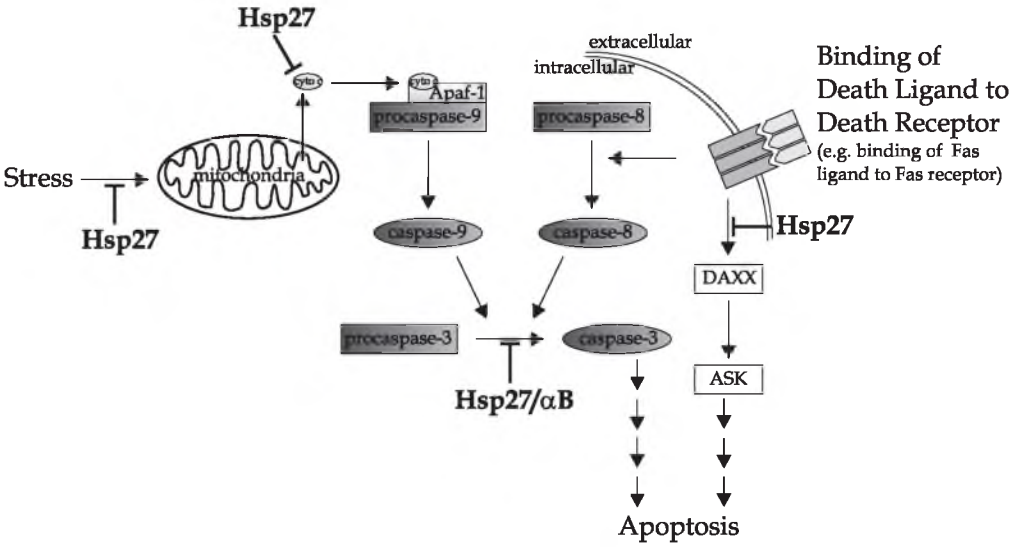

Figure 3. Schematic illustration of the sites of protective action of small heat shock proteins in the apoptotic pathways
In the mitochondrial pathway (depicted on the left) HSP27 interferes with the signal that promotes the release of cytochrome c from the mitochondria. HSP27 can further interact with cytochrome c directly, inhibiting the apoptosome complex (composed of procaspase-9, Apaf-1 and cytochrome c). In the death receptor pathway (depicted on the right) HSP27 interferes with the Daxx pathway, probably by binding to Daxx and thus preventing interaction of Daxx with Ask and Fas. Both HSP27 and αB-crystallin have been shown to directly interact with procaspase-3, preventing its maturation into the active enzyme. (Figure is based on [36])

protection against apoptosis [105], and phosphorylation of αB-crystallin at serine 59 seems to be necessary and sufficient to protect against apoptosis [106].

αA-crystallin can also protect against apoptosis and has 2-3 fold higher anti-apoptotic activity than αB-crystallin [107]. Also for αA-crystallin it has been documented that mutation (R116C) makes it less effective in protection against apoptosis [107].

The protection by sHSPs against apoptosis has been found in many different cell types using many different apoptotic inducers, but there has also been a report that sHSPs may promote apoptosis [108]. Besides the protection against stress-induced apoptosis, sHSPs also seem to be involved in the protection against apoptosis during cell differentiation. During early cell differentiation, HSP27 and αB-crystallin are upregulated and inhibition of expression aborts the differentiation processes and induces apoptosis. In embryonic stem cells and olfactory neuroblasts, HSP27 seems essential for preventing the cells from undergoing apoptosis during differentiation [109,110] and a reduction of HSP27 expression aborts the differentiation. In myoblasts, αB-crystallin, but not HSP27, protects against differentiation-induced apoptosis [104].

The roles of other sHSPs in apoptosis remain to be studied. Since besides HSP27 and αB-crystallin also HSPB2 and HSPB3 are upregulated during differentiation it can be speculated that they may also have anti-apoptotic properties.

Involvement in the cytoskeleton

The cytoskeleton is a dynamic structure providing strength and internal organization to cells. It consists of microfilaments/actin, intermediate filaments (vimentin, desmin,

glial fibrillary acidic protein, lamin, keratin and neurofilament proteins) and tubulin/microtubules, which form a functional unit together. Several observations have linked sHSPs to the cytoskeleton. One of the first indications that sHSPs are somehow involved in the cytoskeleton, came from the identification of HSP27 as an inhibitor of actin polymerization [17,111]. HSP27 probably inhibits actin polymerization by capping the actin filaments at their elongating ends, preventing further growth of the polymer. Phosphorylation of HSP27 regulates the inhibitory activity since only unphosphorylated low molecular weight HSP27 is able to inhibit actin assembly, while unphosphorylated multimers and phosphorylated low molecular weight species are devoid of this inhibitory activity [112]. It has also been suggested that αB-crystallin can inhibit actin polymerization [113]. *In vitro*, αB-crystallin is able to stabilize actin filaments and prevents their cytochalasin-induced depolymerization in a phosphorylation-dependent manner [114]. αB-crystallin expression in glioma cells stabilizes filamentous actin organization [115]. Besides HSP27 and αB-crystallin, also HSP20 has been described as an actin-associated protein, but reports on the role of HSP20 phosphorylation are contradictory [116,117]. It has been speculated that HSP20 interacts with specific elements of the contractile machinery in muscle - actin and myosin light chains - and in that way modulates vasorelaxation [66]. One of the more recently identified sHSPs, cvHSP, has been shown to bind filamin [22], an actin-binding protein that promotes actin polymerization as well as attachment of membrane proteins to actin filaments (reviewed in [118]).

With respect to intermediate filaments (IFs), αB-crystallin has been best studied. Interactions between αB-crystallin and IFs have been noted in muscle, lens, and astrocytes [72,119,120]. Association of αB-crystallin with IFs has been detected after stress [77,121], during mitosis [122] and even in unstressed cells [123]. *In vitro*, αB-crystallin inhibits the polymerization of IFs independent of phosphorylation [119]. Thus, in contrast to interaction with actin, the interaction of αB-crystallin with IFs does not seem to depend on αB-crystallin phosphorylation. Also, interactions have been found with soluble IFs as well as intact IFs [119,123], indicating that the assembly status of the filaments does not affect binding, again in contrast to the results found with actin. Increased αB-crystallin expression in the absence of stress can modify the organizational state of IF [124], and expression of a mutant αB-crystallin (R120G) is linked to an autosomal dominant desmin-related myopathy [125], a disease which is characterized by desmin aggregates (see next section). Reports on interactions of HSP27 with IFs are scarce and are restricted to co-localizations, which have been detected in unstressed and stressed cells [76,123,126].

Whereas the relations of sHSPs to actin and intermediate filaments have been studied extensively, much less in known about their relation with tubulin/microtubules. HSP27 has been found to associate with tubulin [127], but is unable to protect microtubules when overexpressed [128]. Also αB-crystallin associates with tubulin, in a temperature-dependent manner, and shows *in vitro* chaperone-like activity towards tubulin [129]. In contrast to HSP27, αB-crystallin is able to protect microtubules when overexpressed [128]. αB-crystallin phosphorylated at Ser-59 is localized at the microtubule organizing centers during mitosis [130]. Besides the association with tubulin, interactions with the microtubule motor protein dynein have been detected.

HSPB9 and also other sHSPs can interact with TCTEL1, a component of dynein (Chapter 6). Dynein is involved in the movement of vesicles, cellular organelles and chromosomes, and TCTEL1 is, amongst others, important for cargo specificity.

Role in diseases

sHSPs have been implicated in a variety of diseases, including diseases caused by protein aggregation, cancer, and auto-immunity. Since many sHSPs possess *in vitro* chaperone-like activity, it can be speculated that they play a role in inclusion body diseases. Many results are available from studies on HSP27 and αB-crystallin. Elevated levels of HSP27 and/or αB-crystallin have been detected in neuro-degenerative diseases such as Alzheimer's [131], Parkinson's [132], Creutzfeldt-Jakob [132,133], and Alexander's [15,134]. Interestingly, in Huntington's disease αB-crystallin decreases in expression over the course of disease [135]. Besides elevated levels, also depositions of HSP27 and αB-crystallin have been found in the brains of patients with various neurological diseases. The role of sHSPs in human diseases with respect to protein aggregation remains elusive. Overexpression of αB-crystallin decreases the number of inclusions found after overexpression of GFAP and restores GFAP to a normal filamentous organization [136], suggesting that sHSP upregulation may be a response to abnormal IF organization in an attempt to restore the normal IF network. In Huntington's disease HSP27 suppresses cell death without suppressing poly(Q) aggregation [137] indicating that not the aggregates *per se* are the most harmful to cells.

A mutation in αB-crystallin, in which arginine 120 is replaced by glycine, is linked to another type of protein aggregation disease, namely autosomal dominant desmin-related myopathy [125]. This disease is characterized by adult onset and an accumulation of desmin aggregates, but also cataract has been observed. Cells transfected with the mutant αB-crystallin also accumulate desmin/αB-crystallin aggregates [125]. *In vitro* studies of αB-crystallin R120G have shown that it has an altered structure and a defective chaperone-like activity [138]. Interestingly, a mutation at the corresponding position in αA-crystallin (arginine 116 to cysteine) is linked to autosomal congenital cataract [14]. In mice, another mutation in αA-crystallin (arginine 54 to histidine) is also linked to cataract [139].

Since cancer cells within a tumor are exposed to stressful conditions such as insufficient blood supply, and since cells overexpressing sHSPs are more resistant to damaging conditions, the question has arisen whether or not tumors overexpressing sHSPs are more resistant to treatment. In this respect HSP27 has been best studied as a possible predictive/prognostic factor in cancer (for review see [140]). In specific cases, HSP27 expression is indeed negatively correlated with the outcome of the disease, but also positive correlations or no correlation at all have been found. It thus seems that no general conclusion can be drawn, possibly due to the limitations of the studies. Besides HSP27, also HSPB8 is exclusively expressed in estrogen-receptor-positive breast cancer cell lines, and thus has a potential to serve as a breast cancer biomarker [23]. We identified HSPB9 as a cancer/testis associated gene (Chapter 6), but the relevance of this finding with respect to disease outcome is unclear.

Five of the sHSPs (αA- and αB-crystallin, HSP27, HSPB2 and HSPB10) have been described as autoantigens in various diseases. αB-crystallin has been proposed to be a key autoantigen in multiple sclerosis [141], and serum concentrations of

antibodies against αA- and αB-crystallin are correlated with the severity of this disease [142]. In patients with glaucoma, autoantibodies against αA-, αB-crystallin, and HSP27 have been detected [143], while HSPB2 is a muscle autoantigen in thyroid associated ophthalmopathy [144]. Obstruction of the male reproductive tract results in generation of HSPB10 autoantibodies in rats [145].

HSPB2 is selectively upregulated in skeletal muscles of myotonic dystrophy patients, which may suggest an involvement in the pathogenesis of this disease [19]. Modulation of cvHSP expression in obesity suggests that cvHSP may be associated with obesity and related metabolic disorders [22]. Overexpression of HSPB8 in heart results in myocardial hypertrophy [34]. sHSPs are thus involved in a very broad spectrum of diseases showing that they may function in many different cellular processes.

OUTLINE OF THIS THESIS

Small heat shock proteins have been identified as molecular chaperones *in vitro*, but their *in vivo* function is still poorly understood. The main purpose of this thesis was to gain more insight into the unique and overlapping roles that small heat shock proteins play in normal and stress situations. In order to achieve this goal, we chose to compare the stress response of several small heat shock proteins. Small heat shock proteins, being chaperones, are able to bind unfolding proteins, while proteasomes are able to degrade them. Therefore, we investigated a possible functional relationship between small heat shock proteins and proteasomes (Chapter 2) and found an interesting way in which cells deal with unfolding proteins when they can not be degraded. All small heat shock proteins tested showed co-localization with actin stress fibers upon proteasomal inhibition, and we proposed that actin is used as storage place to clear the cytoplasm from possible harmful aggregates.

In order to understand the unique and overlapping functions of small heat shock proteins it is a prerequisite to first know the actual number of small heat shock proteins that are present within a human being. The amount of data in databases has increased immensely in the past few years and the publication of cvHSP, identified by computational search of tissue-selective expression of expressed sequence tags [22], prompted us to search the databases for more, until then, unknown small heat shock proteins. This search resulted in the identification of HSPB8 and HSPB9 (Chapter 3). Characterization of the small heat shock protein features of HSPB8 is described in Chapter 4, and shows that its expression and behaviour is very similar to, but not exactly the same as that of other small heat shock proteins. Data on the tissue- and development-specific expression pattern of HSPB8 in pigs is presented in Chapter 5, and the results are compared to HSP20, HSPB2 and cvHSP. Finally, in Chapter 6 testis-specific HSPB9 is further characterized, a unique member which is specifically expressed in normal testis and in tumors from different origins.

Even though the results presented in this thesis have not elucidated the exact function(s) of small heat shock proteins, they have increased our insight. In Chapter 7, the most important results are summarized and discussed with implications for further research.

Translocation of small heat shock proteins to the actin cytoskeleton upon proteasomal inhibition

Pauline Verschuure [1]
Yvonne Croes [1]
Paul R.L.A. van den IJssel [2]
Roy A. Quinlan [2]
Wilfried W. de Jong [1]
Wilbert C. Boelens [1]

[1] *Department of Biochemistry, Nijmegen Center for Molecular Life Sciences, University of Nijmegen, Nijmegen, The Netherlands*
[2] *Department of Biochemistry, University of Dundee, Dundee, Scotland, UK*

J. Mol. Cell. Cardiol. (2002) **34**: 117-128

The role of small heat shock proteins (sHSPs) as molecular chaperones is still poorly understood. We therefore investigated the effect of proteasomal inhibition on sHSPs in the rat cardiac myoblast cell line H9c2. Proteasomes are responsible for controlled degradation of intracellular proteins. Inhibition of their activities leads to accumulation of unfolded proteins, which can form insoluble 'aggresomes' together with proteasomes and heat shock proteins HSP70 and HSP90. We here report that upon proteasome inhibition, αB-crystallin and HSP25 translocate from the detergent-soluble cytosolic fraction to the detergent-insoluble nuclear/cytoskeletal fraction. Although phosphorylation of both αB-crystallin and HSP25 is induced, this does not seem to be essential for the translocation. Immunocytochemistry revealed that αB-crystallin and HSP25, which show a diffuse cytoplasmic staining in unstressed H9c2 cells, colocalize with F-actin upon proteasomal inhibition. After transfection in H9c2 cells, other sHSPs (αA-crystallin, HSP20, HSPB2 and HSPB3) showed similar translocation to the actin cytoskeleton. The redistribution of sHSPs upon proteasomal inhibition may reflect a mechanism by which cells are protected from damaged intracellular proteins by sequestering them on the cytoskeleton.

INTRODUCTION

Mammals express at least nine different small heat shock proteins (sHSPs), known as αA-crystallin, αB-crystallin, HSP27 (HSP25 in rodents), HSP20, HSPB2, HSPB3 [21], cvHSP/HSPB7 [22], HSPB8 and HSPB9 [27]. They are characterized by the so-called α-crystallin domain, a conserved sequence of about 85 residues. sHSPs form large complexes, which may contain more than one type of subunit. sHSPs fulfil diverse functions. They act as chaperones by binding unfolding proteins [4], help to inhibit apoptosis [105,146], convey thermotolerance to cells [92], and can associate with the cytoskeleton. HSP27, αB-crystallin, HSP20 and HSPB2 have been shown to associate with actin and desmin filaments in cardiac tissue and stressed cardiomyocytes [69,70,72]. In several other cell types, colocalization of αB-crystallin with intermediate filaments has been observed. The interaction can be induced by different types of stress [77], and has also been detected in unstressed cells with specific antibodies [123]. αB-crystallin may also contribute to the stability of actin filaments, since reducing the expression of αB-crystallin with antisense cDNA in glioma cells was found to lead to a disorganized microfilament network [115]. Furthermore, *in vitro* it has been shown that α-crystallin, a lens-specific complex of αA- and αB-crystallin, is able to stabilize actin filaments and prevent cytochalasin-induced depolymerization [114].

α-Crystallin has been reported to have a low affinity for the 20S proteasome [147,148], and αB-crystallin is *in vitro* indeed able to bind C8/α7, an α-type proteasomal subunit [149]. Since αB-crystallin can bind unfolding proteins, while proteasomes are able to degrade them, we were interested in

a possible functional relation between αB-crystallin and proteasomes. From that perspective, we investigated the effect of MG132, a reversible, cell-permeable proteasome inhibitor, on αB-crystallin and other sHSPs in the rat cardiac myoblast cell line, H9c2.

The ubiquitin-proteasome system is the major extra-lysosomal pathway for controlled degradation of intracellular proteins in eukaryotes. It plays a key role in many cellular processes, ranging from cell-cycle control to differentiation and cellular immune response [150]. Inhibition of the proteasome, e.g. by lactacystin or MG132, blocks the rapid degradation of short-lived regulatory proteins and abnormal polypeptides, and the slower degradation of long-lived proteins [151]. This leads to the formation of aggresomes [152], activation of stress kinases [153], induction of heat shock proteins [154] and may eventually cause apoptosis [155]. Aggresomes contain misfolded proteins, but also the 20S proteasome, ubiquitin, HSP70 and HSP90. Aggresome formation is thought to provide a cytoprotective role by clearing the cytoplasm from potentially toxic aggregates. The interaction of sHSPs with actin stress fibers upon proteasomal inhibition, as described in this work, may represent a similar mechanism to clear the cytoplasm from possibly harmful aggregates.

MATERIALS AND METHODS

Cloning

For expression of Green Fluorescent Protein (GFP) fusion products, the cDNAs of sHSPs were cloned into the pEGFP-c1 vector (Clontech, Palo Alto, CA, USA) at the 3' end of GFP. N-terminal fusion was chosen because it has been shown that an N-terminally fused protein does not affect the complex size and chaperone function of αB-crystallin [156]. The complete coding regions of wild type human αB-crystallin, a non-phosphorylatable mutant (S19A, S45A, S59A), and two phosphorylation-mimicking mutants (S19D, S45D and S59D) [157], and of rat αA-crystallin [158] were cloned into the BglII site with a GCC linker between the BglII site and the start codon. The complete coding regions of HSPB2, HSPB3, and HSP20 were isolated from a rat heart cDNA library by PCR and cloned into the BglII site of pEGFP-c1 with the start codon adjacent to the BglII site. Due to the creation of a restriction site, HSPB2 contains a Ser2Ala substitution. GFP-2B(1-40) contains the 40 N-terminal amino acid residues of the coxsackie B3 virus protein 2B (gift from F.J. van Kuppeveld [159]) fused to GFP.

Cell culture and stress treatments

The rat cardiac myoblast cell line H9c2 and the rat glioma cell line C6 were cultured in DMEM (GIBCO, Breda, The Netherlands) supplemented with 10% heat-inactivated fetal calf serum, 100 U/ml penicillin and 200 µg/ml streptomycin. The cells were incubated at 37°C in a humidified atmosphere containing 5% CO_2. Transient transfections were performed with Lipofectamine (Life Technologies, Breda, The Netherlands) according to the supplier's manual. Proteasomes were inhibited by addition of MG132 or lactacystin (both from Calbiochem, Bad Soden, Germany) to the medium. Heat shock was performed by complete immersion of the cell culture dishes in a water bath of the desired temperature.

Detergent solubility

Stressed and control cells were harvested by trypsinization, and centrifugation in a Minifuge RF (Hereaus, Hanover, Germany) (5 min at 100 x g, 4°C). Cells were washed

once with medium and twice with ice-cold phosphate-buffered saline (PBS) containing 1 mM phenylmethanesulfonyl fluoride. Cells were resuspended in ice-cold lysis buffer (10 mM Tris pH 7.5, 10 mM NaCl, 5 mM $MgCl_2$, 1 mM phenylmethanesulfonyl fluoride and 0.5% Triton X-100) and centrifuged (5 min at 300 x g, 4°C). The supernatant was used as detergent-soluble fraction. The pellet was washed once with lysis buffer and then used as detergent-insoluble fraction.

Electrophoresis and Western blot analysis

SDS-PAGE was performed following standard procedures. For Western blot analysis, proteins were transferred electrophoretically to a nitrocellulose membrane (Schleicher&Schuell, Dassel, Germany), and the membrane was incubated successively with primary antibodies and with alkaline phosphatase-conjugated secondary antibodies (Promega, Leiden, The Netherlands). The primary antiserum for detection of αB-crystallin was raised in rabbits against the C-terminal 13 amino acid residues of αB-crystallin. For immunofluorescence, the antibodies were affinity purified using the C-terminal peptide. HSP25 was detected with a polyclonal antiserum against mouse HSP25 (a gift from Dr. A. Zantema, Leiden). Antibodies specific for each of the three phosphorylated serines of αB-crystallin were raised in rabbits using three peptides corresponding to internal sequences of human αB-crystallin, containing phosphorylated serine 19 (residues 15-23), serine 45 (residues 41-49) and serine 59 (residues 55-63). Antibodies specific for phosphorylated serine 15 of HSP27 were raised in rabbits using a peptide corresponding to internal sequences of human HSP27. Antibodies recognizing phosphorylated serine 82 of human HSP27 (serine 86 in rat sequence) were monoclonal. The phosphoserine-specific antibodies were affinity purified. Affinity isolated actin antibody was obtained from Sigma.

Indirect immunofluorescence

Cells were grown on glass coverslips and allowed to attach overnight before stress treatment. After treatment cells were washed with PBS, fixed with 3% paraformaldehyde for 15 min, washed again with PBS, and permeabilized with 0.2% Triton X-100 for 10 min. F-actin was detected using TRITC-conjugated phalloidin (Sigma, Zwijndrecht, The Netherlands). Primary antibodies were used as described above. A FITC-conjugated anti-rabbit IgG (DAKO, Glostrup, Denmark) was used as the second antibody. After incubations coverslips were washed three times with PBS and mounted in a solution of 10% Mowiol (Hoechst, Frankfurt, Germany) with 1.2% diaza-bicyclooctane. Cells were examined by confocal laser scanning microscopy (BIO-RAD MRC 1000; Kr/Ar laser; COMOS software, Hercules, CA, USA).

RESULTS

αB-crystallin and HSP25 become detergent-insoluble upon inhibition of proteasomal activity

We investigated a possible change in distribution of αB-crystallin in H9c2 cells after inhibition of proteasomal activity with MG132, a reversible and cell-permeable proteasome inhibitor. Following treatment with MG132, H9c2 cells were lysed in a buffer containing 0.5% Triton X-100, and separated in a detergent-soluble cytoplasmic and a detergent-insoluble nuclear/cytoskeletal fraction. Under normal conditions, αB-crystallin was almost exclusively found in the soluble fraction

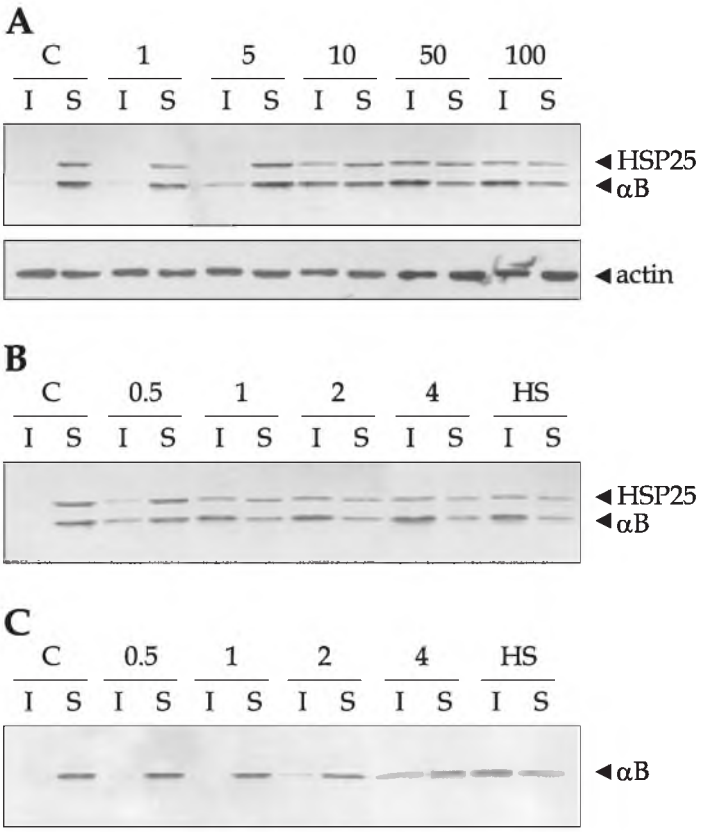

Figure 1. αB-crystallin and HSP25 translocate to the detergent-insoluble fraction upon proteasomal inhibition in a concentration- and time-dependent manner
Untreated control cells (lanes C) and stressed cells (other lanes) were separated into detergent insoluble and -soluble fractions (lanes I and S, respectively). Each fraction was subjected to SDS PAGE and immunoblotting with anti-αB-crystallin antibody, anti-HSP25 antibody (A C) and anti actin antibody (A, lower panel). (A) H9c2 cells treated for 4 h with increasing concentrations of the proteasome inhibitor MG132 (1, 5, 10, 50 or 100 μM MG132, respectively). (B) H9c2 cells treated with 50 μM MG132 for 0.5, 1, 2 or 4 h, respectively. HS, cells heat shocked at 44°C for 20 min. (C) C6 glioma cells treated with 50 μM MG132 for 0.5, 1, 2 or 4 h, respectively. HS, cells heat shocked at 44°C for 20 min.

(lanes C in Fig. 1A,B), while after heat shock it was predominantly in the insoluble fraction (lanes HS in Fig. 1B), as observed in other cell types [160,161]. Inhibition of proteasomal activity similarly led to insolubilization of αB-crystallin, dependent on the concentration of MG132, and reaching a maximum at 10 μM (Fig. 1A; 1-100 μM for 4 h). The level of insolubilization also depends on the incubation time, reaching after 4 h a level similar to that after heat shock (Fig. 1B; 0.5-4 h at 50 μM MG132). Insolubilization seems irreversible, even after a recovery period of up to 96 h (data not shown).

To determine whether the redistribution of αB-crystallin upon proteasomal inhibition is a more general cellular response, C6 glioma cells were subjected to the inhibitor, too. In these cells also αB-crystallin translocates to the detergent-insoluble fraction, although the dynamics is considerably slower (Fig. 1C). Since H9c2 cells also contain HSP25, it allowed us to investigate whether proteasome inhibition had the same effect on the detergent-solubility of HSP25. As for αB-crystallin, HSP25 was almost exclusively found in the detergent-soluble fraction in normal conditions and translocated in a concentration- and time-dependent manner to the insoluble fraction upon inhibition of the proteasome with MG132 (Fig. 1A,B). The extent of insolubilization after 4 h at 50 μM MG132 is similar to that after heat shock, although the percentage of insolubilized HSP25 (approximately 50%) is not as high as that of αB-crystallin (approximately 70%).

To determine whether actin filament organization is affected by proteasome inhibition, we stained the Western blots with anti-actin antibody (Fig. 1A, lower panel). In unstressed cells, actin is distributed equally between the detergent-soluble and detergent-insoluble fractions. Upon proteasomal inhibition, we found a small change in this ratio. There seemed to be slightly more actin in the detergent-soluble fraction.

αB-crystallin and HSP25 are phosphorylated upon proteasomal inhibition

Proteasome inhibitors can induce HSP70 and HSP25/27 expression [162] and activate stress kinases [153]. We did not observe increased expression of αB-crystallin or HSP25 in H9c2 cells after proteasomal inhibition (data not shown). However, we clearly detected an increase in phosphorylation of αB-crystallin as compared to unstressed cells and a minor increase of HSP25 phosphorylation (Fig 2, cf. lanes C with I and S). Since αB-crystallin can be phosphorylated on serines 19, 45 and 59, we investigated these phosphorylation sites separately after two hours of proteasome inhibition, when αB-crystallin is distributed approximately equally between the soluble and insoluble fractions (see Fig. 1B). In untreated H9c2 cells, no phosphorylated αB-crystallin is found (Fig. 2A, lane C). Upon proteasomal inhibition, pronounced phosphorylation of serine 59 was observed, equally distributed over the insoluble and soluble fractions (lanes I and S). However, phosphorylation of serine 19 or serine 45 could not be detected. In HSP25, which can be phosphorylated at serines 15 and 82, both sites are already phosphorylated in untreated cells (Fig. 2B, lane C). Upon proteasomal inhibition, the distribution of phosphorylated HSP25 between soluble and insoluble fraction is similar to that of the total HSP25, as is true for αB-crystallin. These results indicate that there is no preference for either phosphorylated or unphosphorylated αB-crystallin or HSP25 to translocate to the insoluble fraction, and that the same serines are phosphorylated in the soluble and insoluble fraction.

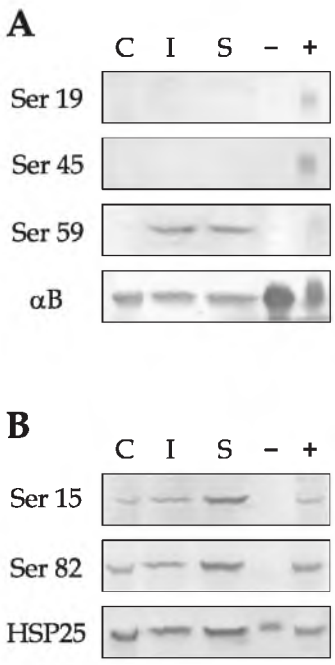

Figure 2. Phosphorylation of αB-crystallin and HSP25 does not affect their insolubilization

H9c2 cells were untreated (C) or exposed to 50 μM MG132 for 2 h and separated into detergent-insoluble (I) and soluble (S) fractions.

(**A**) Fractions subjected to SDS-PAGE and immunoblotting with anti-αB-crystallin antibody (αB) or with antibodies specific for each of the phosphorylated serines (Ser 19, Ser 45 and Ser 59). Recombinant αB-crystallin (-) and α-crystallin isolated from calf lens (+) were used as negative and positive controls, respectively.

(**B**) Fractions subjected to SDS-PAGE and immunoblotting with anti-HSP25 antibody (HSP25) or with antibodies specific for each of the phosphorylated serines (Ser 15 and Ser 82). Recombinant HSP25 (-) and H9c2 cells treated for 1 h with 100 μM sodium arsenite (+) were used as negative and positive controls, respectively.

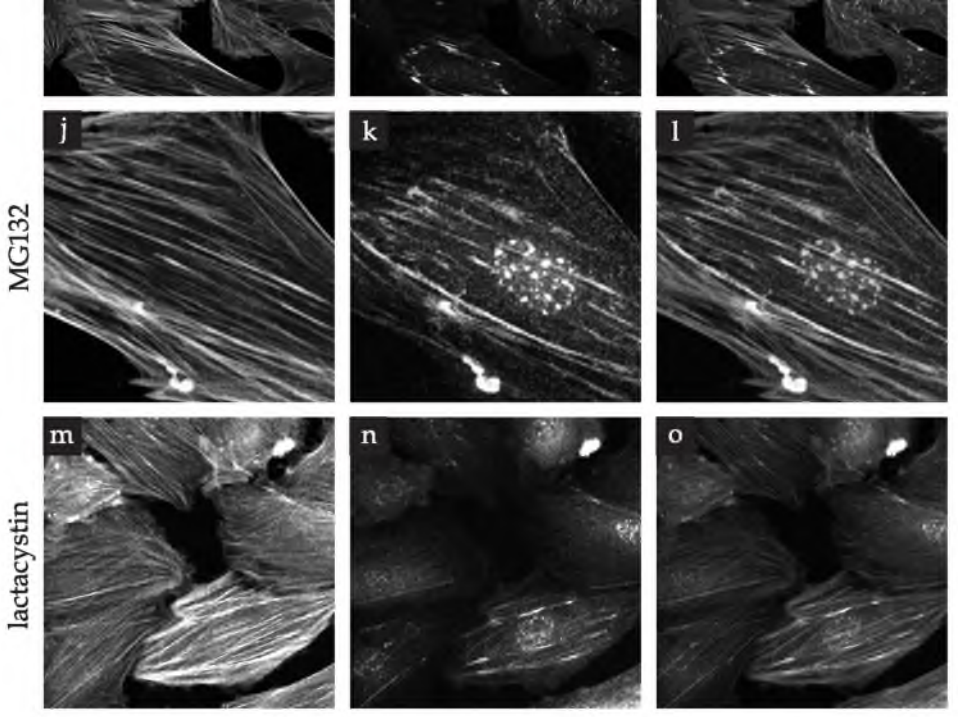
MG132
lactacystin
j
k
l
m
n
o

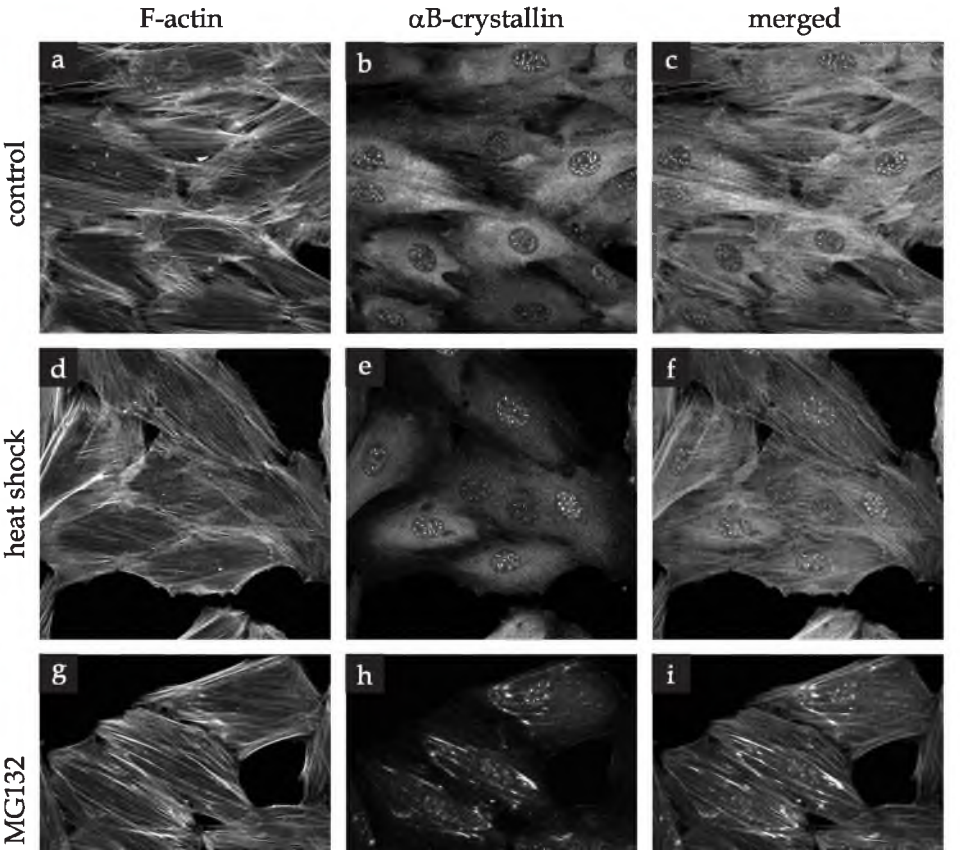
F-actin
αB-crystallin
merged
control
heat shock
MG132
a
b
c
d
e
f
g
h
i

αB-Crystallin translocates to the actin cytoskeleton upon inhibition of proteasomal activity

The translocation of αB-crystallin to the detergent-insoluble fraction was further examined by immunocytochemistry. Under normal conditions αB-crystallin was found throughout the cytoplasm (Fig. 3b). Note that specific regions in the nucleus are also stained, due to crossreactivity of the αB-crystallin antiserum with a nuclear protein [69]. After heat shock, αB-crystallin seemed to have the same distribution as in control cells (Fig. 3e) even though it had become detergent-insoluble (Fig. 1B).

After proteasomal inhibition, the staining of αB-crystallin concentrated into bright fibers and lumps in the central region of the cells, reminiscent of actin fibers (Fig. 3h). Double staining indeed revealed colocalization of αB-crystallin with F-actin as present in stress fibers (Fig. 3i,l). However, stress fibers are not uniformly decorated with αB-crystallin, and not all αB-crystallin colocalizes with F-actin. Removal of the inhibitor after the incubation did not reverse the association with stress fibers (data not shown), in agreement with the lack of resolubilization of αB-crystallin (see above). Also, another proteasome inhibitor, lactacystin, induced a similar pattern of αB-crystallin (Fig. 3n), indicating that the redistribution is indeed a response to the inhibition of proteasomes.

We also tested the effect of proteasome inhibition on αB-crystallin localization in other cell lines. In the skeletal muscle myoblast cell lines L6 and C2 from rat and mouse, respectively, colocalization of αB-crystallin and stress fibers could be observed (data not shown), although less pronounced than in H9c2. Colocalization was not observed in C6 glioma cells (data not shown), possibly because these cells have much fewer stress fibers. In C6 glioma cells αB-crystallin may become triton-insoluble (Fig. 1C) by binding to other cellular structures. Thus colocalization of αB-crystallin and stress fibers upon proteasomal inhibition is not a universal mechanism.

Phosphorylation of αB-crystallin is not crucial for the translocation

To investigate whether phosphorylation of αB-crystallin is indeed, as for insolubilization (cf. Fig. 2A), not important for the colocalization with stress fibers, we constructed GFP fusion proteins and transiently expressed them in H9c2 cells. First we examined the localization of GFP-αB-crystallin (wild type). It had a diffuse cytoplasmic distribution under non-stress conditions (Fig. 4A, panel e), similar to that of endogenous αB-crystallin (cf. Fig. 3b). After incubation with MG132, GFP-αB-crystallin was redistributed and decorated the actin stress fibers (Fig. 4B, panel e) similarly to wild type αB-crystallin (cf. Fig. 3h), indicating that the fused GFP did not interfere with the relocalization process. GFP on its own and with a control fusion protein, GFP-2B(1-40), mainly gave a diffuse distribution throughout the nucleus and cytoplasm, although in the periphery of the cell some fiber-like structure could be seen (Fig. 4A, panels b,k). Neither control protein showed the relocalization upon proteasomal inhibition that was found for αB-crystallin

Figure 3. Immunocytochemical localization of αB-crystallin and F-actin in control and stressed cells
Control H9c2 cells (a-c), cells heat shocked at 44ºC for 20 min (d-f), cells treated with 50 μM MG132 for 4 h (g-l), and cells treated with 25 mM lactacystin for 4 h (m-o) were fixed, permeabilized, and double-stained with anti-αB-crystallin antibody (b,e,h,k,n) and TRITC-conjugated phalloidin (a,d,g,j,m). Merged images are also shown (c,f,i,l,o). Areas of overlap appear yellow. Cells were examined by confocal laser scanning microscopy. Cell shown in (j-l) is an enlargement. A colour version of this image is available on page 115.

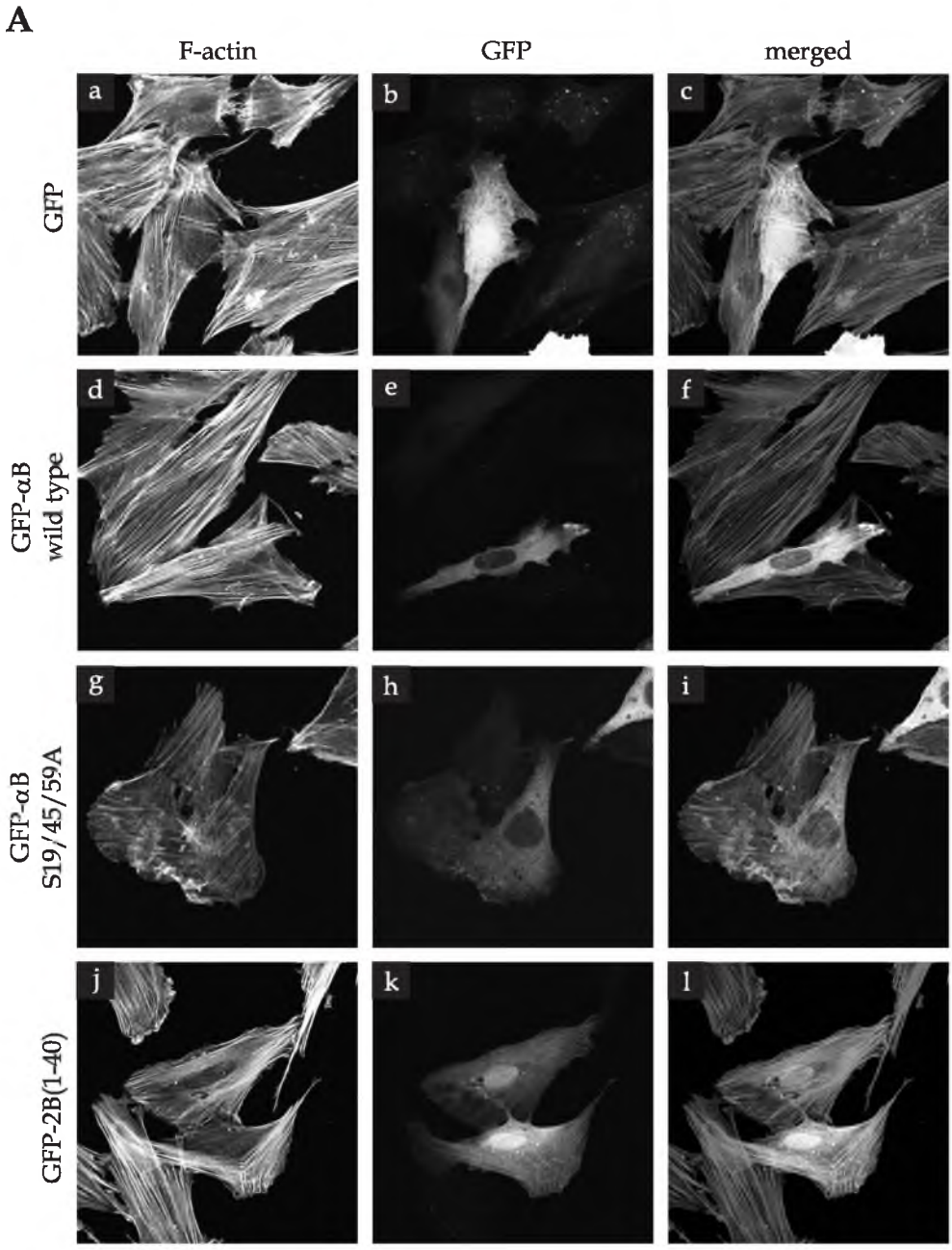

Figure 4. **Phosphorylation of αB-crystallin is not involved in translocation to F-actin upon proteasomal inhibition**
H9c2 cells were transiently transfected with GFP-fusion constructs and examined by confocal laser scanning microscopy directly **(A)** or after a 4 h incubation with 50 μM MG132 **(B)**. Cells were transfected with GFP (a-c), GFP-αB-crystallin wild type (d-f), a non-phosphorylatable GFP-αB-crystallin S19A, S45A, S59A (g-i) or GFP-2B(1-40) (j-l). A colour version of this image is available on pages 116-117. *Continued on next page.*

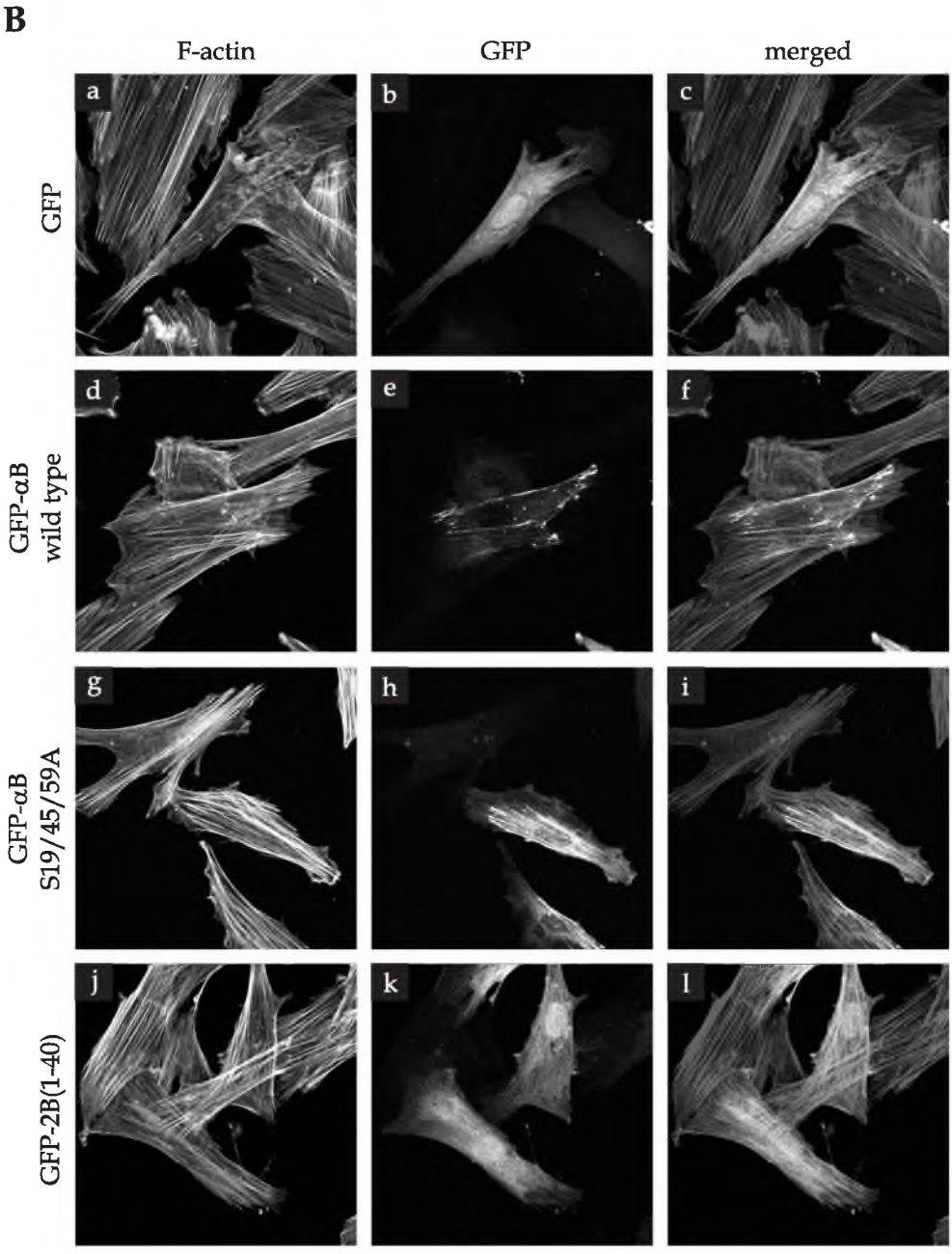

Figure 4. *Continued.*

(Fig. 4B, panels b,k). A non-phosphorylatable GFP-αB-crystallin mutant (S19A, S45A, S59A) [157] was still able to localize along stress fibers after incubation with MG132 (Fig. 4B, panel h). Also two GFP-αB-crystallin mutants in which phosphorylation was mimicked (S19D, S45D, and S59D) were distributed normally in non-stressed cells and localized with stress fibers after proteasomal inhibition (data not shown). Thus phosphorylation of αB-crystallin seems irrelevant for the interaction with stress fibers.

Other sHSPs translocate to stress fibers as well

To determine whether the colocalization with stress fibers upon proteasomal inhibition is specific for αB-crystallin, five other sHSPs, namely HSP25, αA-crystallin, HSP20, HSPB2 and HSPB3, were examined. The endogenous cytoplasmic HSP25 shows a similar redistribution to αB-crystallin (cf. Fig. 3h), from a diffuse localization in unstressed cells (Fig. 5i) to a localization along actin stress fibers after incubation of H9c2 cells with MG132 (Fig. 5j). Since αA-crystallin and HSP20 could not be detected immunologically in H9c2 cells, while specific antisera for HSPB2 and HSPB3 were not available, these sHSPs were transiently expressed in the H9c2 cells as GFP fusion proteins. All these GFP-sHSPs showed a cytoplasmic localization in untreated cells (Fig. 5a,c,e,g) and a redistribution after incubation with MG132 similar to GFP-αB-crystallin (Fig. 5b,d,f,h; cf. Fig. 4B, panel e), suggesting that the behavior of αB-crystallin upon proteasomal inhibition is typical for sHSPs.

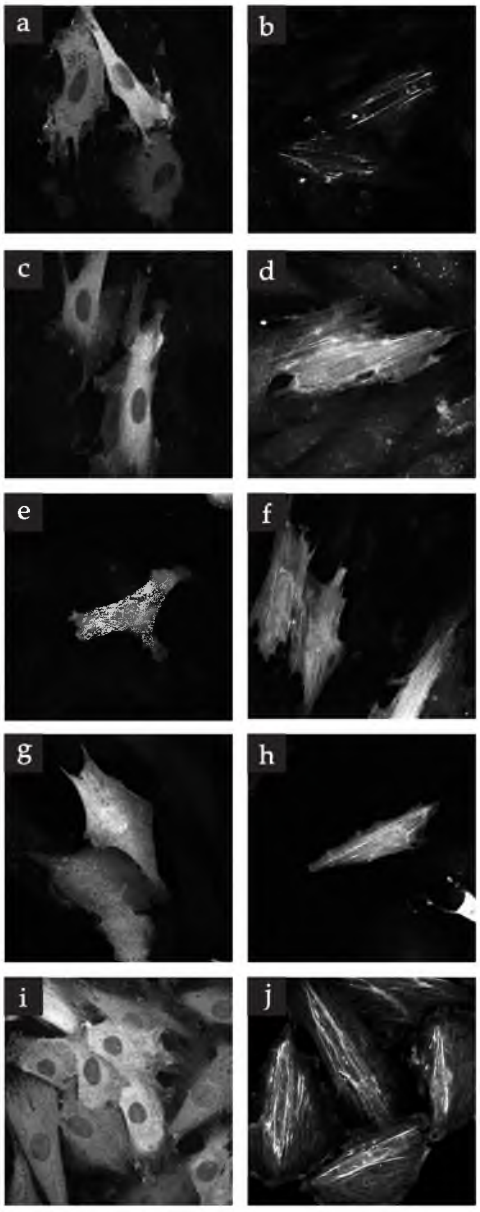

Figure 5. sHSPs colocalize with actin stress fibers in H9c2 cells upon proteasomal inhibition
Localization before (a,c,e,g,i) or after proteasomal inhibition (b,d,f,h,j) of GFP-αA-crystallin (a-b), GFP-HSP20 (c,d), GFP-HSPB2 (e,f), or GFP-HSPB3 (g,h) transiently transfected in H9c2 cells and endogenous HSP25 in untransfected H9c2 cells (i,j). Cells were fixed and incubated with a polyclonal antiserum against HSP25 and a secondary antibody fused to FITC (i,j) or examined directly (a-h) by confocal laser scanning microscopy. A colour version of this image is available on page 118.

DISCUSSION

Upon proteasomal inhibition, αB-crystallin and the other investigated sHSPs (αA-crystallin, HSP25, HSP20, HSPB2 and HSPB3) become actin-associated, with a fiber-like appearance in combination with lumps. Since sHSPs can form complexes containing more than one type of subunit [18,163,164] it can not be excluded that some sHSPs indirectly associate with actin stress fibers via binding to other sHSPs. Redistribution of sHSPs can also be induced by other forms of stress, such as heat shock (Fig. 3e, [19,161]) hypoxia-reoxygenation [165-167], and serum starvation [77], but these stresses do not induce stress fiber-association. Furthermore, the insolubilization of αB-crystallin upon proteasomal inhibition is irreversible, in contrast to insolubilization of sHSPs after heat shock [69], oxidative stress [168] and ischemia [167]. Importantly, the insolubilization of αB-crystallin and HSP25 upon proteasome inhibition seems to be phosphorylation independent. Also after ischemic pre-conditioning, phosphorylation of αB-crystallin seems not be important for the insolubilization [166]. However, in some cases, such as insolubilization of αB-crystallin and HSP25 upon hypoxia-reoxygenation [165,167] and formation of pathological inclusions [169], phosphorylation might be important. It thus appears that the interaction between sHSPs and stress fibers upon proteasome inhibition is fundamentally different from the relocalizations induced by other types of stress.

Although insolubilization of αB-crystallin upon proteasomal inhibition takes place in all four cell lines tested, the colocalization with F-actin is not the same. The skeletal muscle myoblast cell lines L6 and C2 do show colocalization, but not to the same extent as in H9c2 cells. In C6 glioma cells no colocalization with actin stress fibers could be detected. This may be due to the fact that these cells contain fewer of such fibers, or that a specific type of actin assembly is needed for efficient binding. It also is possible that αB-crystallin interacts with intermediate filaments in these cells, since such interaction is enhanced upon stress, too [77,123]. We were, however, not able to detect colocalization with intermediate filaments.

The main question of course is why αB-crystallin and other sHSPs do associate with actin stress fibers upon proteasomal inhibition. One possibility is that actin itself, by partial degradation or unfolding, becomes a target for sHSPs. The role for sHSPs could then be to protect the integrity of the actin stress fibers. Sakamoto *et al.* [165] have also suggested that stabilization of actin filaments by HSP27 contributes to protection against heat shock. We found no conspicuous changes of actin stress fibers upon proteasomal inhibition (Fig. 3, compare panels a and g), although actin become slightly more soluble upon proteasomal inhibition (Fig. 1A, lower panel). The soluble fraction may contain both G- and F-actin [170]. sHSPs could interfere with this solubilization by binding to the insoluble actin. However, since only part of the actin filament seems to become decorated with sHSPs, this 'protective' effect might be limited.

Alternatively, unfolding proteins of a kind that would normally be degraded by the proteasome, may accumulate during proteasome inhibition, and become substrates for sHSPs. It may be beneficial for the functioning of the cell to sequester the sHSP-substrate complexes from the cytoplasm by binding them to the actin cytoskeleton. This would resemble the formation of aggresomes, suggested to be a cellular response to the presence of aggregated, misfolded proteins, and

possibly serving to clear the cytoplasm from harmful aggregates [152]. However, in the case of aggresomes, the aggregates are transported along microtubules to a single site in the cell, whereas we find αB-crystallin present in several lumps along actin stress fibers. Of course, still other explanations can be envisaged, and further research is needed to try to understand the functional relevance of the interaction of sHSPs with the actin stress fibers.

Acknowledgement

We thank Dr. Paul Muchowski for the mutant αB-crystallin clones.

3

Characterization of two novel human small heat shock proteins: protein kinase-related HSPB8 and testis-specific HSPB9

Guido Kappé [*,1]
Pauline Verschuure [*,1]
Ria L.A. Philipsen [2]
André A. Staalduinen [2]
Paul van de Boogaart [2]
Wilbert C. Boelens [1]
Wilfried W. de Jong [1]

[*] *Both authors contributed equally*
[1] *Department of Biochemistry, Nijmegen Center for Molecular Life Sciences, University of Nijmegen, Nijmegen, The Netherlands*
[2] *N.V. Organon, Oss, The Netherlands*

Biochim. Biophys. Acta (2001) **1520**: 1-6

Using search profiles based on the conserved α-crystallin domain that is characteristic for small heat shock proteins (sHSPs), we traced two new human sHSPs. One of these, being the eighth known human sHSP and thus named HSPB8, was recently described as a serine-threonine protein kinase (H11), but not identified as an sHSP [25]. Northern blotting showed that HSPB8/H11 is predominantly transcribed in skeletal muscle and heart, like most other sHSPs. The other, named HSPB9, is specifically expressed in testis, notably in the spermatogenic cells from late pachytene spermotocyte stage till elongate spermatid stage. While mammalian sHSPs are generally highly conserved, mouse HSPB9 shows 38% sequence difference with human HSPB9, which may confirm its sex-related role.

INTRODUCTION

The family of small heat shock proteins (sHSPs) has multiple representatives in most organisms [6,171]. They range in monomeric size from 12 to 42 kDa, and are characterized by a conserved C-terminal 'α-crystallin domain' of 80-100 residues. This domain has an IgG-like fold [7,172], and is preceded by an N-terminal domain which is more variable in length and sequence. There often is a short and freely flexing C-terminal extension [173]. sHSPs generally form large and dynamic homo- or heteromeric complexes of up to 700 kDa in certain cases, which may readily dissociate and exchange subunits [174,175]. Dimeric building blocks of subunits are arranged in a globular structure around a central region of lower density [7,176]. The dynamic and open structure of sHSPs, combined with the presence of accessible hydrophobic surfaces and polar C-terminal extensions, is essential for their chaperone-like properties [177]. This is the *in vitro* ability to bind unfolding proteins and keep them in solution. Bound proteins are kept in a folding-competent state and may be refolded in conjunction with HSP70 [4,178,179]. Most sHSPs are constitutively expressed at considerable levels, and many can be upregulated upon heat and other forms of stress, thereby enhancing cellular survival.

In human and other mammals, seven different sHSPs have been described until now. The long known αA- and αB-crystallins are both abundant proteins in the eye lens, while αB-crystallin additionally occurs at considerable levels in heart, striated muscle and kidney [180]. Also the five other sHSPs (HSP27 [181], HSP20 [18], HSPB2 [50], HSPB3[21] and cvHSP [22]) are all expressed to different extents in heart and striated muscle, and most of them at lower levels in various other tissues [30]. HSP27 and αB-crystallin are expressed at increased levels in various tumors and neurodegenerative diseases [85], and are among others implicated in regulating apoptosis [146] and maintaining cytoskeletal integrity [182].

The various sHSPs in an organism are likely to have related and complementary functions. To better understand the width of functioning of the human sHSP family, it is important to know the actual number and properties of the gene products belonging to this family. Such a goal comes within reach, assuming that virtually all human gene transcripts will be represented in the EST

databases by now. We here report the tracing of two new human sHSPs from these databases, their expression pattern in different tissues, and a brief comparison with the other human sHSPs.

MATERIALS AND METHODS

sHSP search in EST databases

A PILEUP alignment of the conserved α-crystallin domains of the seven known human sHSPs (corresponding with positions 95 - 188 in Fig. 1, see also EMBL Nucleotide sequence database http://www.ebi.ac.uk, alignment ALIGN_000032) was used to make a search profile with PROFILEMAKE v4.50. To have a broader search potential, another profile was obtained from an alignment of the α-crystallin domains of 40 very diverse prokaryotic and eukaryotic sHSPs [6], which gave a similar result as the human α-crystallin profile. The profiles were used as queries to search for ESTs of unknown human sHSPs in the complete public EST database, using Compugen's implementation of the PROFILESEARCH algorithm. The annotations of all hits were screened for keywords like "crystallin", "HSPB2", "MKBP", "HSPB3", "protein 27", "shock 27", and "p20" that would identify the EST as a known sHSP. Human ESTs that were not identified as sHSPs in this way were checked for homology to known sHSPs using Compugen's implementation of a translated Smith and Waterman search on the SWISSPROT database. Only those ESTs that showed homology to known sHSPs were checked to assess whether they represented a known or unknown sHSP, using a BLAST search on the EMBL database.

Northern blot analyses

The tissue distribution of HSPB8, HSPB9 and HSP27 mRNAs were analyzed using Human Multiple-tissue Northern blots (CLONTECH). cDNA fragments corresponding to the complete open reading frame of each sHSP were radiolabeled using the Random Primers DNA Labeling System (GibcoBRL) and used as probes. The blots were first probed with HSPB9 cDNA and subsequently with HSPB8 cDNA. Thereafter the blots were stripped and reprobed with HSP27 cDNA. HSPB8 and HSPB9 cDNAs

Figure 1. Alignment of the novel human HSPB8 and HSPB9 with the other seven known human sHSPs and *Methanococcus jannaschii* HSP16.5

The alignment was obtained using PILEUP, and improved by manual editing. Identical or highly conserved residues in at least 8 of the 10 sequences are in black; in 5-7 of the sequences in gray. Below the human sHSPs is the predicted secondary structure as obtained from their multiple alignment, using the PHD program [251] at the PredictProtein server of the University of Columbia (maple.bioc.columbia.edu/pp/). The bottom line presents the actual secondary structure of MjHSP16.5 as assigned from the crystal structure [7]. Arrows and cylinders represent β-strands and α-helices, respectively, of which the gray arrow indicates a weakly predicted β-strand. Accession numbers are: AJ302068 (HSPB9), Q9UKS3 (HSPB8/H11), Q9UBY9 (HSPB7/cvHSP), O14558 (HSPB6/HSP20), P02511 (HSPB5/αB), P02489 (HSPB4/αA), Q12988 (HSPB3), Q16082 (HSPB2/MKBP), S39199 (HSPB1/HSP27). The presented HSPB8 sequence has 53W, as in various ESTs, rather than 53C as documented for H11 [25]. The human sHSPs are here indicated as "HSPB" in accordance with the rules of the Human Gene Nomenclature Committee (http://www.gene.ucl.ac.uk/nomenclature/). Because the new sHSPs are the eighth and ninth members of this family found in man, we name them HSPB8 and HSPB9. Considering HSP27 as HSPB1, and HSPB2 [50], HSPB3 [21] and HSPB7 (acc. nr.: NM_014424) already being in use, this would leave HSPB4 through HSPB6 for αA-crystallin, αB-crystallin and HSP20, respectively. The indications HSPB4 and HSPB5 for αA- and αB-crystallin would avoid any confusion about their being genuine sHSPs. However, considering the priority of the name α-crystallin, given in 1894, and its established usage, it seems undesirable to actually replace their names, leaving HSPB4 and HSPB5 as possible formal indications. In the case of human HSP27 (also named HSP28) and rodent HSP25, the use of HSPB1 would make it immediately clear that we are dealing with the corresponding, orthologous protein in different species.

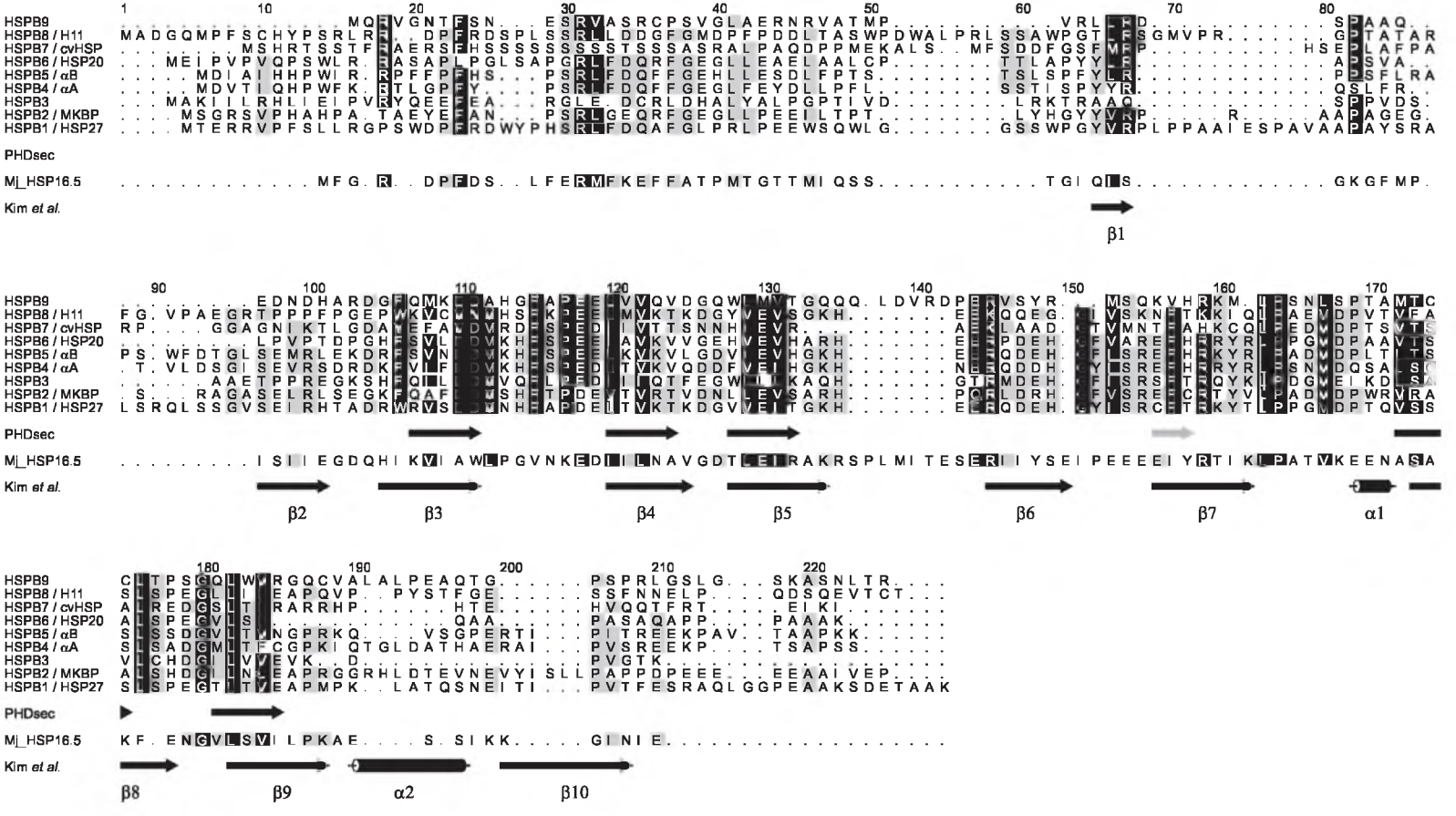
HSPB9
HSPB8 / H11
HSPB7 / cvHSP
HSPB6 / HSP20
HSPB5 / αB
HSPB4 / αA
HSPB3
HSPB2 / MKBP
HSPB1 / HSP27
PHDsec
MJ_HSP16.5
Kim et al.
β1
β2
β3
β4
β5
β6
β7
α1
β8
β9
α2
β10

were amplified by PCR from a human placental cDNA library and from human genomic DNA, respectively.

In situ hybridization

Mouse testis tissue was fixed in 4% buffered formalin for 24 h at room temperature. Paraffin sections (5 µm) were dewaxed, rehydrated, treated with proteinase K (1 µg/ml) and acetylated for 5 min with 0.25% acetic anhydride in 0.1 M triethanolamine buffer. Sections were treated for 2 h at hybridization temperature with prehybridization mix, containing 52% formamide, 21 mM Tris, 1 mM EDTA, 0.33 M NaCl, 10% dextran sulphate, 1x Denhardt's solution, 100 µg/ml salmon sperm DNA, 100 µg/ml tRNA and 250 µg/ml yeast total RNA, and subsequently incubated overnight (16 h) at 42°C or 50°C with hybridization mix, consisting of prehybridization mix with the following additions: 0.1 mM DTT, 0.1% sodium thiosulphate, 0.1% SDS and 200 ng/ml digoxigenin-labeled probe. Slides were then washed in 2x SSC (300 mM NaCl, 30 mM sodium citrate pH 7.0), followed by washes in 1x SSC and 0.1x SSC at hybridization temperature. Sections were digested with 20 µg/ml ribonuclease A in 0.6 M NaCl, 20 mM Tris, 10 mM EDTA for 1 h at 37°C, washed with PBS and buffer 1 (100 mM maleic acid, 150 mM NaCl), and incubated for 30 min with blocking solution (1 g/ml BSA (Sigma) in buffer 1) and for 1 h at room temperature with anti-digoxigenin conjugated to alkaline phosphatase (Roche), diluted 1:500 in blocking solution. After two washes in buffer 1, the slides were stained with Nitro blue tetrazolium/5-bromo-4-chloro-3-indolyl phosphate (Sigma) and counterstained with Mayer's hematoxylin (Sigma) 1:5 for 3 sec. Slides were mounted in Kaiser's glycerol gelatin. Videoprints were made (VY-170, Hitachi) using a 3-CCD camera (HV-C10A, Hitachi) on a Nikon Optiphot microscope.

Table 1. Characteristics of the human sHSPs

Protein name	p*I* [a]	Mass (kDa) [a]	Length (aa) [a]	% sequence identity between orthologues [b]	% sequence identity with [c]		Intron positions and phases [d]	Chromosomal location [e]
					HSPB8	HSPB9		
HSPB9	9.0	17.5	159	62.2	23.2	100	intronless	17q21
HSPB8/H11	4.7	21.5	196	94.4	100	23.2	133 (1), 162 (2)	12
HSPB7/cvHSP	6.5	18.6	170	94.7	23.6	25.2	87 (1)	1p36.23-p34.3
HSPB6/HSP20	6.4	16.8	157	91.1	37.9	32.3	98/99, 146/147	19q13.1
HSPB5/αB	7.4	20.2	175	97.7	35.5	26.8	98/99, 146/147	11q22.3-q23.1
HSPB4/αA	6.2	19.9	173	94.8	31.5	28.7	98/99, 146/147	21q22.3
HSPB3	5.9	17.0	150	88.0	29.9	20.9	intronless	5q11.2
HSPB2/MKBP	4.8	20.2	182	97.3	39.4	20.9	40 (1)	11q22-q23
HSPB1/HSP27	6.4	22.8	205	84.9	29.9	28.1	133 (1), 162 (2)	7q11.2

[a] Calculated with PEPTIDESORT of the GCG PACKAGE. [b] Amino acid sequence identity as determined between human and mouse (or rat in case of HSPB2 and HSPB6) orthologous sHSPs. [c] Amino acid sequence identities as determined by pairwise comparisons of HSPB8 and HSPB9 with the other human sHSPs. [d] Intron positions refer to the position numbers in Figure 1. Positions separated by a slash indicate phase 0 introns (between codons); phase 1 and 2 introns interrupt codons after the first and second codon position, indicated as (1) and (2), respectively. Note that the HSPB8 gene might contain more than two introns. [e] Chromosomal localizations obtained from the OMIM Database (HSPB1 – HSPB5), AC002398 (HSPB6), AF155908 (HSPB7), NM-014365 (HSPB8) and AC003104 (HSPB9).

Results and Discussion

Database search

Searching the translated EST database with two sHSPs profiles yielded 90 human ESTs that matched the search profiles (*E* value below 1), but were not annotated as being known human sHSPs. Using these 90 ESTs for homology searches in the SWISSPROT database showed 37 of them to have obvious homology with known sHSPs. A BLAST search on the EMBL database identified 33 of these as known human sHSPs, leaving two unknown proteins, represented by two ESTs each. These were considered as novel sHSPs because of their convincing sequence similarity with known sHSPs (see below).

Protein kinase-related HSPB8

For one of the retrieved new sHSPs, the mRNA sequence turned out to be present in the database (accession No. AF133207). It was recently reported as coding for a protein, designated as H11, which is similar to the protein kinase (PK) domain of the multifunctional herpes simplex virus type 2 ribonucleotide reductase, and has Ser-Thr-specific PK activity [25]. H11 expression appears to be required for the growth of human melanoma cells. Remarkably, the conspicuous sequence relationship with the sHSP family was not mentioned [25], although more recent annotations do recognize the homology with sHSPs (AF191017, AF250138). Considering that this protein H11 clearly is an sHSP, we propose to use the formal name HSPB8 for it (see legend of Fig. 1). A draft sequence of a genomic fragment (AC009819) located on chromosome 12 contains the gene for HSPB8. Aligning the mRNA with its gene reveals the presence of at least two introns (see Table 1).

The cDNA for HSPB8 was amplified from a cDNA library of human placenta. Its sequence was determined and differed at a single position from the published H11 mRNA sequence ([25]; see legend of Fig. 1). The deduced amino acid sequence is aligned with the other human sHSPs in Fig. 1. This 196-residue HSPB8 has a remarkably low p*I*, 4.7. The cDNA was used as a probe for Northern blotting on mRNA from various human tissues (Fig. 2A, upper panels). The transcript is approximately 2.2 kb in length. The HSPB8 gene is most abundantly transcribed in skeletal muscle, heart and placenta, and to lesser extent in many other organs. No expression was found in blood.

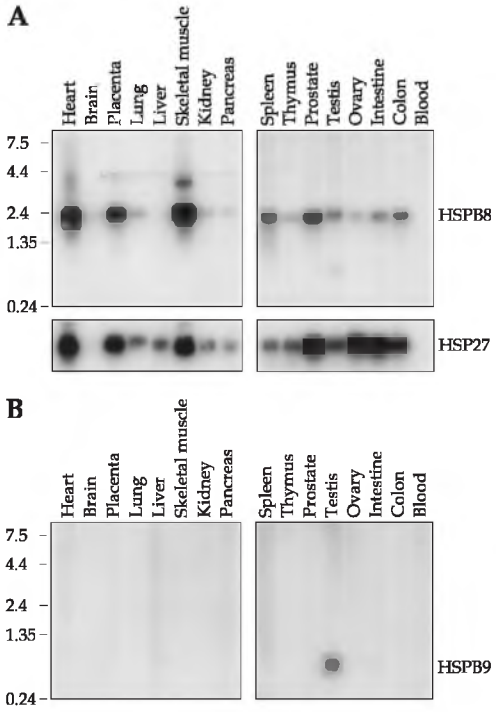

Figure 2. Northern blot analysis of HSPB8, HSPB9 and HSP27 expression

Human multiple tissue Northern blots (CLONTECH) were probed successively with HSPB8 cDNA (**A**, upper panels) and HSPB9 cDNA **(B)**, and HSP27 cDNA (**A**, lower panels). Each lane contains approximately 2 µg of purified poly(A)+ RNA isolated from the indicated tissues. Marker sizes are indicated in kb. Note that blots A were exposed overnight whereas blots B were exposed for 5 days.

As compared with the expression patterns of αB-crystallin, HSP20, HSP27, HSPB2 and HSPB3, as published by Sugiyama *et al.* [30], who used corresponding CLONTECH blots, the expression pattern for HSPB8 is most similar to that of HSP27 (Fig. 2A, lower panels).

Testis-specific HSPB9

The second unknown human sHSP, which we propose to name HSPB9, was also found as part of a genomic DNA fragment (AC003104) originating from chromosome 17. An alignment of this genomic fragment with the ESTs for HSPB9 revealed a continuous open reading frame, encoding a protein of 159 residues. Since the gene is intronless, we could amplify the cDNA for HSPB9 directly from human genomic DNA. The sequence was determined, and the deduced amino acid sequence aligned in Fig. 1. In contrast to HSPB8, this protein is unusually basic, with a p*I* of 9.0.

Northern blotting showed that among the represented human tissues, HSPB9 was exclusively transcribed in testis (Fig. 2B). This is in agreement with the EST database results, which additionally indicate its occurrence in lung and germ cell tumors. The transcript is exceptionally small, just approximately 0.8 kb, leaving only approximately 300 nucleotides for the polyA-tail and the 5' and 3' UTRs.

Mouse being a more convenient experimental model than human, we also determined the sequence of the mouse gene for HSPB9 (accession nr. AJ302069). The deduced amino acid sequence turned out to be remarkably different from the human HSPB9 (Table 1). The possibility that the mouse gene is not the orthologue of human HSPB9 can be dismissed, considering the shared presence of unique sequence characteristics, not found in other sHSPs (e.g., the sequence ASRCPSVxLAERNxVATMP-VRL at positions 33-65 in Fig. 1).

In situ hybridization was performed on testis sections of adult and immature mice. In all the seminiferous tubules of adult mice

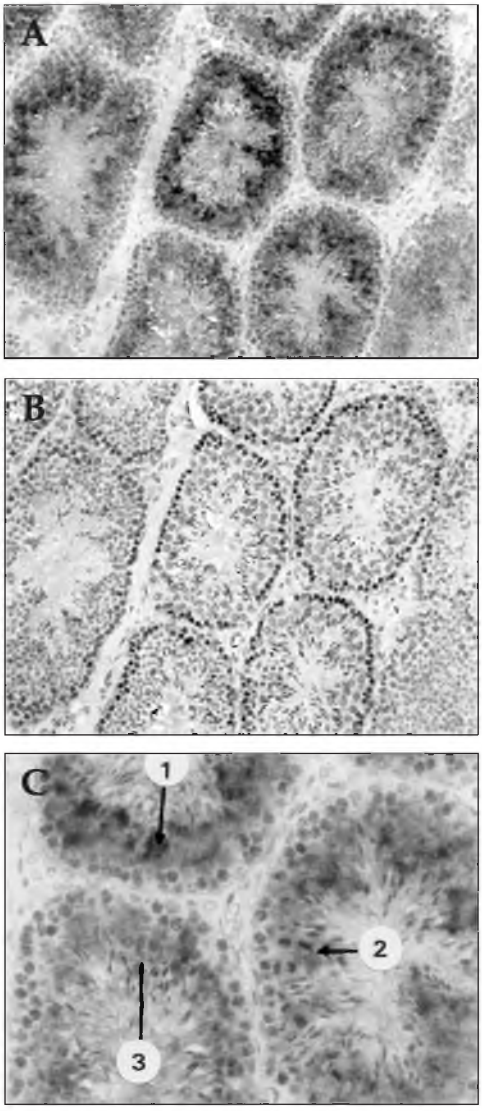

Figure 3. *In situ* hybridization of testis of adult mice with antisense HSPB9 probe (A,C) and sense HSPB9 probe (B)

A dark brown staining was only obtained with the antisense probe, representing HSPB9 mRNA signal. All stained cells are localized in the seminiferous tubules. The stained cells indicated in the higher magnification (C) are diplotene (1) and stage XII (2) spermatocytes, and round spermatids (3). A colour version of this image is available on page 118.

the HSPB9 probe hybridized to specific stages of germ cells (Fig. 3A,C). Spermatogenesis in the seminiferous tubules can be subdivided in three different phases: the proliferative phase in which spermatogonia divide, the meiotic phase in which genetic material in spermatocytes is recombined and segregated, and the spermiogenic phase in which round spermatids transform through elongate spermatids into spermatozoa. On the basis of the staging of spermatogenesis described by Russell [183] the HSPB9 positive germ cells were identified. A high expression of HSPB9 was found in diplotene and stage XII (meiosis I and II) spermatocytes, round spermatids and step 9-12 elongate spermatids, and a somewhat lower expression in late pachytene spermatocytes and step 13-15 elongate spermatids. No signal was detected in Sertoli cells, spermatogonia, leptotene, zygotene, early pachytene spermatocytes and spermatozoa. Also in the testis of 16-days old mice the first HSPB9 expression can be detected in pachytene spermatocytes, but the number of stained cells in the testis increased with age: in 24-days old mice all tubuli contained stained cells (data not shown). The control sections of adult and immature testis incubated with the sense probe gave no signal (Fig. 3B). Interestingly, also HSP25 - the mouse orthologue of HSP27 - has been reported to be expressed during spermatogenesis, but at somewhat earlier stages: leptotene, zygotene and early pachytene [184].

Comparisons with other sHSPs

The nine human sHSPs, indicated as HSPB1-9, are aligned in Fig. 1; the reasons for using the names HSPB1-9 are given in the legend. This alignment reveals that the sequences between positions 106 and 184 are best conserved, corresponding with the location of the α-crystallin domain. In that same region the homology with the archaeal MjHSP16.5 is also clearly detectable. The similarities in the N-terminal domain are limited to some scattered short motifs (PF, SRL, LR), which are even absent in HSPB3 and mostly so in HSPB7/cvHSP. In the C-terminal extensions no overall similarities can be recognized. The secondary structure predictions suggest that at least six of the ten β-strands as observed in the α-crystallin domain of MjHSP16.5 [7] may also be present in the human sHSPs. The contact site for model substrates, which has been located between β3 and β4 [185], is also conserved. Three β strands were not predicted, of which two, β1 and β6, are probably absent in human sHSPs based on systematic analyses of spin-labeled αA-crystallin mutants [172].

The diversity of the human sHSPs is also evident from Table 1. It reveals that HSPB8 and HSPB9 indeed have the most extreme p*I* values within the family. The amino acid sequence identities of HSPB8 and HSPB9 with the other human sHSPs reflect that both, but especially HSPB9, have highly diverged from all others. Also the dispersal over different chromosomes (apart from αB-crystallin and HSPB2, which are oriented head-to-head on chromosome 11 [50]), and the variety in intron positions witness for the seniority of the gene duplications that have resulted in the present mammalian sHSP family. The percent sequence identity between orthologous human and rat or mouse sequences shows that all sHSPs are highly conserved in mammals (between 88% and 98% identity), with the exception of HSPB9 (62% identity). It has been observed that sex-related genes, i.e. genes that are involved in fertilization, spermatogenesis or sex determination, have a high rate of nonsynonymous substitutions [186,187]. This might be due to periods of positive

selection acting on such genes during speciation, thus creating reproductive barriers between speciating populations. The increased rate of change of HSPB9 thus supports the idea that it has some important sex-related role.

With nine expressed and quite divergent sHSPs, mammals now compare well with other organisms in which multiple sHSPs have been described. This reaches numbers of at least 12 in *Bradyrhizobium japonicum* [188], 14 in *Cenorhabditis elegans* [189], 13 in *Xenopus laevis* [190] and over 20 in higher plants [191]. In contrast, *Saccharomyces cerevisiae* has only two sHSPs, and quite a few bacteria can even do without (G.K. unpublished data), demonstrating that the presence of so many different sHSPs is not a universal requirement.

NOTE ADDED IN PROOF

HSPB8 has also been identified by Benndorf *et al.* who designated it HSP22 [24].

ACKNOWLEDGEMENTS

We thank Vivian Keijsers for analysing the HSP27 expression on Northern blot and Jack Leunissen for advice about the database searches.

Expression and stress response of the mammalian small heat shock protein HSPB8

Pauline Verschuure [1]
Lisa U. Wunderink [1]
Dominic P.H.M. Heuts [1]
Wilfried W. de Jong [1]
Wilbert C. Boelens [1]

[1] *Department of Biochemistry, Nijmegen Center for Molecular Life Sciences, University of Nijmegen, Nijmegen, The Netherlands*

Manuscript in preparation

The human genome encodes ten quite diverse members of the small heat shock protein (sHSP) family. Seven of them are highly expressed in various types of muscle, but their functional diversity and complementarity remain poorly understood. Amongst these, one of the most intriguing is HSPB8 (also named H11 kinase, E2IG1 and HSP22), which reportedly has kinase activity, is estrogen inducible, and mediates cell growth. Nevertheless, the basic features of HSPB8 as a heat shock protein, such as expression patterns, stress behaviour and complex formation, have not yet been characterized. We therefore compared HSPB8 with other mammalian sHSPs, notably HSP27/B1, HSP20/B4 and αB-crystallin/HSPB6. We show that, in the muscle myoblast cell line C2, HSPB8 is not upregulated during differentiation, only slightly after heat shock, and markedly after arsenite treatment. Interestingly, even though HSPB8 is regulated by estrogen at the mRNA level in the human breast cancer cell line MCF-7, there is no effect at the protein level. Stress induces phosphorylation of HSPB8 in the mouse C2 cells, but not in human HeLa cells. In the C2 cells HSPB8 becomes partially detergent-insoluble after heat shock or proteasomal inhibition, but not after arsenite or H_2O_2 stress. Resolubilization of HSPB8 is independent of protein translation. Glycerol density gradient centrifugation of C2 and HeLa cell extracts shows that HSPB8 forms complexes, which are distinct from αB-crystallin complexes and cofractionate with the smaller complexes of HSP27. It can be concluded that HSPB8 is a stress responsive protein with a unique combination of features.

INTRODUCTION

The human small heat shock protein (sHSP) family, characterized by a conserved 'α-crystallin' domain of about 85 residues, comprises ten members [13] of which HSP27 and αB-crystallin are the best known representatives (for recent sHSP reviews, see [12,192,193]). Most sHSPs have *in vitro* chaperone-like activity and can form homo- and hetero-oligomeric complexes. Their expression is often induced in response to diverse stimuli like heat shock, oxidative stress and heavy metals. Typically, they can confer thermotolerance to cells when overexpressed, and are believed to protect the cytoskeleton by associating with it. HSP27 and αB-crystallin are upregulated in degenerative diseases and tumors, and have been shown to inhibit apoptosis. Despite their ubiquity and apparent physiological importance, little is known about the precise functioning and possible complementarity of the various sHSPs in the cell.

Until 1997 four human sHSPs had been described: the eye lens proteins αA-crystallin/HSPB5[1] and αB-crystallin/HSPB6, of which the latter is also abundant in heart and other muscle, and HSP27/HSPB1 (HSP25 in rodents)[2] and HSP20/HSPB4, which have highest expression in muscle. Since then six more sHSPs have

[1] The ten human sHSPs have been given the formal names HSPB1-10 in accordance with the guidelines of the HUGO Gene Nomenclature Committee.

[2] For convenience we will use HSP27 in this paper to indicate both human HSP27 and mouse HSP25.

been identified: MKBP/HSPB2 [50], HSPB3 [21], cvHSP/HSPB7 [22], HSPB8 [25], HSPB9 [27] and ODF1/HSPB10 [13], of which the first four again typically occur in muscle, while the last two are testis-specific. Although most of these novel sHSPs are abundantly expressed, they have not yet received much attention in the literature. However, initial studies have shown some interesting and unique characteristics for some of them. HSPB2 was identified as an interactor and activator of Myotonic Dystrophy Protein Kinase [19], cvHSP may be associated with obesity and related metabolic disorders [22], and HSPB8 has been reported to have kinase activity [25]. HSPB9 apparently is a cancer/testis-associated gene (Chapter 6), while HSPB10 has been extensively studied as sperm tail ODF1 [194,195], but was not earlier recognized as a sHSP.

HSPB8 appeared in the literature under several names. As H11 kinase it was found to have some similarity to the protein kinase domain of the large subunit of Herpes Simplex Virus type 2 ribonucleotide reductase, but was not recognized as a sHSP [25]. H11 kinase can be phosphorylated and its expression in melanoma cells and keratinocytes is associated with cell growth. Others have shown the overexpression of H11 kinase in ischemic heart and found it to be a mediator of cardiac cell growth and hypertrophy [34]. The same gene product, named E2IG1 and now recognized to be sHSP-related, was identified as a transcript that is induced upon estrogen treatment of estrogen-sensitive breast cancer cell lines [23]. As HSP22 it was found as a yeast two-hybrid interactor of a mimick of phosphorylated HSP27 [24]. Recombinant HSP22 itself could be phosphorylated *in vitro* by protein kinase C, casein kinase-2 and p44 mitogen-activated protein kinase, but not by mitogen-activated protein kinase-activated protein kinase 2 (MAPKAP-2).

The formal name HSPB8 was proposed when the same protein was found as the eighth human sHSP by searching databases with the conserved α-crystallin domain [27]. Northern blot analysis showed highest expression of HSPB8 in heart and skeletal muscle, a pattern similar to HSP27. Because important features of HSPB8 as a novel sHSP have not yet been described, we analyzed its expression, stress behaviour, complex formation and phosphorylation in different cell lines, and compared it to other sHSPs. The results show that HSPB8 behaves in these respects very similar to - but not exactly the same as - HSP27 and HSP20, despite the large sequence differences.

MATERIALS AND METHODS

Cell culture and stress treatments

The mouse myoblast cell line C2 was cultured in Dulbecco's Modified Eagle's Medium (DMEM; GibcoBRL) supplemented with 20% heat-inactivated fetal calf serum, 100 U/ml penicillin and 200 µg/ml streptomycin. The human HeLa cell line was cultured in the same medium supplemented with 10% heat-inactivated fetal calf serum. The human breast cancer cell line MCF-7 was cultured in DMEM without phenol red, supplemented with 10% heat-inactivated fetal calf serum. The cells were incubated at 37°C in a humidified atmosphere containing 5% CO_2. C2 cells were differentiated from myoblasts into myotubes by growing the cells for 5-7 days in medium supplemented with 10% serum and the formation of myotubes was visually checked. Heat shock was given by complete immersion of the cell culture flasks in a waterbath at the desired temperature and recovery took place at normal culture conditions. Arsenite

treatment was performed by adding sodium arsenite (Baker) to the medium with a final concentration of 100 µM. Estradiol treatment was performed by seeding MCF-7 cells in flasks and incubation for 48 h in DMEM without phenol red, supplemented with 10% charcoal/dextran-treated fetal bovine serum (Hyclone) before adding 17β-estradiol (Sigma) to a final concentration of 10^{-8} M. Proteasomes were inhibited by incubation with 50 µM MG132 (Calbiochem) for 4 h. H_2O_2 treatment was performed by addition of freshly diluted H_2O_2 to a final concentration of 250 µM.

Detergent solubility

Detergent-soluble and -insoluble fractions were obtained as described before [196]. In brief, cells were lysed in buffer (10 mM Tris pH 7.5, 10 mM NaCl, 5 mM MgCl2, 1 mM phenylmethanesulfonyl fluoride and 0.5% Triton X-100) and centrifuged (5 min at 300 x g at 4°C). The supernatant was used as detergent-soluble fraction and the pellet as detergent-insoluble fraction.

Electrophoresis and Western blot analysis

Sodium dodecyl sulfate polyacrylamide gel electrophoresis (SDS-PAGE) was performed using standard procedures. Isoelectric focusing (IEF) was performed as described before [197] using the Protean II system (Biorad). In brief, cell extract was made in 8 M urea, 2% 3-[(3-cholamido-propyl) dimethylammonio] 1-propane-sulfonate (CHAPS) and mixed with an equal volume of sample buffer (2.4% ampholine mixture, 8 M urea, 2% Triton X-100, 1% 2-mercaptoethanol, 1% bromophenolblue). The sample was then applied on a gel containing 8 M urea, 2.4% ampholine mixture and 5% acrylamide, and the gel was run at 150 V for 30 min and subsequently at 200 V for 2.5 h. For isoelectric focussing of HSPB8, the ampholine mixture consisted of 16% ampholine pH 3.5-10 and 84% ampholine pH 2.5-5, while for isoelectric focussing of HSP27 the ampholine mixture consisted of 16% ampholine pH 3.5-10, 42% ampholine pH 2.5-5 and 42% ampholine pH 5-7. Before Western blotting, the isoelectric focusing gel was incubated in buffer (6 M urea, 30% glycerol, 50 mM Tris, 2% SDS) for 10 min.

For Western blot analysis, proteins were transferred electrophoretically to a nitrocellulose membrane (Schleicher & Schuell) or polyvinylidene fluoride membrane (Millipore) after SDS-PAGE and isoelectrofocussing, respectively. The membrane was incubated with primary antibodies and subsequently with either alkaline phosphatase-conjugated (Promega) or peroxidase-conjugated (Dako) secondary antibodies. The primary antiserum for detection of HSPB8 was raised in rabbits using a peptide corresponding to aminoacids 179-193. Antibodies against αB-crystallin, mouse HSP27 and HSP20 have been described before [196,198]. Antibodies against human HSP27 and the inducible HSP70 were from Stressgen. Affinity-isolated actin antibody was obtained from Sigma and antibody against desmin was from BioGenex.

RNA isolation and quantitative real time RT-PCR

Control and stressed cells were harvested in Trizol (GibcoBRL) and total RNA was isolated according to the manufacturer's protocol. Genomic DNA was removed by DNase I treatment (GibcoBRL). DNase I was heat inactivated before reverse transcription. cDNA for quantitative analysis was generated with Superscript II reverse transcriptase (GibcoBRL) using random hexamer primers and 2 µg of total RNA. The amount of RNA was quantified by quantitative real-time polymerase chain

reaction (PCR) with the GeneAmp 5700 Sequence Detection System (Applied Biosystems) using the Sybr Green kit (Eurogentec). The PCR signal from control RNA, isolated from unstressed cells, was arbitrarily set to 1. All other signals were calculated compared to this. Furthermore, a PCR with a control primerset (glyceraldehyde-3-phosphate dehydrogenase; GAPDH) was included and all PCR signals were corrected for this value. The following primersets were used: for human HSPB8 5'-TGCACAG-CTTCAAGCCAGAG-3' and 5'-CCTCCACG-TATCCATCTTTGGT-3'; for human GAPDH 5'-ATCCCATCACCATCT-TCCAGG-3' and 5'-GCATCGCCCCACTTG-ATTT-3'.

Yeast two-hybrid assay

To generate the yeast two-hybrid vectors, the full length cDNAs of human HSP27, human αB-crystallin, rat HSP20, human HSPB2 and rat αA-crystallin were cloned in frame with the LexA-DNA binding domain of the slightly modified pEG202 (bait) plasmid, while the full length cDNA of human HSPB8 was cloned in frame with the transcription activation domain of the slightly modified pJG4-5 (prey) plasmid (both plasmids kindly provided by Roger Brent, Molecular Sciences Institute, Berkeley).

For the interaction screening, yeast strain EGY48 (*ura3 trp1 his3 3LexA-operator-LEU2*; Clontech) was transformed with bait, prey and reporter plasmids. Transformants were selected on plates lacking histidine, uracil and tryptophan. After induction of the prey, expression activation of the *LacZ* reporter was determined.

Glycerol gradient centrifugation

Sedimentation analysis was carried out using a Sorvall Discovery 100 ultra-centrifuge with a Th 641 rotor. Samples were layered on top of 5-40% glycerol gradients (in 50 mM Tris pH 7.5, 50 mM NaCl, 0.5% NP-40) created with the Gradient Master (Bio-Comp) in 12 ml tubes and centrifuged at 40000 rpm for 16 h at 4°C. After centrifugation, 0.5 ml fractions were collected

Table 1. Expression of HSPB8 in various cell lines

Cell line	Type of cell line	HSPB8 expresssion [a]		
		RT-PCR	NB	WB
HeLa	human cervical cancer	+ [b]	+ [b]	+ [b,c]
G361	human melanoma	+ [d]	+ [d]	+ [d]
SK-MEL-31, SK-MEL-2	human melanoma	+ [d]		
A431	human keratinocytes		+ [b]	+ [b,c]
C2	mouse myoblast			+ [c]
L6	rat myoblast			+ [e]
L929	mouse fibroblast			+ [e]
MCF-7, T-47-D, ZR-75-1, UACC-821	human estrogen receptor (+) breast cacer		+ [f]	+ [c]
MDA-MB-157, MDA-MB-435, MDA-MB-453, SkBr3	human estrogen receptor (-) breast cancer		- [f]	
293	ad.-immortalized human embryonic kidney	- [b,d]	- [b,d]	- [b,d]
H9c2	rat cardiomyoblast			- [e]

[a] as determined by reverse transcription polymerase chain reaction (RT-PCR), Northern blotting (NB), or Western blotting (WB); [b] reference [252]; [c] this paper, see Figures; [d] reference [25]; [e] this paper, data not shown; [f] reference [23]; +, expression ; -, no expression; blanks, not determined; ad., adenovirus

from the top of the tubes. The molecular mass standards used were albumin (66 kDa), aldolase (158 kDa), catalase (232 kDa) and thyroglobulin (669 kDa).

RESULTS

HSPB8 can be detected in cell lines from different origin

Because we wanted to compare properties of HSPB8 to those of other sHSPs, and muscle is the only tissue that expresses several sHSPs at high levels (e.g., [30]), we examined HSPB8 expression in several myoblast cell lines (C2, L6, and H9c2), as well as in some other cell lines. Results are summarized in Table 1, together with data from earlier studies. Amongst the myoblast cell lines, we could detect HSPB8 in C2 and L6, but not in H9c2. We chose to use C2 cells for most of the further experiments, since these contain highest expression of HSPB8 and can efficiently be differentiated into myotubes. Interestingly, HSPB8 expression was also detected in L929, a cell line that has often been used because of its presumed lack of sHSPs (e.g., [199]).

HSPB8 is not upregulated upon muscle cell differentiation

Expression of sHSPs can be regulated during muscle differentiation [30]. We therefore investigated the protein levels of HSPB8 during differentiation of mouse myoblast C2 cells. Differentiation into multinucleated myotubes by lowering the serum content of the medium, was confirmed morphologically (not shown) and was evident biochemically from the appearance of desmin, a muscle-specific protein, upon Western blot analysis (Fig. 1). Reaction with various sHSP antisera showed that HSPB8 and HSP27 are not detectably upregulated during differentiation, in

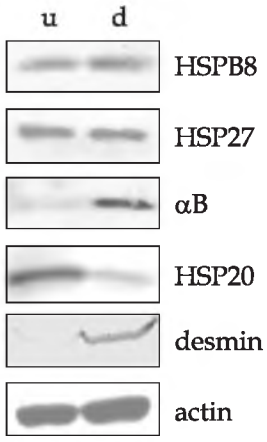

Figure 1. HSPB8 expression during myogenic differentiation of the mouse myoblast cell line C2
Extracts of undifferentiated (u) and differentiated (d) cells were subjected to SDS-PAGE and immunoblotting with antibodies against the proteins indicated on the right.

contrast to HSP20 and αB-crystallin which show a pronounced downregulation and upregulation, respectively. These results for HSP27, HSP20 and αB-crystallin are very similar to what has been described by Sugiyama *et al.* [30], and demonstrate that as for muscle differentiation HSPB8 may behave most similar to HSP27.

HSPB8 is slightly upregulated upon heat shock, but better by arsenite

Since heat-inducibility is characteristic for HSPs, we investigated the effect of heat shock on the expression of HSPB8 in C2 cells at different temperatures and after different recovery periods (Fig. 2). HSPB8 tends to show a minor increase in protein expression, most similar to that of HSP20. In contrast, HSP27 and αB-crystallin are both upregulated to a great extent, notably 24 h after a heat shock of 44°C or 45°C. As a control for the stress response, expression of the well-known stress-inducible HSP70 was found to show an upregulation comparable to HSP27 and αB-crystallin. Since regulation

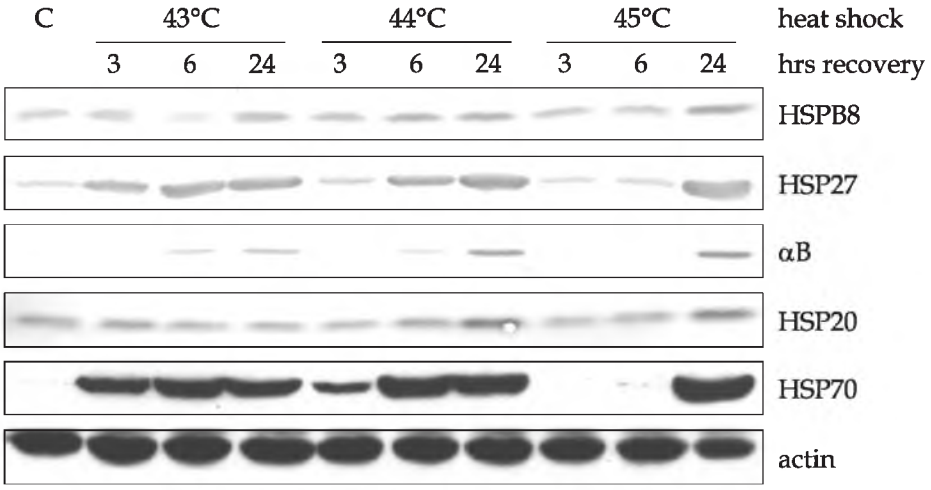

Figure 2. HSPB8 expression after heat shock
The mouse myoblast cell line C2 was heat shocked for 30 minutes at 43, 44 or 45°C, and then recovered at 37°C for 3, 6 or 24 hours. Total cell extracts were subjected to SDS-PAGE and immunoblotting with antibodies against the proteins indicated on the right. C, control cells kept at 37°C.

of sHSP gene expression primarily takes place at the transcription level, we also followed the HSPB8 mRNA expression during recovery after heat shock. HSPB8 mRNA was quantified by real-time RT-PCR and normalized for GAPDH mRNA. Surprisingly, no clear change in HSPB8 mRNA levels could be detected after the investigated temperatures and recovery periods (data not shown).

Since sHSPs can differentially be induced by various types of stress [200], we also examined HSPB8 expression in C2 cells exposed to sodium arsenite. Increased levels of HSPB8 were now observed, as well as increases in HSP27, αB-crystallin and HSP70 levels, all with similar kinetics (Fig. 3). The increase of HSPB8 became visible 4 h after addition of arsenite and protein levels remained elevated for at least 24 h. HSP20 was not upregulated, emphasizing the stress-specific regulation of the different

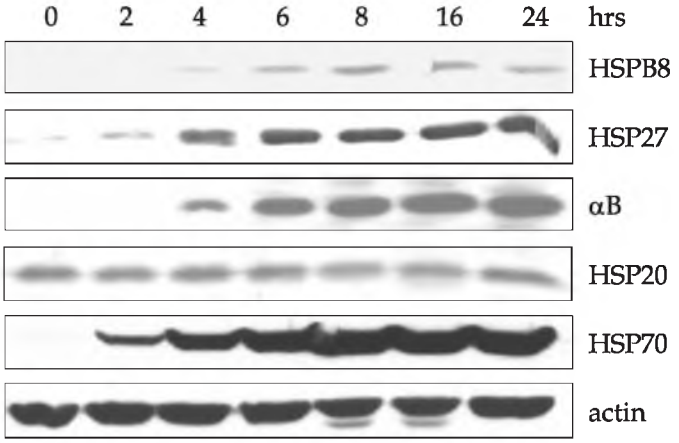

Figure 3. HSPB8 expression upon arsenite stress
The mouse myoblast cell line C2 was exposed to 100 μM sodium arsenite for 0, 2, 4, 6, 8, 16 or 24 hours. Cell extracts were subjected to SDS-PAGE and immunoblotting with antibodies against the proteins indicated on the right. Note that the intensity of HSPB8 staining was reduced compared to Figs. 1 and 2 (compare lane u in Fig. 1, lane C in Fig. 2, and lane 0 in Fig. 3).

sHSPs. Also after arsenite treatment the expression of HSPB8 mRNA was analyzed by real-time RT-PCR and indeed found to be increased, confirming enhanced transcription. The maximal increase was approximately 3.5-fold, 5 h after the start of arsenite exposure (data not shown). These results indicate that HSPB8 is indeed a stress-responsive protein.

HSPB8 mRNA is upregulated upon estrogen treatment, but HSPB8 protein is not

In a recent study [23] upregulation of HSPB8 mRNA was found as an effect of estrogen action. To assess whether HSPB8 is also upregulated at the protein level, we used the same estrogen-responsive cell line, MCF-7, and cultured it in medium with charcoal/dextran-treated serum to reduce the level of hormones and growth factors. Also phenol red was removed from the medium since it may have estrogenic activity on some cells [201]. The MCF-7 cells were then treated with 10^{-8} M 17β-estradiol, and HSPB8 expression was followed by Western blotting (Fig. 4A). We did not observe an increase of HSPB8 nor of HSP27, the only other detectable sHSP in this cell line. Also, HSP70 levels were not induced (data not shown). Furthermore, we tested if adding non charcoal treated fetal calf serum and phenol red had an effect on protein expression levels, but also under these conditions HSPB8, HSP27 and HSP70 levels remained constant, indicating that the used culture conditions do not seem to have an effect (data not shown). Wondering whether these results also meant that HSPB8 mRNA was not upregulated in our estradiol-treated MCF-7 cells, we performed real-time RT-PCR. Surprisingly, we indeed found that mRNA levels had increased upon estrogen treatment (Fig. 4B). The maximal increase is approximately 5-fold after 2-4 h of estrogen treatment. Thus even though HSPB8 mRNA levels are already increased after two hours, HSPB8 protein levels are not detectably increased even after 24 h.

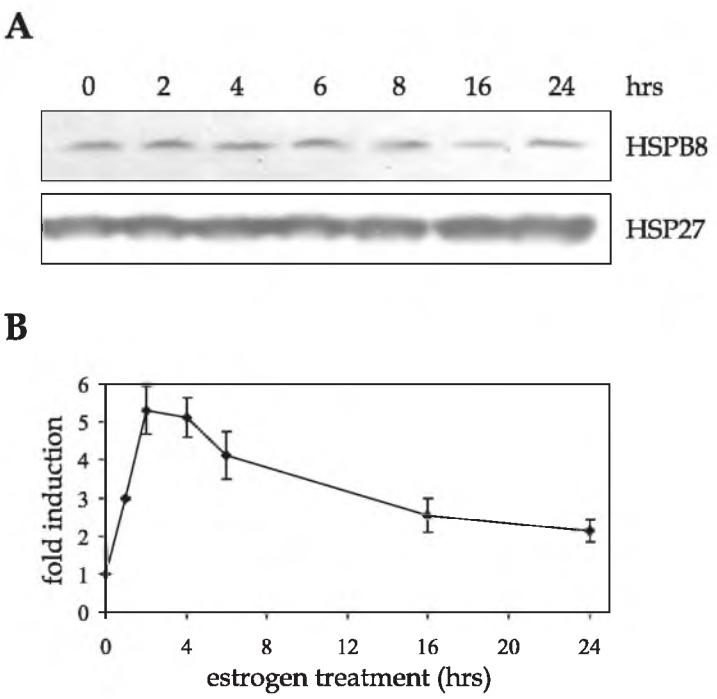

Figure 4. HSPB8 mRNA is upregulated upon estrogen treatment, but HSPB8 protein is not

The human breast cancer cell line MCF-7 was treated with 10^{-8} M 17β-estradiol for the indicated times. **(A)** Cell extracts were subjected to SDS-PAGE and immunoblotting with antibodies against HSPB8 and HSP27. **(B)** Total RNA was extracted from the cells and HSPB8 mRNA was quantified by real-time RT-PCR. All PCR signals were normalized compared to GAPDH expression, as measured by real-time RT-PCR. The HSPB8 signal from untreated control cells was set at 1.

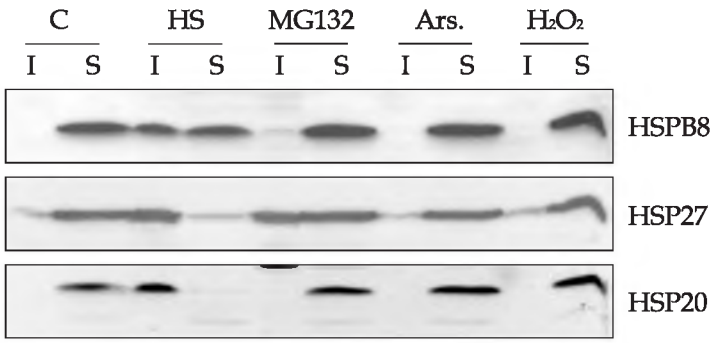

Figure 5. HSPB8 translocates to the detergent-insoluble fraction upon heat shock, but not upon other stress treatments
The mouse myoblast cell line C2 was left untreated (C), heat shocked at 45°C for 30 minutes (HS), treated with 50 μM proteasome inhibitor for 4 hours (MG132), treated with 100 μM sodium arsenite for 1 hour (Ars.) or exposed to 250 μM H_2O_2 for 1 hour (H_2O_2). Directly after treatment cells were separated into detergent-insoluble and detergent-soluble fractions (lanes I and S, respectively). Each fraction was subjected to SDS-PAGE and immunoblotting with antibodies against the proteins indicated on the right.

HSPB8 translocates to the detergent-insoluble fraction upon heat shock, but not upon other stress treatments

For several sHSPs it has been reported that they can associate with the cytoskeleton or redistribute to the nucleus upon stress treatment (review see [202]). We therefore investigated a possible change in distribution of HSPB8 in C2 cells directly after treatment of the cells with a heat shock, a proteasome inhibitor, sodium arsenite or hydrogen peroxide (Fig. 5). Following treatment, the cells were harvested and lysed in a buffer containing 0.5% Triton X-100 and separated into a detergent-soluble cytoplasmic fraction and a detergent-insoluble nuclear/cytoskeletal fraction. In control, unstressed cells HSPB8 was found exclusively in the soluble fraction (lanes C). After a heat shock approximately 50% of HSPB8 translocated to the insoluble fraction (lanes HS), while after proteasomal inhibition only a very minor fraction translocated to the insoluble fraction (lanes MG132). Both sodium arsenite and hydrogen peroxide did not have an effect on the solubility of HSPB8 (lanes Ars. and H_2O_2). HSP27 and HSP20 show a more pronounced translocation after heat shock, but are - like HSPB8 - also hardly affected by arsenite and H_2O_2. In contrast to HSPB8 and HSP20, upon proteasome inhibition approximately 50% of HSP27 becomes insoluble. Unfortunately, our HSPB8 antiserum or even affinity purified antibodies could not be used for immunofluorescence detection of the protein, probably due to a too low expression level. We thus were unable to determine whether the insoluble HSPB8 is associated with the cytoskeleton or is redistributed to the nucleus.

HSPB8 solubility can be restored after heat shock and this resolubilization is independent of translation

It has been shown for αB-crystallin that heat-induced insolubilization is a reversible process [69,167]. It is therefore interesting to establish whether this is also true for HSPB8. After a 44°C heat shock, C2 cells were recovered at 37°C and harvested at different recovery times. Fig. 6A shows that after six hours, no HSPB8 can be found in the detergent-insoluble fraction anymore. Heat shock at 43°C or 45°C resulted in less or

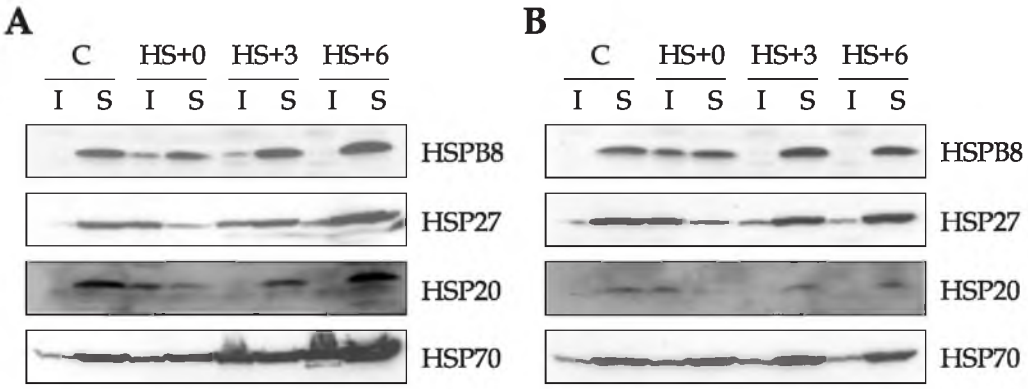

Figure 6. HSPB8 solubility can be restored after heat shock, independent of *de novo* protein synthesis
(A) C2 cells were left untreated (C) or heat shocked at 44°C for 30 minutes and harvested directly after heat shock (HS+0), or recovered at 37°C for 3 hours (HS+3) or 6 hours (HS+6). After treatment cell extracts were separated into detergent-insoluble and -soluble fractions (lanes I and S, respectively). Each fraction was subjected to SDS-PAGE and immunoblotting with antibodies against the proteins indicated on the right. **(B)** The experiment in Fig. 6A was repeated in the presence of the translational inhibitor cycloheximide (10 μg/ml).

more HSPB8, respectively, in the insoluble fraction directly after heat shock, and required a correspondingly shorter or longer time, respectively, for recovery into the soluble phase (data not shown).

The resolubilization of HSP27 is slower than that of HSPB8, probably due to the fact that insolubilization of HSP27 directly after heat shock is higher. During the recovery period increasing amounts of HSP27 in the soluble fraction are also the result of induced expression (cf., Fig. 2). HSP70, which is already partially present in the insoluble fraction in unstressed cells, is not insolubilized to a great extent directly after heat shock, but the amount of insoluble HSP70 seems to further increase during the recovery period. This might be due, too, to the large increase of total HSP70 (cf., Fig. 2). Like HSPB8, the detergent-insoluble HSP20 resolubilizes during recovery.

Rather than the insoluble HSPB8 becoming soluble again, it is also possible that the insoluble HSPB8 is degraded and new, soluble HSPB8 synthesized. To distinguish between these possibilities, we added cycloheximide to the medium before the heat shock and repeated the experiment. Cycloheximide completely inhibited *de novo* protein synthesis, as is evident from the absence of induction of HSP27 and HSP70 (compare lanes HS+6 in Fig. 6A and 6B). In Fig. 6B it can be seen that cycloheximide does not diminish the appearance of HSPB8 in the soluble fraction, confirming that it is the existing insoluble protein that resolubilizes. The resolubilization even seems to be somewhat faster than without cycloheximide, since 3 h after heat shock, no HSPB8 was found in the insoluble fraction anymore (compare lanes HS+3 in Fig. 6A and 6B). Also HSP27 solubility is restored in the presence of cycloheximide and, like HSPB8, recovery seems faster than without cycloheximide. The same applies to HSP20.

HSPB8 forms oligomeric complexes

It has been reported that two types of heteromeric sHSP complexes exist in muscle cells [30]. One complex consists of HSP27, αB-crystallin and HSP20, and the other of HSPB2 and HSPB3. To assess the interactions of HSPB8 with other sHSPs we first used the yeast two-hybrid system.

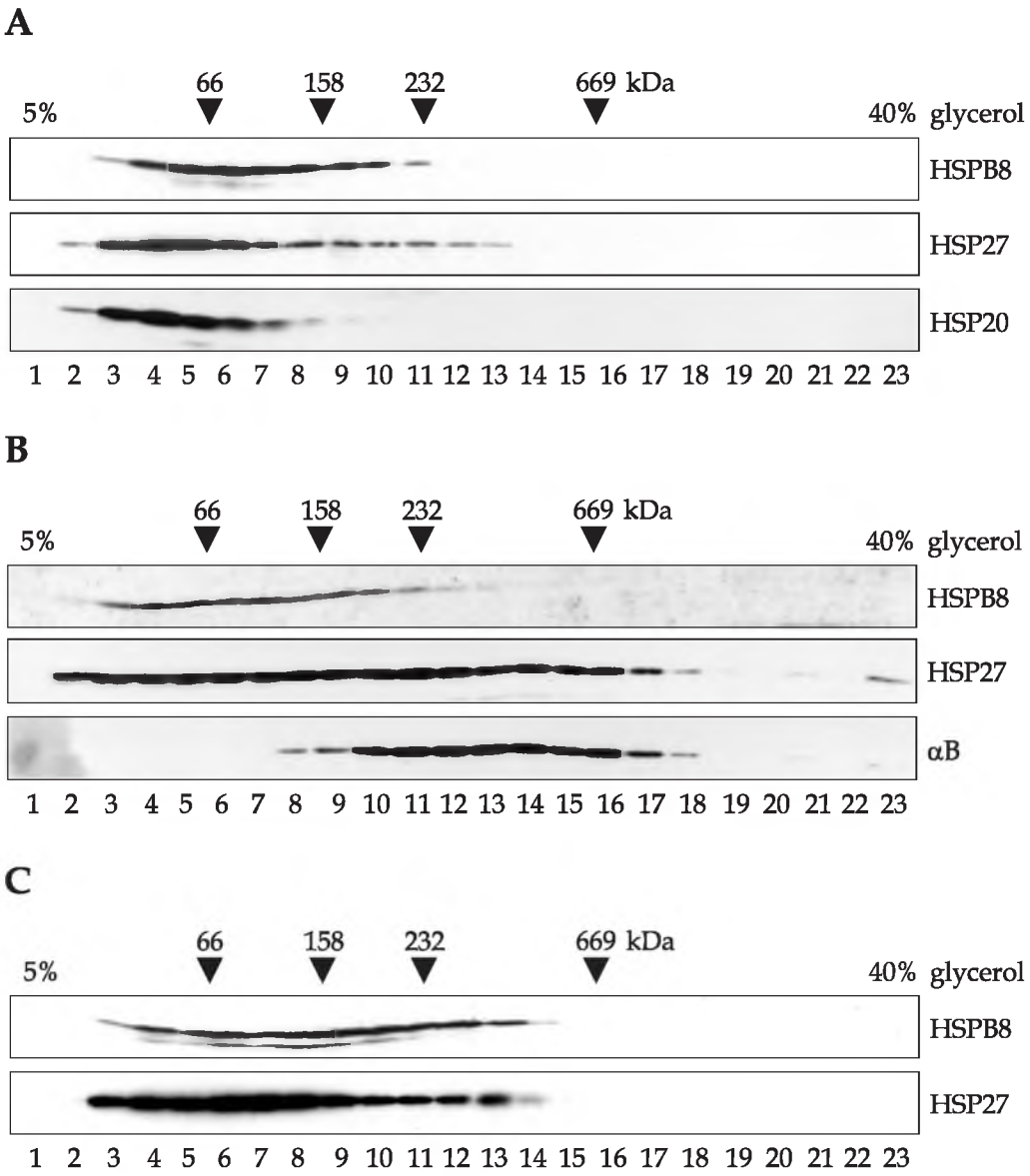

Figure 7. HSPB8 complexes in C2 and HeLa cells

Extracts from undifferentiated **(A)**, and differentiated C2 cells **(B)** as well as HeLa cells **(C)** were fractionated by centrifugation on a glycerol density gradient (5-40%) and analyzed by SDS-PAGE and immunoblotting with antibodies against the proteins indicated on the right. Arrowheads indicate the molecular masses (kDa) of marker proteins.

Table 2. Interaction of HSPB8 with other sHSPs as determined in the yeast two-hybrid system

	Interaction with HSPB8
HSP27	++
αB-crystallin	+
HSP20	++
HSPB2	-
αA-crystallin	-
empty vector [a]	-

+ interaction; ++ strong interaction; - no interaction;
[a] empty vector (expressing only the DNA binding domain) is used as a negative control.

Table 2 shows that HSPB8 can interact with HSP27, αB-crystallin and HSP20, but not with HSPB2, suggesting that HSPB8 might be present in a complex with the former three sHSPs in muscle. Interestingly, and confirming the specificity of the assay, HSPB8 did not interact with αA-crystallin, the lens-specific sHSP that shows 60% identity to αB-crystallin.

To study whether endogenous HSPB8 is indeed present in oligomeric complexes, C2 and HeLa cell extracts were fractionated by glycerol gradient ultracentrifugation and analyzed by immunoblotting. In un-differentiated C2 cells, HSPB8 can be detected in complexes with a molecular mass varying from approximately 40 to 250 kDa (Fig. 7A). HSP27 displays a broader range (±40 to 400 kDa), while HSP20 is more uniform in size (±40 to 150 kDa). In differentiated C2 cells (Fig. 7B), the HSPB8 complex has a size identical to that in undifferentiated cells. In these differentiated cells, we were unable to detect HSP20, but could detect αB-crystallin (cf. Fig. 1). The latter is found in high molecular weight complexes (±150 to 1000 kDa), indicating that HSPB8 and αB-crystallin are present in distinct complexes. Interestingly, HSP27 now shows a much broader sedimentation profile (±40 to 1000 kDa) possibly due to the disappearance of HSP20 or the presence of αB-crystallin. In HeLa cells, which have no detectable αB-crystallin or HSP20, the complexes in which HSPB8 and HSP27 occur have similar sizes (Fig. 7C) like in undifferentiated C2 cells, albeit over a somewhat broader mass range (±40 to 500 kDa).

Acidic isoforms of HSPB8 are formed in C2 cells upon exposure to stress, but not in HeLa cells

Several post-translational modifications have been described for sHSPs, of which phosphorylation is the most prominent and best studied [203]. We therefore studied the possible changes in isoelectric point of HSPB8 in response to stress in C2 and HeLa cells, using isoelectric focusing and subsequent Western blot analysis. As shown in Fig. 8A, HSPB8 in untreated cells is present in two major forms with different isoelectric points, and a minor more acidic one. After heat shock, the upper band disappears and the most acidic band becomes pronounced. Inhibition of proteasomes does not affect the isoforms of HSPB8, while after both arsenite- and H_2O_2-treatment, all three forms of HSPB8 are detected. Since Benndorf *et al.* [24] showed that HSPB8 can be phosphorylated *in vitro*, it is most likely that the more acidic HSPB8 bands are phosphorylated isoforms.

The same samples were also analyzed for HSP27 (Fig. 8B). Mouse HSP27 can be phosphorylated at serines 15 and 86. In control cells the unphosphorylated (p_0) and monophosphorylated (p_1) forms are most prominent, but also the diphosphorylated (p_2) form can be seen. After all types of stress used here, the unphosphorylated HSP27 disappears and the mono- and diphosphorylated isoforms become the major products. In contrast to HSPB8, there is not much difference in the response to the

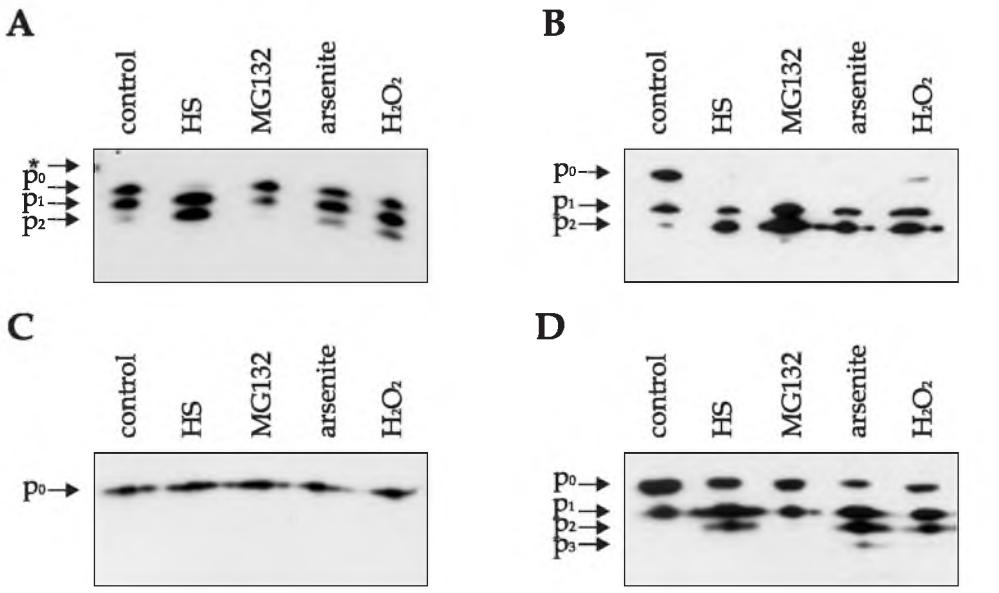

Figure 8. Different isoforms of HSPB8 are present in control and stressed C2 cells, but not in HeLa cells
C2 cells **(A,B)** or HeLa cells **(C,D)** were left untreated (control), heat shocked at 45°C for 30 minutes (HS), treated with 50 μM proteasome inhibitor for 4 hours (MG132), treated with 100 μM sodium arsenite for 1 hour (arsenite) or exposed to 250 μM H_2O_2 for 1 hour (H_2O_2). Cells were harvested and analyzed on isoelectric focusing gel followed by Western blot analysis. (A,C) An IEF gel with a pH range of 2.5-5 was used and immunoblotting was performed with HSPB8 antiserum. (B,D) An IEF gel with a pH range of 2.5-7 was used and immunoblotting was performed with HSP27 antiserum. Unphosphorylated forms are indicated with p_0, and mono-, di- and triphosphorylated forms with p_1, p_2 and p_3, respectively. The * in panel A indicates the position of unphosphorylated recombinant human HSPB8, which is predicted to have a higher isoelectric point than unmodified mouse HSPB8 (5.0 versus 4.9; calculated using http://scansite.mit.edu/calc_mw_pi.html).

different types of stress, suggesting that different kinases and/or pathways are responsible for the modification of HSPB8 and HSP27.

In HeLa cells, we could not see any modification of HSPB8, neither in control cells nor in stressed cells (Fig. 8C), while HSP27 was already partially phosphorylated in control cells, and became more phosphorylation after heat shock, arsenite and peroxide stress (Fig. 8D). The four isoforms of HSP27 correlate with the unphosphorylated HSP27 and the three reported phosphorylation sites of human HSP27 (serines 15, 78 and 82).

DISCUSSION

Heart and skeletal muscle are the only tissues that simultaneously express seven of the ten known sHSPs (αB-crystallin, HSP27, HSP20, cvHSP, HSPB2, HSPB3 and HSPB8), which raises the question whether and how they are functionally complementary. Some of these sHSPs are not expressed in undifferentiated muscle cells (αB-crystallin, HSPB2, HSPB3) while others (HSP27, HSP20) are already present before differentiation [30]. We showed here, that HSPB8, like HSP27, is already present in undifferentiated C2 cells, and that protein levels remain constant during differentiation. Interestingly, HSP20 levels drop after C2 cell

differentiation, indicating that each sHSP is regulated in a unique way during differentiation. These results indicate the different need that undifferentiated and differentiated cells have for a specific composition of sHSPs.

A difference in sHSP regulation was also found after stress in the C2 cell line. Whereas HSP27 and αB-crystallin are upregulated upon heat shock, the effect on HSPB8, as for HSP20, is very minor. HSPB8 is slightly upregulated as a protein, but mRNA levels remain constant. This discrepancy could be due to a more stable protein or to more efficient translation after heat shock. The absence of heat inducibility at the mRNA level has earlier been reported for HSPB2, HSPB3 and HSP20 [30]. Interestingly, we found that expression of HSPB8 is induced by arsenite, very similar to HSP27 and αB-crystallin. With arsenite, no induction of HSP20 was detected. The different inducibility of a single sHSP after different forms of stress has been shown before, indicating the presence of independent stress-specific signaling pathways (e.g. [167,200]).

It has been reported that HSPB8 mRNA is upregulated upon estrogen treatment [23]. We could confirm this observation, but did not see an accumulation of HSPB8 protein. A similar discrepancy between mRNA and protein accumulation in response to estrogen treatment has earlier been reported for HSP27 [204,205] and for IGFBP-4 [206], and suggests translational regulation besides transcriptional regulation. In the same cell line that we used (MCF-7), the discrepancy between mRNA and protein levels has been seen before for cyclophilin 40 after heat shock, and was found to be due to a higher protein turnover [207]. Whether this is also the case for HSPB8, remains to be tested.

Under normal conditions, HSPB8 is a detergent-soluble protein, becoming partially and reversibly insoluble after certain types of stress (Figs. 5 and 6), as has been described for other sHSPs [69,77,196]. The extent of insolubilization differs greatly between the types of stress and the different sHSPs ([19,73,196,208], this paper). The reason why sHSPs become reversibly detergent-insoluble is unclear, but is likely due to different kinds of interactions, such as association with actin and intermediate filaments as has been shown for HSP27, αB-crystallin, HSP20 and HSPB2 [116,196], and may occur both in unstressed cells [123] and after stress [77].

Phosphorylation of sHSPs may take place in response to stress, as has been described for HSP27 and αB-crystallin, but has also been reported under other conditions such as cell division (αB-crystallin, [63]) and cyclic nucleotide-dependent vasorelaxation (HSP20, [65]). Each sHSPs seems to be phosphorylated by a unique set of kinases: HSP27 by MAPKAPK-2, αB-crystallin by MAPKAPK-2, p44/42 mitogen-activated protein kinase and protein kinase A, and HSP20 by cyclic GMP-dependent protein kinase/protein kinase A (review [209]). Since HSP27 phosphorylation is induced by a variety of stresses, while HSPB8 phosphorylation is only seen after heat shock (Fig. 8), and since Benndorf *et al.* [24] showed that HSPB8 could not be phosphorylated *in vitro* by MAPKAPK-2, we conclude that phosphorylation of HSPB8 and HSP27 is mediated by different kinases. The fact that we see phosphorylation of HSPB8 in C2 cells but not in HeLa cells probably reflects that cells of different origin may have different stress responses.

Phosphorylation decreases the complex size of HSP27 and HSP20 [116,208], while phosphorylation of αB-crystallin only has a minor effect on its complex size [62]. For

HSPB8 the estimated complex sizes in C2 and HeLa cell extracts range between 40-250 kDa and 40-500 kDa, respectively (Fig. 7), while phosphorylation of HSPB8 is approximately 50% in C2 cells and absent in HeLa cells (Fig. 8). This suggests that also for HSPB8 complex size is reduced by phosphorylation.

In muscle cells, sHSPs have been found in two heteromeric complexes, one composed of HSP27, αB-crystallin and HSP20, and the other of HSPB2 and HSPB3 [30]. The tissue distribution of HSPB8 is more similar to that of HSP27, αB-crystallin and HSP20, which are expressed in a wider variety of tissues, than to that of HSPB2 and HSPB3, which are specifically expressed in muscle [27,30]. Surprisingly, our sedimentation data (Fig. 7) suggest that HSPB8 is present in a complex distinct from the αB-crystallin containing complex, although in the yeast two-hybrid system both proteins can interact. It is possible that HSPB8 forms a complex with HSP27 and HSP20 *in situ,* because of the (partial) overlap in their sedimentation profiles and the interactions found in the yeast two-hybrid system. Although HSPB8 did not show any interaction with HSPB2 in this system, it cannot be excluded that HSPB8 is also part of the HSPB2/HSPB3 complex because both complexes have similar sizes [30]. Phosphorylation of HSP27 reduces the complex size of HSP27 [208] and it is very interesting that HSPB8 cofractionates with the smaller and not with the larger HSP27 complexes (Fig. 7B), suggesting that HSPB8 prefers to interact with phosphorylated HSP27 as has been shown by Benndorf *et al.* [24].

In summary, despite their considerable sequence difference [13], HSPB8 seems to behave very similar to HSP27 upon myoblast differentiation, arsenite stress, estrogen treatment, stress-induced insolubilization and complex formation, but differs in its response to heat shock and stress-induced phosphorylation. Of course, we have to be careful in extrapolating the results since the phenomena described in this paper may well be cell type- or tissue-specific. Since seven of the ten known sHSPs are expressed in the same tissues – heart and skeletal muscle –the question remains why we have so many of them. They all have their own specific properties and react slightly different under different conditions. It seems plausible that a certain set of sHSPs is expressed because that specific combination is optimal under the given conditions, but it will be a formidable task to entangle the roles of each individual sHSP and their mutual interactions.

ACKNOWLEDGEMENTS

We thank Luc Rietveld and Sander Granneman for their assistance with the real-time RT-PCR and sedimentation analyses, respectively.

Expression of small heat shock proteins HSPB2, HSPB8, HSP20 and cvHSP in different tissues of the perinatal developing pig

Pauline Verschuure [1]
Caroline Tatard [2]
Wilbert C. Boelens [1]
Jean-François Grognet [2]
Jean Claude David [2]

[1] *Department of Biochemistry, Nijmegen Center for Molecular Life Sciences, University of Nijmegen, Nijmegen, The Netherlands*
[2] *Ecole Nationale Supérieure Agronomique de Rennes, Rennes, France*

Eur. J. Cell Biol. (2003), in press

Recently, we have described the developmental expression of the small heat shock proteins (sHSPs) HSP27/HSPB1 and αB-crystallin/HSPB6 in different tissues of pigs from almost full term foetuses to three years old adults [210]. The data described in this report extends this study to four other members of the sHSP family (HSP20/HSPB6, cvHSP/HSPB7, MKBP/HSPB2 and HSPB8). We studied expression of these proteins in porcine lens, brain, heart, liver, kidney, lung, skeletal muscle, stomach and colon, and found a ubiquitous expression of HSP20 and HSPB8 as earlier reported for HSP27 and αB-crystallin. In contrast, cvHSP and HSPB2 expression is essentially restricted to heart and muscle. During development, the sHSPs tend to (temporarily) increase in stomach, liver, lung, kidney, hippocampus and striatum, while expression in heart is more or less constant and a large variation is found in sHSP expression patterns in skeletal muscle. In cerebellum and cortex a temporary decrease of HSP20 and HSPB8 is observed directly after birth. The major impact of this study is that each tissue seems to have a unique profile of sHSP expression, which varies during development and may reflect the need of a particular tissue to maintain at all stages an optimal chaperoning machinery to protect against physiological stress.

INTRODUCTION

Heat shock proteins are a group of highly conserved proteins, that are constitutively expressed in most cells under normal physiological conditions [3]. They exert housekeeping functions in normal cell metabolism as well as protective functions under stress conditions. Their synthesis is increased during stresses such as exposure to elevated temperatures, heavy metals, amino acids analogues and physiological changes. Heat shock proteins can be divided into five unrelated families (HSP100, HSP90, HSP70, HSP60 and the small heat shock proteins (sHSPs)) based on their monomeric size as well as specific function.

sHSPs are the most diverse family amongst the heat shock proteins. They are characterized by the presence of the so-called α-crystallin domain, a stretch of 80-100 amino acids in the C-terminal half of the proteins [6]. Their function is not well understood, but *in vitro* they display chaperone-like activity, while *in vivo* they are able to protect cells against stress. Besides the more general protective effect against stress, sHSPs have been implicated in specific cellular processes. For example, HSP27 and αB-crystallin are involved in the modulation of cytoskeleton and inhibition of apoptosis (reviewed in [36,202]). Furthermore, sHSPs play a role in inclusion body diseases, such as neurodegenerative disorders [85], cataract [14,125], and desmin-related myopathy [125], in autoimmune diseases such as multiple sclerosis [141] and in cancer [140], in which the expression of sHSPs appears to be linked to the oncogenic status of cells. Amongst the ten mammalian sHSPs (formally indicated as HSPB1-10), the eye lens-specific αA-crystallin/HSPB5 and the

more generally expressed αB-crystallin/HSPB6 and HSP27/HSPB1 have been known for long and are best studied so far. Seven other sHSPs have more recently been identified: MKBP/HSPB2, HSPB3, HSP20/HSPB4, cvHSP/HSPB7, HSPB8, HSPB9 and HSPB10 [13]. Mammalian sHSPs are expressed in a wide variety of tissues which often contain multiple sHSPs. Heart and skeletal muscle are two tissues in which even up to seven sHSPs (HSP27, αB-crystallin, HSP20, HSPB2, HSPB3, cvHSP, and HSPB8) are expressed at the same time and at relatively high levels. Expression of sHSPs is known to be regulated during development and differentiation [211]. Some sHSPs may even be required for the differentiation of specific cell types [38] or might protect certain differentiating cell types from going into apoptosis [104]. Regulation of expression is considered to be primarily at the level of transcription. Recent work from one of our laboratories has reported such regulated expression for HSP27 [212] and αB-crystallin [210], as well as for the unrelated HSP70/HSC70 [213] and HSP90 [214] in a perinatal model of pig development. However, scarce information is available on the tissue expression of other sHSPs during development. Since αA-crystallin is lens-specific and HSPB9 and HSPB10 are both testis-specific, we omitted these sHSPs in the present investigation. We studied expressions of HSP20, cvHSP, HSPB2, and HSPB8 during development in nervous and non-nervous tissues, with a special interest in heart, skeletal muscle and brain.

Materials and Methods

Animals

All experimental procedures were carried out in accordance to the European Convention for the Protection of Vertebrate Animals used for Experimental and other Scientific Purposes (Council of Europe nr. 123, Strasbourg 1985) and the French Ministry of Agriculture for the use and care of laboratory animals. All animals used were Large White strain. They were obtained from INRA, St Gilles. All animals were from separate litters. Experiments were performed using foetus, newborn, 1 h, 4 h, 8 h, 1 day, 2 day, 5 day, 10 day, 28 day and 3 year old animals. Four separate animals were used for each point. Foetuses were obtained following electrical killing of the mother a day before presumed term (at day 114 of gestation). Until 28 days of age, piglets were kept with their mother. Following 5 min inhalation of chloroform, foetuses and piglets until 28 days of age were killed by decapitation at indicated times. Three year old animals were killed in commercial slaughterhouses. Tissues were immediately sampled and kept at –80°C. The relative expression of the sHSPs was determined in different tissues: lens, whole brain, cerebellum, cortex, hippocampus, striatum, heart, liver, kidneys, lungs, skeletal muscle (semitendinosus), and two parts of the gastrointestinal tract (stomach and proximal-colon).

Preparation of protein homogenates

For protein extraction, tissues were minced and placed in extraction buffer (TEX buffer 1X: 60 mM Tris-base pH 6.8, 10% glycerol, and 3% sodium dodecyl sulfate (SDS)) with 5% β-mercaptoethanol and the protease inhibitor Antagosan (Hoechst Laboratories, Paris, France). Tissues were homogenised in Ultra Turrax at maximum speed for 1 min in ice and centrifuged at 26500 x g for 15 min. Supernatants were collected and kept at –20°C for no longer than one week before use. Protein concentrations were measured according to

Lowry *et al.* [215] using an Elisa plate reader (Argus 300, Packard).

Gel electrophoresis and Western blot analysis

Equal amounts of proteins were loaded on 13% acrylamide gel with a 4% stacking gel. Electrophoresis was performed in buffer containing 25 mM Tris pH 7.6, 0.1% SDS and 0.2 M glycine. Following migration, proteins were transferred to Hybond C membranes (Amersham Biosciences, Freiburg, Germany) during 75 min using buffer containing 25 mM Tris pH 7.6, 0.1% SDS, 0.2 M glycine and 20% methanol. Blots were washed four times in TBST buffer (20 mM Tris pH 7.6, 12.5 mM NaCl and 0.5% Tween-20), soaked in Ponceau Red during 1 min for molecular weight marker (Sigma, Lyon, France) revelation and washed again four times in TBST buffer for 5 min each. Membranes were blocked for 1 h at room temperature in TBST buffer containing 5% milk powder at room temperature and then incubated overnight with the primary antibody at a dilution of 1:1000. The antiserum for detection of HSP20 has been described before [198]. The primary antisera for detection of rat HSPB2 and rat HSPB3 were raised in separate rabbits using the recombinant proteins. The primary antisera for detection of human cvHSP and HSPB8 were raised in separate rabbits using peptides, corresponding to amino acids 156-170 (cvHSP) and 179-193 (HSPB8), coupled to keyhole limpet hemocyanin (Pierce, Etten-Leur, The Netherlands). Following overnight incubation at room temperature, blots were washed 5 x 5 min in TBST buffer and 5% milk powder containing the secondary antibody diluted 1:1000 (anti-rabbit IgG peroxidase-coupled from Sigma). Following 5 x 5 min washes in TBST buffer, bands were revealed using diamino-benzidine (Sigma) in 30 ml buffer containing 60 mM Tris pH 6.8, 0.2% hydrogen peroxide and 200 µl 0.8% $NiCl_2$. After staining, membranes were washed in distilled water and dried at 37°C in oven. Representative westerns are given in the figures. To check for equal protein loading of each lane, all membranes were tested for the expression of β-actin, using anti-β-actin antibody (Sigma, ref. 9044) and a peroxidase-coupled secondary antibody (Sigma) both at a dilution of 1:5000. Examples are given in Figs. 2 to 4.

Standardisation

To compare densities, membranes were scanned using a phosphor imager (Quantum Appligene, Illkirch, France). Expression of HSP20 in the cerebellum at 10 days of age was arbitrary given a value of 100 and other densities were compared to this value. Data is presented as means ± SEM (Standard Error of Measurement; N = 4). Data was analysed using the ANOVA procedure (Analysis of Variance) of the statistical analysis system (SAS Institute, Cary, NC, USA) with Dunnett post-hoc comparison between means at post-foetal times and foetal time. Differences between means were considered significant when $p < 0.01$.

RESULTS

Specificity of the polyclonal antibodies

To study the expression of HSP20, HSPB2, HSPB3, cvHSP and HSPB8, we used rabbit polyclonal antisera raised against rat recombinant proteins (HSP20, HSPB2 or HSPB3), or against a peptide corresponding to the human sequence of cvHSP or HSPB8. These obtained antisera recognize recombinant human proteins on Western blot (Fig. 1 and data not shown). To analyse if the antisera also specifically recognize the porcine proteins, protein extracts from 5 day

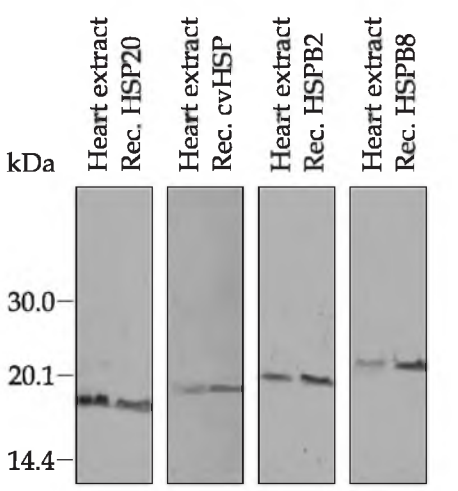

Figure 1. Western blot analysis showing the specificity of the used antisera

Total extract from 5 day old porcine heart (Heart extract) and recombinant (Rec.) human HSP20, cvHSP, HSPB2 or HSPB8 were separated by SDS-PAGE and analysed using the antibodies against the proteins indicated at the bottom. Molecular weights of marker proteins are indicated on the left.

old pig heart were used (Fig. 1). The HSPB3 protein could not be detected in the heart extract (data not shown), despite the fact that this tissue probably has the highest expression of HSPB3 [30], and for this reason this antiserum was not used for further experiments. The other antisera specifically detected one band in the pig heart extract. The positions of the bands (16.8, 18.6, 20.2 and 21.5 kDa for HSP20, cvHSP, HSPB2 and HSPB8, respectively) are similar to the recombinant proteins and are clearly distinct from each other, indicating that these antisera are specific and do not cross-react with the other sHSPs.

Tissue distribution of HSP20, HSPB2, cvHSP and HSPB8 in pig

As a first step in investigating the developmental expression of HSP20, HSPB2, cvHSP and HSPB8, we studied their

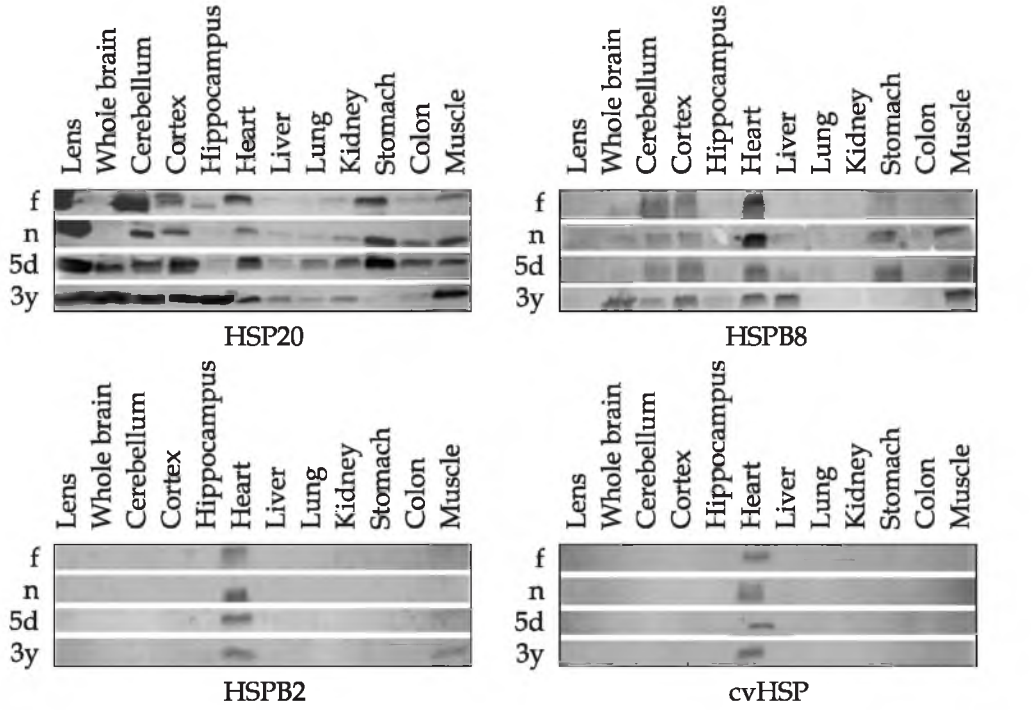

Figure 2. Tissue-specific expression of HSP20, HSPB8, HSPB2 and cvHSP at different developmental stages

Extracts of the tissues indicated at the top were obtained from foetus (f), newborn (n), 5 days old (5d) and 3 years old (3y) pigs. Samples containing 100 µg of protein were subjected to SDS-PAGE and immunoblotting with antibodies against the indicated proteins.

expression in a number of different tissues at four stages. Although there have been studies in which the tissue distribution of some of these was examined (e.g. [30]), this is the first report that examines all four proteins on the same basis. As depicted in Fig. 2, the tissue distribution of both HSP20 and HSPB8 is ubiquitous. Interestingly, the expression levels of both proteins vary between the different tissues and the developmental stages (see also Figs. 3-5). HSP20 can be detected in all tissues tested, while HSPB8 is found in all tissues except for lens. In contrast to HSP20 and HSPB8, the tissue distribution of cvHSP and HSPB2 is more restricted, showing only detectable expression in heart and muscle. For HSPB2, besides heart and muscle, also a faint band was observed in 5 day- and 3 year-old porcine liver.

Relative expression of HSP20 and HSPB8 in different regions of the developing brain

Because of the special involvement of cerebellum, cortex, hippocampus and striatum in stress, developmental studies were first focused on these regions. For this purpose, protein extracts from these regions were obtained at different developmental stages with special attention to the period directly after birth. Expression of HSP20 and HSPB8 was quantified by Western blot analysis and compared to foetal levels (Fig. 3). In both cerebellum and cortex, HSP20

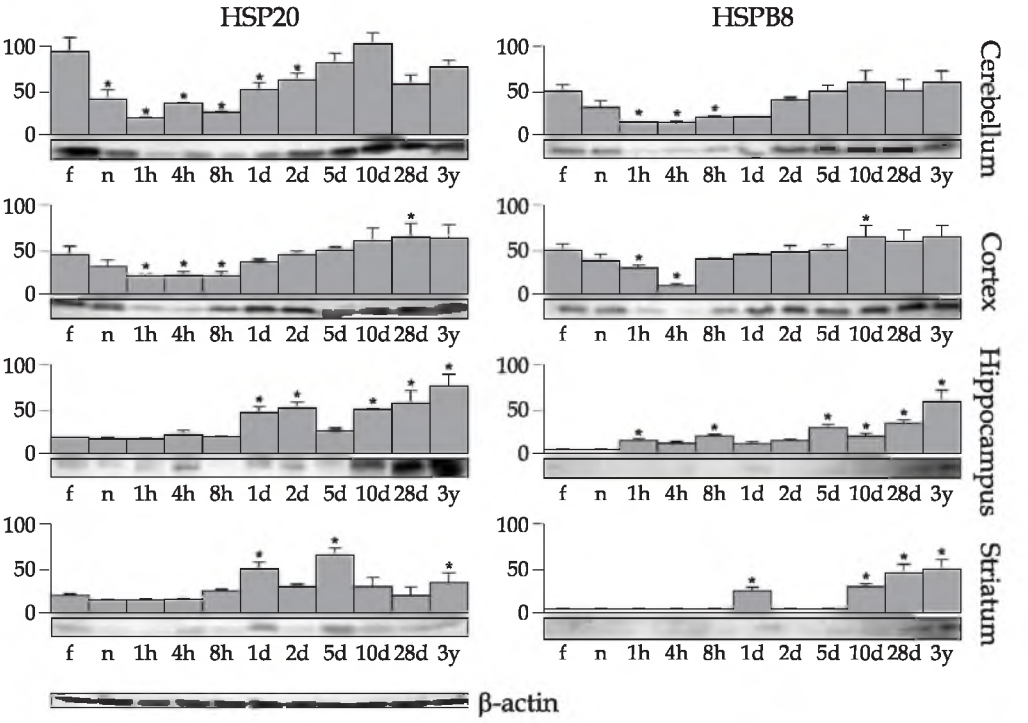

Figure 3. Developmental expression of HSP20 and HSPB8 in porcine cerebellum, cortex, hippocampus and striatum
Samples were obtained at different stages of development (from left to right: foetus, newborn, 1 hour, 4 hours, 8 hours, 1 day, 2 days, 5 days, 10 days, 28 days and 3 years old animals). A total of 100 µg of protein per lane was subjected to SDS-PAGE and immunoblotting with antibodies against the proteins indicated at the top. Expression was quantified and values, given in arbitrary units, are the mean ± SEM of four independent experiments. A representative Western blot is shown below each quantification diagram. All blots were additionally stained for β-actin to check for equal protein loading and an example is given for hippocampus (left lowest panel). * Significantly different from foetus ($p < 0.01$).

and HSPB8 levels drop directly after birth. Already one hour after birth their expression is significantly lower than in foetus and expression remains lower for several hours (cortex) or days (cerebellum). However, at later stages, expression levels increase again back to foetal levels or even higher. In hippocampus and striatum, expression of HSP20 and HSPB2 was relatively low in foetuses and newborns. Expression was found to increase with age and significant higher expression was found about one day after birth. As was already shown in Fig. 2, we could not detect HSPB2 and cvHSP in brain.

Developmental expression of HSP20 and HSPB8 in liver, lung and kidney

Previous study has revealed that two other members of the sHSP family, αB-crystallin and HSP27, are expressed in liver, lung and kidney, and that their expression generally increases during development [210]. Therefore, we examined whether HSP20 and HSPB8 levels are also developmentally regulated in these tissues. As depicted in Fig. 4, in liver HSP20 increases after birth and levels do not seem to change during development. Initially, HSPB8 levels are constant in liver development, but – in contrast to HSP20 levels - they show a sharp increase at relatively late stages (28 days, 3 years). In lung, the developmental expression of HSP20 is very similar to that of HSPB8, with the exception of newborn, in which HSP20 is temporarily upregulated as compared to foetus while HSPB8 is not. For both proteins expression is low in foetus and increases eight hours after birth. Both HSP20 and HSPB8 expression remains high, but drops back to foetal levels at the 3 years time point. Also in kidney, HSP20 and HSPB8 expression is low in foetus with a slight temporal increase directly after birth for HSP20. Then they increase with age starting at day one for HSP20 and day ten for HSPB8. No decrease at 3 years as was seen in lung was observed for HSP20 and HSPB8 in kidney. HSPB2 and cvHSP could not be detected in these tissues (Fig. 2).

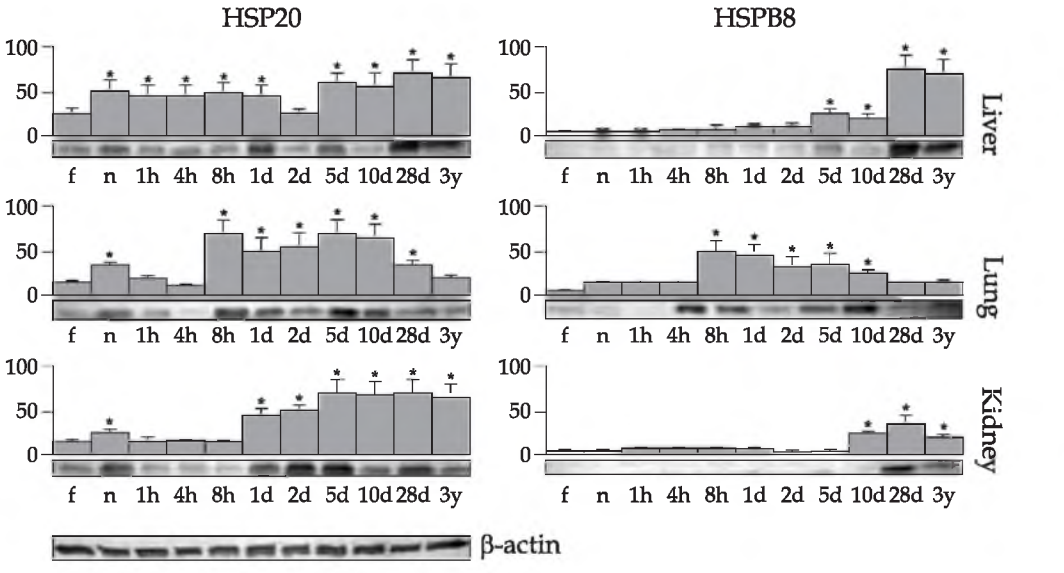

Figure 4. Developmental expression of HSP20 and HSPB8 in liver, lung and kidney
Legends as for Figure 3. Lowest panel left represents the expression of β-actin in liver.

Developmental expression of HSP20, cvHSP, HSPB2 and HSPB8 in heart, muscle and stomach

Since seven different sHSPs are expressed in heart and muscle, a major challenge lies in the identification of overlapping and unique roles of these sHSPs. A better understanding may come from the knowledge of the pattern of expression during development of heart and muscle. We therefore examined the developmental expression of HSP20, cvHSP, HSPB2 and HSPB8 in these tissues (Fig. 5). In the porcine heart, an almost constant level of expression of HSPB8 and cvHSP is found during development, while HSP20 levels increase in the later stages of development and HSPB2 levels are already increased at birth, remain higher than in foetus, but decrease again at the 3 years time point. In muscle, all four tested sHSPs are increased with age as compared to foetus, either already at birth (HSP20), or starting about one day following birth (cvHSP, HSPB2 and HSPB8). However, the increase in HSPB2 and cvHSP at day 1 seems to be only temporal. In older animals (28 days, 3 years) expression is higher again. HSP20 and

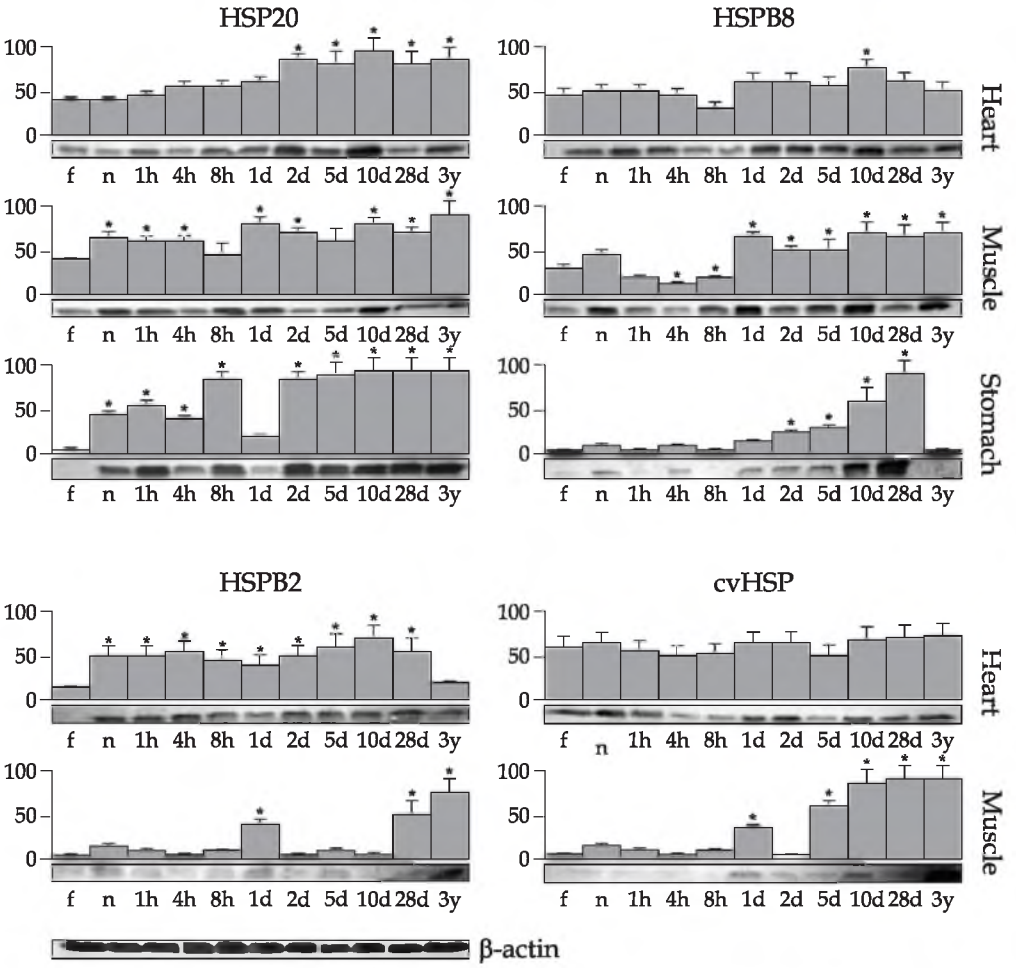

Figure 5. Developmental expression of HSP20, HSPB8, HSPB2 and cvHSP in heart, muscle and stomach
Legends as for Figure 3. Lowest panel left represents the expression of β-actin in stomach.

HSPB8 are also expressed in stomach (Fig. 5) and in colon (not shown). In stomach, under the present conditions, HSP20 has a variable expression, which at all time points is higher than foetal level. HSPB8 increases with age in stomach, but after 3 years HSPB8 expression is back to foetal level again.

DISCUSSION

Developmental regulation of sHSPs is common and has been described in organisms as diverse as *Drosophila melanogaster* [216], *Caenorhabditis elegans* [217], *Xenopus laevis* [218], *Saccharomyces cerevisiae* [219] and mammals [211]. The presence of different sHSPs in a single tissue probably reflects the specific need of that tissue at a certain moment. For this reason sHSPs may sometimes be similarly and sometimes differentially regulated during development. In mammals several studies have focussed on heart and muscle, since the expression of most sHSPs is very high in these tissues. Only few reports have compared the tissue distribution or the developmental expression of different sHSPs within one study [32,33]. We and others have previously shown differential regulation of HSP27 and αB-crystallin [32,210]. In order to clarify whether also other sHSPs are differentially regulated during tissue development, we used the same system as we have used before for HSP27 and αB-crystallin. In a first series of experiments, expression of HSP20, HSPB2, cvHSP and HSPB8 was compared in different porcine tissues at four given stages (foetus, newborn, 5 days, 3 years; Fig. 2). In a second series of experiments, expression was compared at eleven different stages of development (ranging from foetus to 3 years) in single tissues (Figs. 3-5).

We show here that HSP20 and HSPB8 are ubiquitously expressed in porcine tissues (Fig. 2) as has been reported before in other animals [18,29,30]. Both are detected in all tissues examined except lens, in which we could detect HSP20, but not HSPB8. Expression of HSP20 in lens has been reported before [18]. The tissue expression patterns of cvHSP and HSPB2 are more restricted and we mainly detected these proteins in heart and muscle. This result is as expected since cvHSP was discovered by a database search for heart-selective expression [22], while HSPB2 is mainly expressed in heart and muscle in rat tissues [30], even though in that study also low expression was found in colon and thymus. When comparing the tissue distribution of the sHSPs described in this report to that of the previously reported αB-crystallin and HSP27 [210], we can conclude that there are two types of expression patterns for sHSPs. αB-Crystallin, HSP27, HSP20 and HSPB8 all show ubiquitous expression with varying concentrations in the different tissues, while the tissue distribution of HSPB2 and cvHSP is largely restricted to heart and muscle. To this last group also belongs HSPB3, on the basis of the published mRNA and protein expression profile [30].

Based on our previous study [210] and the data presented in this paper (Figs. 3-5) we could distinguish seven different types of developmental expression patterns for the porcine sHSPs (Fig. 6). During development, sHSPs tend to (temporarily) increase in stomach, liver, lung, kidney, hippocampus and striatum, while a large variation is found in sHSP expression in skeletal muscle. In cerebellum and cortex a temporary decrease of HSP20 and HSPB8 is observed directly after birth. Remarkably, the developmental expression pattern of a single sHSP varies a lot between tissue types.

During pig development we found constant levels in heart for αB-crystallin,

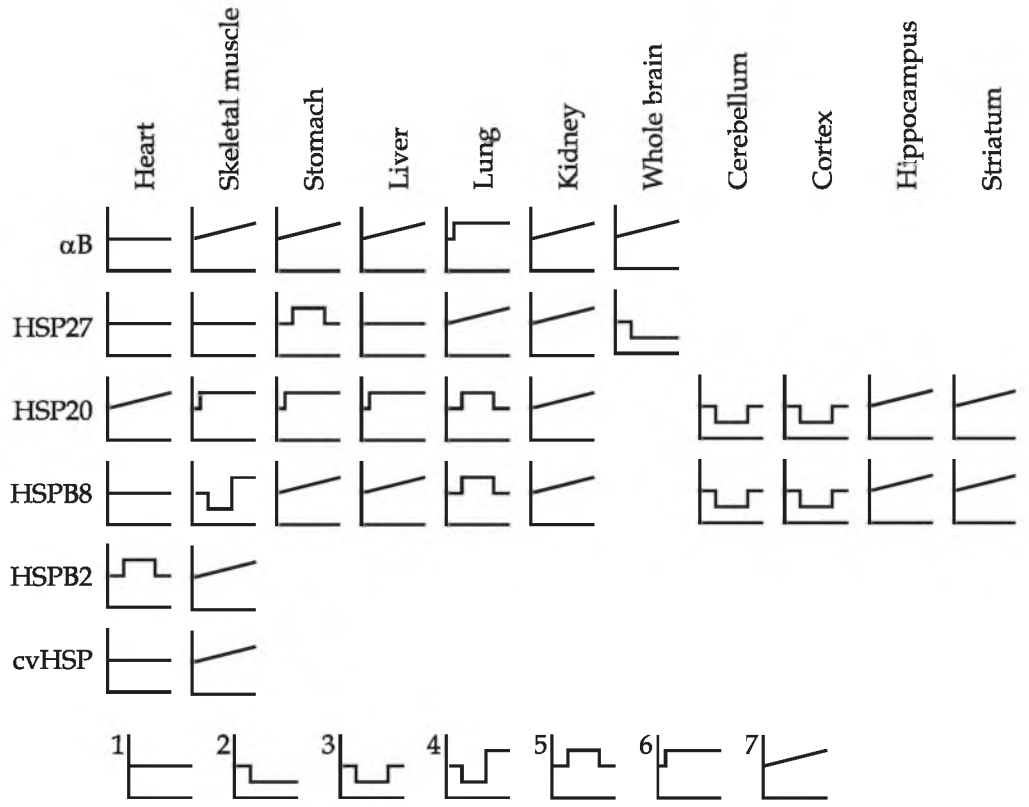

Figure 6. Schematic overview of developmental expression of sHSPs in porcine tissues
Results are taken from our previous study (for αB-crystallin and HSP27; [210]) and from the data presented in this paper. The expression patterns of αB-crystallin (αB), HSP27, HSP20, HSPB8, HSPB2 and cvHSP can be grouped into seven categories. As compared to foetal levels, expression during development is (1) constant, (2) down regulated, (3) temporarily down regulated, (4) temporarily down regulated followed by up regulation, (5) temporarily up regulated, (6) up regulated in newborn and then constant, or (7) up regulated with age.

HSP27, cvHSP and HSPB8 (Fig. 6). Also in the rodent heart αB-crystallin levels remain constant [32], but HSP27 levels decrease after birth [32,33] and HSPB8 expression is not detected in the foetal heart, increases after birth and then decreases significantly with age [34]. Based on semiquantitative analysis of cvHSP mRNA in human adult and foetal heart, it is also very likely that the expression level of cvHSP is not constant [22]. However, porcine HSPB2 first increases in the neonate heart and then decreases to foetal levels, which fits nicely to the expression described in rat and human heart [33]. These data indicate that the differential regulation of sHSPs in certain tissues may sometimes be species specific as was shown before [220].

Developmental expression may occur in response to normal physiological stress. For instance, in kidney the increased expression of αB-crystallin, HSP27, HSP20 and HSPB8 upon development may be due to exposure to toxic environmental or metabolic products. Since lungs are only used after birth, the striking increase in HSP20 and HSPB8 expression eight hours after birth may be a result of their use. In heart, expression of HSPB2 may be a response to oxidative stress experienced during

delivery, but could also be due to increased load on the heart after birth. Extensive use of muscles may result in increase in expression of some sHSPs, since HSP27 and αB-crystallin increase dramatically in rat hindlimb muscle after birth and decrease when the muscle is not used [35]. In this respect it would be interesting to find out if the sharp decrease of HSPB8 expression in the stomach of 3-year old pig (Fig. 5) is due to less stomach activity induced by a reduced food load. Interestingly, in brain, HSP27, HSP20 and HSPB8 (Fig. 6) are strongly decreased already within one hour after birth in cerebellum and cortex. This could be developmentally regulated, in order to try to protect these brain regions against stress before and during delivery.

The major impact of this study is that each tissue seems to have a unique profile of sHSP expression, which varies during development and may reflect the need of a particular tissue during development and protection against physiological stress. The expression profile might be related to specific functions assigned to sHSPs such as modulation of the cytoskeleton and inhibition of apoptosis. For most sHSPs these functions have not been assigned yet and a major future challenge lies in the identification of these functions.

ACKNOWLEDGEMENTS

The authors are grateful to Jana Forejtova who performed initial experiments for the HSPB8 protein, they acknowledge the outstanding technical assistance of J. Lareynie and Ms Herrouin in the processing of manuscript. We are indebted to Wilfried de Jong for critical reading of the manuscript.

Testis-specific human small heat shock protein HSPB9 is a novel cancer/testis-associated gene, and interacts with the dynein subunit TCTEL1

Pauline Verschuure [*,1]
Nicole J.W. de Wit [*,2]
Guido Kappé [1]
Stephen M. King [3]
Wilfried W. de Jong [1]
Wilbert C. Boelens [1]
Goos N.P. van Muijen [2]

[*] *Both authors contributed equally*
[1] *Department of Biochemistry, Nijmegen Center for Molecular Life Sciences, University of Nijmegen, Nijmegen, The Netherlands*
[2] *Department of Pathology, University Medical Center Nijmegen, Nijmegen, The Netherlands*
[3] *Department of Biochemistry, University of Connecticut Health Center, Farmington, CT, USA*

Submitted for publication

Searching EST databases for new members of the human small heat shock protein family, we recently identified HSPB9, which is expressed exclusively in testis as determined by Northern blotting [27]. Here we confirm this testis-specific expression pattern by RT-PCR in a broader range of normal tissues. Interestingly, while screening HSPB9 ESTs, we also noted expression in tumors. Using RT-PCR we confirm HSPB9 expression in tumor cell lines and tumor lesions and therefore conclude that HSPB9 belongs to the steadily growing number of cancer/testis-associated genes. To get a better understanding of the function of HSPB9, we performed a yeast two-hybrid screen to search for HSPB9-interacting proteins. TCTEL1, a light chain component of cytoplasmic and flagellar dynein, interacted in both the yeast two-hybrid system and in immunoprecipitation experiments with HSPB9. Immunohistochemistry showed endogenous expression of HSPB9 in human testis and co-expression with TCTEL1 in the same stages of spermatogenesis. The possible functional significance of this interaction is discussed.

INTRODUCTION

Small heat shock proteins (sHSPs) are molecular chaperones which play a role in many cellular processes (for recent reviews see [12,192,193]). They are often induced upon stress and, when overexpressed, can confer cytoprotection. Various sHSPs associate with and can protect the cytoskeleton. Three sHSPs, HSP27, αA- and αB-crystallin, are able to inhibit apoptosis. Additionally, HSP27 has been identified as a negative prognostic factor in different types of cancer, possibly because its over-expression makes cells more resistant to treatment with anticancer drugs. Several studies showed enhanced growth of tumor cells expressing HSP27 [221].

Ten active genes for sHSPs have been identified in the human genome [13]. Most of them are expressed in a wide variety of tissues, with highest expression in heart and skeletal muscle, but two sHSPs - HSPB9 and HSPB10 - are expressed exclusively in testis [13,27]. HSPB10, or outer dense fiber protein 1 (ODF1) [194] probably serves a structural role in the sperm tail. Nothing is known about the functions and properties of HSPB9, but its expression in testis in combination with finding HSPB9 ESTs in lung and germ cell tumor libraries (this paper), raised the question whether HSPB9 belongs to the growing number of cancer/testis-associated genes (CTAs). These CTAs include a variety of unrelated gene families, like MAGE [222], GAGE [223], SSX [224], NY-ESO [225], XAGE [226,227], SPAN-X/CTp11 [228] and MMA-1 [229]. So far, little is known about functions of CTAs. In normal testis these genes are mainly expressed in primitive germ cells. Malignant transformation is often associated with activation or derepression of silent cancer/testis genes, which results in expression of CTAs in a variable proportion of a wide range of human tumors [225,230]. Another feature of the CTA genes is that most of them are mapped to chromosome X. However, recently several CTAs have been described with other chromosomal localizations [229,231].

In this study, we extensively determined

the expression profile of HSPB9 mRNA in normal and tumor tissues by semi-nested RT-PCR. Additionally, in order to get a better insight into the biological function of HSPB9, we searched for HSPB9-interacting proteins in a yeast two-hybrid screen using HSPB9 as bait. This search identified t-complex testis expressed protein 1 (TCTEL1; TCTEX1 in mouse), a light chain component of dynein [232], as a putative interactor. Immunohistochemistry was performed to visualize the localization of HSPB9 in normal human testis and to determine co-expression of HSPB9 and TCTEL1.

MATERIALS AND METHODS

Human tissue samples and cell lines

Tumor samples were collected during surgery at the University Medical Center Nijmegen (The Netherlands), whereas normal tissues, except for placenta, were derived from autopsies (post-mortem delay less than four hours). All tissue samples were immediately frozen in liquid nitrogen en stored at -80°C until use. For immunohistochemical staining normal testis tissue was formalin-fixed and paraffin-embedded.

Human tumor cell lines were grown in Dulbecco's modified Eagle's medium (DMEM) as described earlier [233,234]. For expression profiling of HSPB9 we examined human tumor cell lines derived from different tumor types, like mammary carcinoma (MDA-MB-231*, MDA-MB-468*, BT-474*), bladder carcinoma (RT4*, T24*), stomach carcinoma (AGS*, KATOIII*, Hs 746T*, MD), lung carcinoma (GLC1, GLC2, GLC3, GLC8, GLCa01, GLCa02, GCLp01 [235]) colon carcinoma (CaCo-2*, LS 174T*, LoVo*, COLO 320*, T84*, HT-29*, SW480*, SW1398 [236]), liver carcinoma (Hep3B*, HepG2*, PLC/RPF/5*, Huh7*) and melanoma (1F6, 530, Mel57, M14, MV1, BLM [234]). A number of these cell lines were generously supplied by the Departments of Human Genetics, Urology and Gastro-enterology, UMC Nijmegen (The Netherlands) and the Department of Pathology, University Hospital of Groningen (The Netherlands). Cell lines indicated with * are from the American Type Culture Collection (Rockville, MD, USA).

RNA isolation

For total RNA isolation from tissue samples, at least 5 frozen slices of 20 µm thickness were squeezed with a pestle in 1 ml RNAzolB™ (Campro, Veenendaal, The Netherlands). After the RNAzolB™ treatment, total RNA was subjected to an additional cleaning step with RNeasy (Qiagen, Hilden, Germany). In the case of cell lines, total RNA was isolated from 2 x 10^7 cultured cells using the RNeasy mini kit (Qiagen). All methods were performed according to the manufacturers' protocols.

RT-PCR analysis

Aliquots of 1 µg of total RNA from human tissue samples and cell lines were reverse-transcribed using M-MLV reverse transcriptase (Promega, Madison, WI, USA). In addition to 200 units of M-MLV RT, the reaction mixture consisted of 250 pmol of random hexadeoxynucleotide primers (Roche Diagnostics GmbH, Penzberg, Germany), 4 µl of RT buffer (250 mM Tris-HCl pH 8.3, 375 mM KCl, 15 mM $MgCl_2$, 50 mM DTT) and 4 µl of 1 mM dNTPs (Roche Diagnostics GmbH), with water added to a final volume of 20 µl. This mixture was incubated 10 min at 25°C, 59 min at 42°C and 5 min at 95°C.

The first round of PCR amplification was carried out in a total volume of 25 µl containing 1 µl reverse-transcribed cDNA, 1.5 µl of $MgCl_2$ solution (25 mM), 2.5 µl of

PCR buffer IV (20 mM $(NH_4)_2SO_4$, 75 mM Tris/HCl pH 9.0 and 0.1% Tween), 5 pmol of each primer (F: 5'-GACTCGGATGCAGA-GAGTCGGTAACACCTTC-3'; R: 5'-TTTTT-TTTTTTTTTTGCTGCAC-3'), 0.15 units of Thermoperfectplus DNA polymerase (Integro, Zaandam, The Netherlands). After 5 min of denaturation at 94°C, 30 cycles of amplification were carried out: 45 sec at 94°C, 45 sec at 64°C, 1 min at 72°C, followed by a 5 min elongation step at 72°C.

For semi-nested PCR, the initial PCR products were diluted 1:100 and then 1 µl was added to the PCR reaction mixture. Both PCR mixture and program were identical to that of the first PCR, except for the reverse primer (R: 5'-CGTCCTCGAGTT-ACCGGGTCAGGTTGGAAGC-3') and the annealing temperature (60°C). For each cDNA sample three independent semi-nested PCRs were performed, and samples were considered HSPB9 positive only if expression was seen in all three experiments.

To verify the HSPB9 specificity of the PCR product sequence analysis was performed. About 25 ng of the PCR product was analyzed using 10 µM specific forward or reverse primer and the ABI PRISM 3700 DNA Analyzer (Perkin-Elmer, Applied Biosystems).

Antisera

Antiserum against human HSPB9 (hHSPB9) was raised in rabbit using a synthetic peptide corresponding to the HSPB9 sequence 137-151 (PEAQTGPSPRLG-SLG). The HSPB9 antibodies were affinity purified using the same peptide. Antibodies against TCTEL1 were isolated by nitrocellulose blot purification [232]. Monoclonal antibodies against the VSV tag were isolated from cell line P5D4 [237] (gift from T.E. Kreis†, Department of Cell Biology, University of Geneva, Switzerland).

Plasmid contructs

For recombinant expression, hHSPB9, which is intronless, was amplified from genomic DNA by PCR using the following primers: forward 5'-CACTCCCATGGAG-AGAGTCGGTAACACCTTC-3' and reverse 5'-CGTCCTCGAGTTACCGGGTCAGGTT-GGAAGC-3'. The PCR fragment was digested with NcoI and XhoI and ligated into the pET16b plasmid (Novagen, Madison, WI, USA). After transformation in *E. coli*, expression of recombinant HSPB9 is induced by addition of IPTG.

To generate the hHSPB9 yeast two-hybrid vectors, the same digested PCR fragment was ligated in frame with the LexA-DNA binding domain of the slightly modified pEG202 (bait) plasmid and with the transcription activation domain of the slightly modified pJG4-5 (prey) plasmid (both kindly provided by R. Brent [238], Molecular Sciences Institute, Berkeley, CA, USA). The N-terminus of hHSPB9 (residues 1-46) was amplified from this vector using the same forward primer and 5'-CATCTCG-AGTTAGTCCTCCTGAGCCGCT-3' as reverse primer. The C-terminus (residues 47-159) was amplified using the same reverse primer and 5'-TTGCCATGGAAAATGACC-ACGCCAGAGA-3' as forward primer. Both N- and C-terminal PCR fragments were digested with NcoI and XhoI and ligated into the pEG202 and the pJG4-5 plasmids.

Mouse HSPB9 (mHSPB9) was amplified from genomic DNA by PCR using the following primers: forward 5'-GGAATTCC-ATATGCAGCGGGTAGGAAGC-3' and reverse 5'-CGAATTCGGATCCCTAAGGA-TTCTTCACACTTTC-3'. The PCR fragment was digested with EcoRI and ligated in frame in the pEG202 and the pJG4-5 plasmids.

pEG-TCTEL1 was created by digesting the pJG-TCTEL1 plasmid, which was picked up by the yeast two-hybrid screen, with

EcoRI and ligating the TCTEL1 fragment into the pEG202 plasmid. pEG-hαB-crystallin and pJG-hαB-crystallin were created by digesting pET16-human αB (gift from P. Muchowski, University of Washington, Seattle, WA, USA) with NcoI and XhoI, and ligating the αB-crystallin fragment into the pEG202 and pJG4-5 plasmids.

For expression in human cell lines, pIRES-HSPB9 was constructed by digesting pEG-HSPB9 with BglII and BamHI, and ligating the HSPB9 fragment into the pIRESneo vector (Clontech, Woerden, the Netherlands). VSV-tagged TCTEL1 was created by amplifying TCTEL1 by PCR using the following primers: 5'-CAGCTCGAGATGGAAGACTACCAGGC-3' and 5'-ATACTCGAGTCAAATAGACAG-TCCGA-3'. The PCR fragment was digested with XhoI, and ligated into the pCIneo vector (Promega) in which the VSV-tag sequence (coding for EIYTDIEMNRLGK) was inserted into the NheI and XhoI restriction sites.

Cell transfections and co-immuno-precipitation

HeLa cells and Hep3B cells were cultured at 37°C in DMEM supplemented with 10% fetal calf serum in the presence of 5% CO_2. Transient transfections were performed using Fugene 6 (Roche Diagnostics GmbH) according to the supplier's manual. For co-immuno-precipitation experiments, cells were harvested one day after transfection and lysed in buffer (50 mM Tris pH 7.5, 100 mM NaCl, 0.5% NP-40) at 4°C. Cell lysate was cleared by centrifugation at 4°C and incubated with protein agarose beads (Kem-En-Tec A/S, Copenhagen, Denmark) coupled with rabbit antibodies against HSPB9. After incubation at 4°C, beads were washed with buffer (50 mM Tris pH 7.5, 100 mM NaCl, 0.05% NP-40) and analyzed on Western blot using anti-vesicular stomatitis virus (VSV) antibodies.

Electrophoresis and Western blot analysis

SDS-PAGE was performed following standard procedures. For Western blot analysis, proteins were transferred electrophoretically to a nitrocellulose membrane (Schleicher & Schuell, Dassel, Germany), and the membrane was incubated successively with primary antibodies and with alkaline phosphatase-conjugated secondary antibodies (rabbit anti-mouse or swine anti-rabbit; Promega).

Yeast two-hybrid screen

For the interaction screening, yeast strain EGY48 (*ura3 trp1 his3 3LexA-operator-LEU2*; Clontech) containing bait plasmid pEG-HSPB9 and LacZ reporter plasmid pSH18-34, was transformed with the library pJG-HeLa (HeLa cell line) or with the library pJG-brain (human fetal brain; both libraries kindly provided by R. Brent). Transformants were selected on plates lacking histidine, uracil and tryptophan. After induction of the prey expression, the transformants were transferred to galactose plates lacking leucine to select for proteins able to interact with the HSPB9 fusion protein. For positive clones, which also gave blue coloring on Xgal containing plates, activation of the LacZ reporter was determined.

In studying the interaction between two proteins, we considered the interaction to be positive when LacZ reporter activation was found in both orientations (i.e. when protein A was used as bait and protein B as prey and *vice versa*).

Immunohistochemistry

Four-micrometer sections of paraffin-embedded normal human testis were mounted on Superfrost microscope slides.

These sections were dewaxed in xylene and rehydrated in a series of graded alcohols. For antigen retrieval, rehydrated slides were placed in citrate buffer (pH 6.0) and heated in a microwave oven to 97°C at 850 W for 5 min. This temperature was maintained with an additional 10 min heating at 350 W. After cooling down to room temperature, the sections were briefly washed with phosphate-buffered saline (PBS, pH 7.4) and preincubated with 20% normal goat serum (Vector Laboratories, Burlingame, CA, USA) for 20 min. The sections were stained in a three-step procedure utilizing the following incubations. Overnight incubation at 4°C with affinity purified polyclonal rabbit antibodies against HSPB9 or TCTEL1, diluted 1:100 and 1:300 in PBS, respectively. Thereafter, the sections were incubated with a biotinylated goat-anti-rabbit antiserum for 30 min, followed by a 45 min incubation with peroxidase-labelled avidin-biotin complex (Vector Laboratories). Between all incubations, sections were washed three times in PBS. 3-amino-9-ethylcarbazole was used as substrate to visualize the bound antibodies. After counterstaining with Meyers haematoxylin, sections were mounted with Imsol.

RESULTS

Expression of HSPB9 mRNA in normal tissues, tumor cell lines and fresh tumor lesions

In a previous study we already demonstrated by Northern blotting that among sixteen normal human tissues HSPB9 was only expressed in testis [27]. Screening of EST databases indicated, besides presence in normal human testis, expression in lung and germ cell tumors (Table 1). As such an expression, restricted to normal testis and several types of tumors, is common for CTAs, we wanted to determine the expression profile of HSPB9 in more detail by performing semi-nested RT-PCR on a panel of thirty normal human tissues, various tumor cell lines and fresh tumor lesions of different tissue origin. Because HSPB9 has an intronless transcript, it was

Table 1. HSPB9 ESTs found in the human EST-database

Library name [a]	Tissue type	Number of ESTs found [b]
NCI_CGAP_Lu24	lung, carcinoid	6/36636
NCI_CGAP_Lu5	lung, carcinoid	4/20359
Human insulinoma	pancreatic islet, benign hyperplasia	4/24367
NCI_CGAP_GC6	pooled germ cell tumors	4/39242
Soares_testis_NHT	normal testis	3/46060
NCI_CGAP_Sub1	pooled NCI_CGAP libraries [c]	1/1584
NCI_CGAP_Sub2	pooled NCI_CGAP libraries [c]	1/1562
Soares_total_fetus_Nb2HF8_9w	total fetus	1/27047
Soares_NFL_T_GBC_S1	pooled normal testis, B-cell and fetal lung	1/65708

[a] As named by the Cancer Genome Anatomy Project, http://cgap.nci.nih.gov/; [b] The number of HSPB9 ESTs found in a library compared to the total number of ESTs sequenced; [c] Contains amongst others the NCI_CGAP_Lu24, NCI_CGAP_Lu5 and NCI_CGAP_GC6 libraries

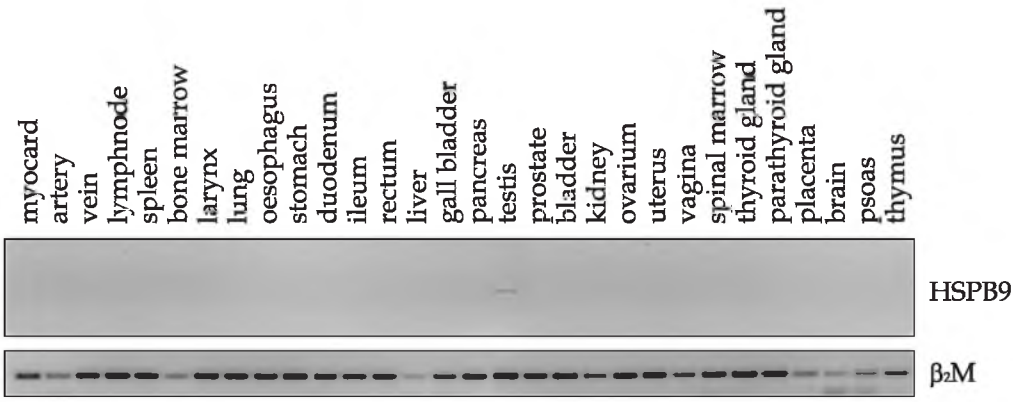

Figure 1. Expression profile of HSPB9 mRNA in normal human tissues, determined by semi-nested RT-PCR
Samples were normalised for the housekeeping gene β_2 microglobulin (β_2M). After 55 rounds of amplification only testis was found positive for HSPB9.

essential to perform PCR analysis that is specific for cDNA and avoids amplification of genomic DNA. Therefore, we designed a primer recognizing seven base pairs of the 3'-specific part of the HSPB9 transcript followed by fifteen base pairs of the poly-A tail. Additionally, we used a high annealing temperature (64°C) to enforce specific amplification of HSPB9 transcripts. Sequence analysis showed HSPB9 specificity of the PCR products. In addition, to ensure that only cDNA was amplified during semi-nested PCR, a sample of genomic DNA was taken along. This sample remained negative in all experiments.

First, we focused on the expression of HSPB9 among normal human tissues. In a first round of amplification (30 cycles) no HSPB9 expression was detectable, most probably due to the high annealing temperature reducing the yield of PCR product. Three independent semi-nested PCRs showed that after 55 cycles HSPB9 expression was only positive in testis (Fig. 1). Five additional cycles of amplification intensified the HSPB9 band in testis, whereas all other normal tissues remained negative (data not shown). These results confirm that expression of HSPB9 is confined to testis.

Also for tumor cell lines and fresh tumor lesions we performed three independent semi-nested PCRs (60 cycles). Table 2 shows that HSPB9 expression was detected in tumor cell lines of lung (5/7), liver (3/4) and melanoma (1/6). As for fresh tumor lesions, we found HSPB9 expression in tumors originated from pancreas (3/5), testis (3/5), ileum (2/4), colon (2/5), lung (2/5) and oesophagus (1/5) (Table 3). However, positivity seen in testis tumors may be influenced by the presence of normal testis tissue.

Table 2. HSPB9 expression in human tumor cell lines determined by RT-PCR

Type of tumor cell line	Semi-nested PCR
lung	5/7 [a]
liver	3/4 [b]
melanoma	1/6 [c]
bladder	0/2
mammary	0/3
stomach	0/4
colon	0/8

HSPB9 positive cell lines: [a] GLC1, GLC2, GLC3, GLCa02, GLC8; [b] Hep3B, PLC/RPF, Huh7; [c] MV1.

Table 3. HSPB9 expression in fresh human malignant tumor tissue samples determined by RT-PCR

Type of malignant tumor tissue	Semi-nested PCR
pancreas	3/5
testis	3/5
ileum	2/4
colon	2/5
lung	2/5
oesophagus	1/5
mammary	0/4

TCTEL1 interacts with HSPB9

To get insight into the biological function of HSPB9, we searched for HSPB9-interacting proteins in a yeast two-hybrid screen using HSPB9 as "bait". Unfortunately, we did not have a testis library available, so we used two different libraries from human origin (HeLa and fetal brain) to transform into yeast. A total of approximately 3 million colonies were screened (HeLa, 2 million; fetal brain, 1 million), and after eliminating false positive colonies, 5 colonies were truly positive. TCTEL1 (t-complex testis expressed protein 1) was found as HSPB9-interacting protein in both libraries, while CTCF (CCCTC-binding factor; zinc finger protein), NUDT5 (nudix hydrolase) and an unknown protein (not similar to a known protein using BLAST search) were only found in the HeLa library. Interestingly, HSPB9 self-interaction could not be detected in the yeast two-hybrid system (data not shown), even though self-interaction has been described for most other members of the sHSP family [30]. Only the HSPB9-TCTEL1 interaction could be confirmed in other systems than the yeast two hybrid (see below), and we therefore focus here on the interaction with TCTEL1.

In the yeast two-hybrid system, TCTEL1 could not bind to the fusion domains alone (DNA binding domain or activation domain), strongly indicating that the HSPB9-TCTEL1 interaction is specific (Table 4). To further characterize this interaction, we made two deletion mutants of HSPB9. Since all sHSPs have a variable N-terminal region and a conserved C-terminal domain (the α-crystallin domain, [6]), one mutant coded for the N-terminus (residues 1-46) and the other for the C-terminus of HSPB9 (residues 47-159). When tested for interaction with TCTEL1, the C-terminus was positive, while the N-terminus was negative (Table 4). This is in accordance with the finding that also other sHSPs interact with TCTEL1 (data not shown), since it is the C-terminus that is conserved between sHSP family members.

We already reported [27] that the sequence identity between human and mouse HSPB9 is unusually low (62% identity, compared to 85-98% for other sHSPs). In contrast, TCTEL1 is almost identical in human and mouse (94% sequence identity). We therefore tested whether mouse HSPB9 could bind human TCTEL1, and found indeed interaction, but not as strong as for human HSPB9 (Table 4). The fact that the interaction is conserved in human and mouse, while the HSPB9 sequence is so divergent, may indicate that it is a relevant feature.

To determine whether the interaction

Table 4. Interaction between TCTEL1 and HSPB9 as determined in the yeast two-hybrid system

	Interaction with TCTEL1
hHSPB9	++
N-hHSPB9 (residues 1-46)	-
C-hHSPB9 (residues 47-159)	++
mHSPB9	+
TCTEL1	++
empty vector [a]	-

+ interaction; ++ strong interaction; - no interaction;
[a] empty vector (expressing only the DNA binding domain or the activation domain) is used as a negative control.

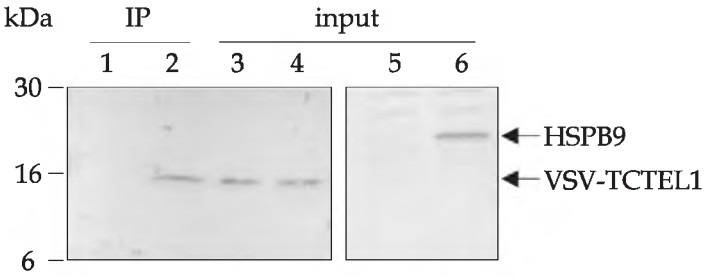

Figure 2. TCTEL1 co-immunoprecipitates with HSPB9
HeLa cells were transiently transfected with 5'VSV-TCTEL1 and either pIRES (control; lanes 1,3,5) or pIRES-HSPB9 (lanes 2,4,6). Cell extracts were used for immunoprecipitation with anti-HSPB9 antiserum (lanes 1,2), and analyzed on Western blot with anti-VSV antibodies. 5'VSV-TCTEL1 expression (0.5% input; lanes 3,4) and HSPB9 expression (5% input; lanes 5,6) in the cell extracts was analyzed on Western blot with anti-VSV antibodies and anti-HSPB9 antiserum, respectively.

between HSPB9 and TCTEL1 as identified in the yeast two-hybrid system can also take place in mammalian cells, we assayed the interaction by co-immunoprecipitation experiments. For that purpose we transiently co-transfected HSPB9 and VSV-tagged TCTEL1 in HeLa cells. By immunoprecipitation with antiserum against HSPB9, VSV-tagged TCTEL1 could be co-precipitated and immunodetected (Fig. 2, lane 2). Precipitation of VSV-tagged TCTEL1 was not detected in cells not transfected with HSPB9 (Fig. 2, lane 1). These results show that interaction between HSPB9 and TCTEL1 can indeed occur in mammalian cells.

Detection of endogenous HSPB9 protein

To try to determine the presence of HSPB9 protein in tumor cell lines, Western blotting was performed using affinity purified anti-HSPB9 polyclonal antibody. Extracts from RT-PCR negative (HT29) and RT-PCR positive (Hep3B and MV1) tumor cell lines were analyzed, as well as transiently transfected HSPB9 in Hep3B cells and recombinantly expressed HSPB9 (Fig. 3). We loaded maximum protein amounts and stained until background signal became apparent. Both recombinantly expressed HSPB9 and transiently transfected HSPB9 were detected as a single band of about 21 kDa, indicating that the antiserum is highly specific. Unfortunately, we were not able to detect endogenous HSPB9 in the tumor cell lines. In extracts from human testis, we were also unable to detect HSPB9 protein (data not shown).

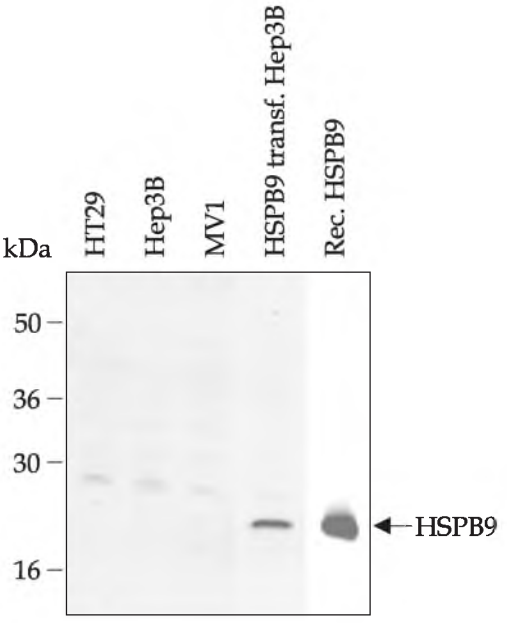

Figure 3. Western blot analysis of HSPB9 expression
RT-PCR negative (HT-29) and positive (Hep3B, MV1) cell lines, Hep3B cells with transiently transfected HSPB9 and recombinant HSPB9 were analyzed on Western blot stained with anti-HSPB9 antiserum. Molecular weight markers are indicated on the left.

Since Western blot analysis may not be sensitive enough to detect HSPB9 when expression is restricted to a small percentage of cells within a tissue, we performed immunohistochemical staining. In normal human adult testis, indeed we found expression of endogenous HSPB9 in only a limited number of cells (Fig. 4A,B). Staining was found in the seminiferous tubuli, specifically in the nuclei of spermatogonia and early spermatids, and a somewhat weaker expression was detected in part of the primary spermatocytes. Leydig cells, Sertoli cells, remaining primary spermatocytes and late spermatids [239] were all negative. Besides staining in the seminiferous tubuli, we, surprisingly, also found weak staining of muscle cells surrounding blood vessels in the interstitial tissue of testis (Fig. 4A). However, our RT-PCR results showed no expression of HSPB9 in other normal tissues, including those containing abundant blood vessels. Even artery and vein samples remained negative (see Fig. 1). The positive staining found in muscle cells in testis must therefore be due to cross-reactivity of the HSPB9 antibodies.

To determine whether HSPB9 and TCTEL1 occur in similar cells, and thus potentially can interact *in vivo*, consecutive paraffin sections of normal human adult testis were stained with anti-HSPB9 and anti-TCTEL1 antibodies. Both HSPB9 and TCTEL1 were found to be expressed in the seminiferous tubuli (Fig. 4E,G). TCTEL1 was located in the cytoplasm, and the most intensive staining was seen in spermatogonia, primary spermatocytes and early spermatids (Fig. 4H). These are the same cells, involved in spermatogenesis, that show a nuclear staining for HSPB9 (Fig. 4F).

DISCUSSION

In a previous study, Northern blotting and *in situ* hybridization (ISH) showed testis restricted expression of HSPB9, and screening EST databases revealed its expression in various types of cancer [27]. These findings suggested that HSPB9 could be a new CTA. A more extensive expression profiling in this study, by semi-nested RT-PCR, confirmed that the expression of HSPB9 is restricted to testis among thirty normal human tissues. Additionally, HSPB9 expression was also found in cell lines derived from malignant tumors of liver, lung and melanoma, and in fresh tumor lesions of various origins (pancreas, testis, ileum, colon, lung and oesophagus). This expression profile clearly shows that HSPB9 indeed can be considered as a CTA.

Immunohistochemical staining showed HSPB9 expression in primitive germ cells (spermatogonia, certain primary spermatocytes) as well as in later stages of spermatogenesis (early spermatids). Staining was nuclear in spermatogonia and early spermatids. For some primary spermatocytes a somewhat weaker signal was detected in the nucleus, whereas other primary spermatocytes remained negative. This disparity in staining might be explained by the fact that primary spermatocytes within a seminiferous tubule can be found in different stages of meiotic division. In our immunohistochemical analyses it was not possible to make a distinction between these stages. The expression pattern of HSPB9 fits that of most other CTAs, which in normal adult testis is primarily restricted to primitive germ cells, e.g. spermatogonia [240,241]. But there are also CTAs that are involved in later stages of sperm maturation [231].

Comparing the immunohistochemical staining with previous ISH data [27], we

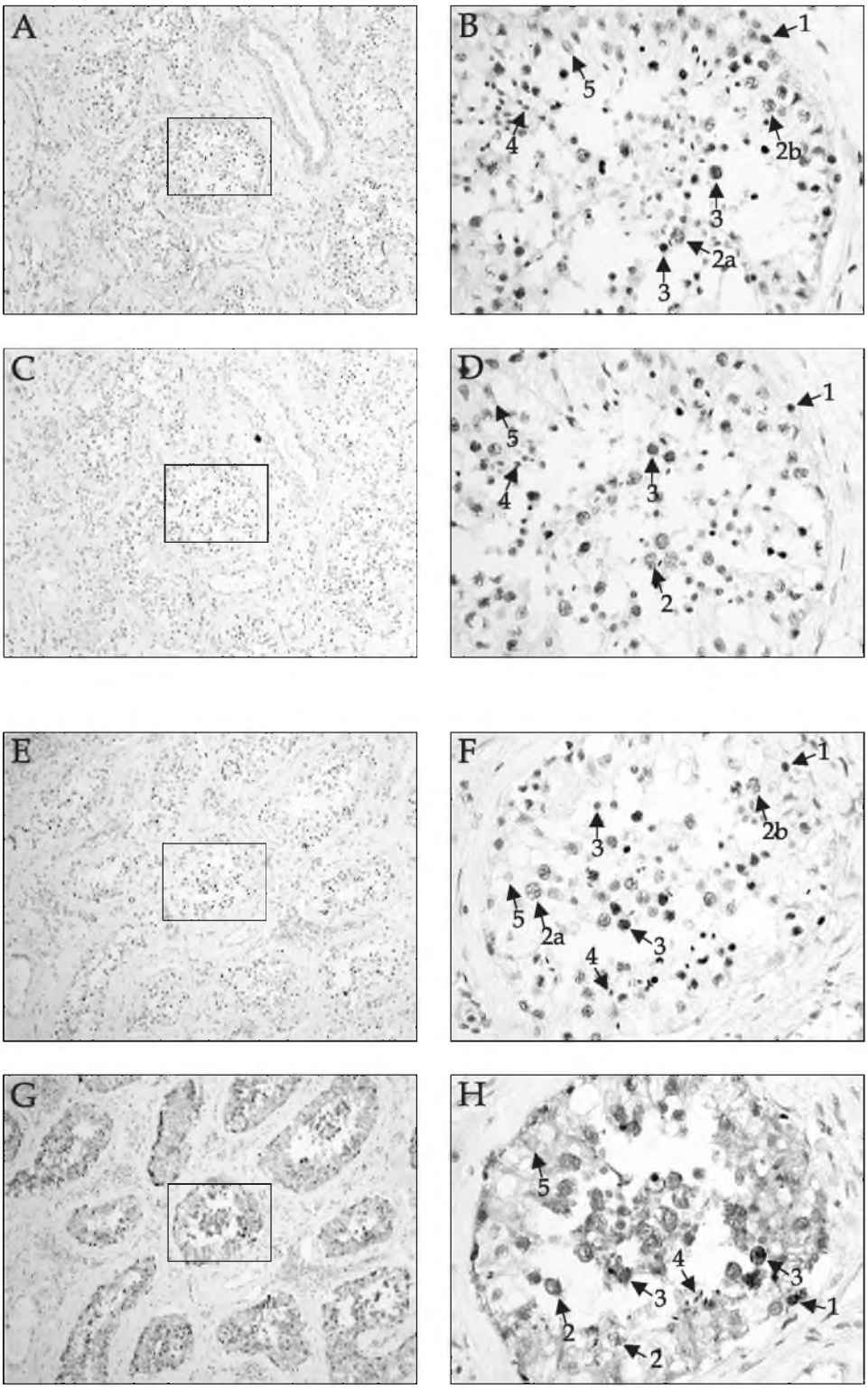
A
B
1
5
4
2b
3
2a
3
C
D
1
5
4
3
2
E
F
1
2b
3
5
2a
3
4
G
H
5
4
3
3
1
2
2

find accordance in the expression of HSPB9 protein and mRNA in part of the primary spermatocytes and spermatids, whereas Sertoli cells, other primary spermatocytes and spermatozoa are negative. Regarding spermatogonia, we see a discrepancy in the absence of mRNA and presence of protein expression. However, this might be due to the fact that the ISH experiment was performed on normal mouse testis, whereas for immunohistochemical staining we used normal human tissue. Also when comparing mRNA and protein expression of another member of the sHSP family that is expressed in testis, HSP27, a similar discrepancy is found. HSP27 mRNA is exclusively found in spermatocytes and is not detected in spermatogonia, spermatids, Sertoli or interstitial cells [184], while HSP27 protein is found in spermatocytes, spermatogonia, spermatids and Sertoli cells [80]. In contrast to HSPB9, HSP27 protein is present in the cytoplasm of cells, a localization more common for sHSPs.

In the yeast two-hybrid and immunoprecipitation analyses we found TCTEL1 as an HSPB9-interacting protein. Expression of TCTEL1 in testis coincides with that of HSPB9. Like for HSPB9 mRNA [27], TCTEL1 mRNA transcription is abruptly initiated at the pachytene stage of meiosis I and persists throughout spermatogenesis [242]. We have shown here that HSPB9 and TCTEL1 are co-expressed as proteins in the same cells during spermatogenesis (Fig. 4), but no subcellular co-localization was detected.

TCTEL1 is a light chain component of dynein. Dyneins are (-) end directed, energy-dependent tubulin motor proteins, and are divided into two functional classes [243]. Axonemal dyneins are located in axonemes of cilia and flagella, and generate the sliding forces between microtubules. Cytoplasmic dyneins are found in most eukaryotic cells, and are involved in the movement of vesicles, cellular organelles and chromosomes. TCTEL1 has been identified as a light chain component of both cytoplasmic dynein [232] and of axonal dynein [244]. For cargo specificity, factors such as dynactin and dynein subunits - like TCTEL1 - have been shown to be important [245].

The interaction of HSPB9 and TCTEL1 could not be corroborated by co-localization studies using immunohistochemical staining. However, since TCTEL1 has a function in transport, one might expect that the interaction occurs only temporarily. This might explain the observed difference in subcellular localization. Additionally, yeast two-hybrid and co-immunoprecipitation experiments provided evidence for interaction of TCTEL1 with other sHSPs, such as HSPB3, cvHSP and HSPB8 (data not

Figure 4. Immunohistochemistry of consecutive paraffin-embedded sections of normal human testis using anti-HSPB9 and anti-TCTEL1 antibodies

(A) Overview of human testis section after immunohistochemical staining using anti-HSPB9 antibodies. Besides nuclear staining of certain cells in the seminiferous tubuli, muscle cells surrounding most of the blood vessels also show weak positive staining. **(B)** Higher magnification of the boxed area in A, comprising seminiferous tubules, demonstrates positive nuclear staining of spermatogonia (1) and early spermatids (3). Late spermatids (4) and Sertoli cells (5) are negative. As for primary spermatocytes (2), some are HSPB9 positive (2a), whereas others show no HSPB9 expression (2b). **(C,D)** Low (10x) and high (40x) magnification of human testis sections leaving out anti-HSPB9 antibodies during immunohistochemical staining (negative control). Spermatogenic cells are numbered as in B.

(E,G) Overview (10x magnification) of consecutive human testis sections after immunohistochemical staining using anti-HSPB9 and anti-TCTEL1 antibodies, respectively. HSPB9 and TCTEL1 are both detected in the seminiferous tubuli of the testis. **(F,H)** Higher magnification of the boxed areas in E and G. Arrows (numbering as in B) show expression of HSPB9 and TCTEL1 in similar cells during spermatogenesis, although they show a nuclear versus cytoplasmic staining, respectively. A colour version of this image is available on page 119.

shown), indicating that transport of sHSPs by dynein may be more general. The actual function of HSPB9 in the nucleus of specific cells during spermatogenesis remains an open question. One might speculate that HSPB9 is involved in imprinting since one of the other yeast two-hybrid interactors is CTCF, a transcription factor whose role in imprinting has been previously described [246]. Furthermore, since no testis library was available for our yeast two-hybrid screen, we may have missed possible testis-specific interactors of HSPB9, which could shed more light on its (nuclear) function. Unravelling the biological role of HSPB9 may also contribute to a better understanding of the involvement of CTAs in cancer development.

ACKNOWLEDGEMENT

S.M.K. is supported by National Institutes of Health grant GM51293.

7

General discussion—Summary

The small heat shock proteins (sHSPs) form a family of molecular chaperones, which are present in almost all organisms. All members contain a conserved C-terminal domain, the α-crystallin domain, while the N-terminus is variable [6]. They typically have a monomeric mass ranging between 16 and 25 kDa and can form homo- and heteromeric complexes. However, our knowledge about sHSP structures and functions is very limited. Even though recently two eukaryotic sHSPs have been crystallized, resolving (part of) their structure [7,8], still not much is known about the actual functions of sHSPs. They can bind unfolding proteins *in vitro* and transfer them to other HSPs in order to be refolded [5]. *In vivo* they can confer thermotolerance to cells when overexpressed, protect cells against apoptosis, are involved in the organization of the cytoskeleton and play a role in many diseases. In the introduction of this thesis (Chapter 1) small heat shock proteins are described in more detail. Since not all sHSPs possess the aforementioned characteristics, a major challenge lies in the unraveling of the exact function(s) of each sHSP. This thesis describes the exploration of characteristics and functions of members of the mammalian sHSP family both under normal physiological conditions and in stress situations.

MAMMALIAN SMALL HEAT SHOCK PROTEINS AND THE PROTEASOME

Efforts to understand the functions of proteins often include identification and characterization of other cellular proteins with which they can interact. Thus one clue for the function(s) of sHSPs may come from the identification of proteins that can bind these sHSPs. α-Crystallin, the lens-specific complex composed of two of the sHSPs (αA- and αB-crystallin), has been shown to have a certain affinity for the 20S proteasome [147,148]. Furthermore, in a yeast two-hybrid screen using αB-crystallin as 'bait' 99% of the interacting proteins turned out to be the proteasomal subunit HC8 [149]. Since αB-crystallin can bind unfolding proteins, while proteasomes play a critical role in cell survival by keeping the cytoplasm clear of unwanted proteins, we investigated a possible functional relationship between αB-crystallin and proteasomes (Chapter 2). We reported that upon proteasome inhibition, αB-crystallin and HSP27 translocate from the detergent-soluble, cytosolic fraction to the detergent-insoluble, nuclear/cytoskeletal fraction independent of phosphorylation. Immunocytochemistry revealed that αB-crystallin and HSP27, which show a diffuse cytoplasmic staining in unstressed cells, colocalize with F-actin upon proteasomal inhibition. Other sHSPs (αA-crystallin, HSP20, HSPB2 and HSPB3) showed similar translocation to the actin cytoskeleton. We suggested that the redistribution of sHSPs upon proteasomal inhibition may reflect a mechanism by which cells are protected from damaged intracellular proteins by sequestering them on the cytoskeleton. Our proposed mechanism was positively

commented on by M. Sussman, who further explored this suggestion by literature study [247].

Published data suggests that proteasomes degrade defective protein products and when they can not keep up, for instance when their activity is inhibited, indigestible inclusions called aggresomes can form [152]. In contrast to the co-localization with actin that we found in our study, aggresomes are associated with tubulin. They can be found at a juxtanuclear site within a cell, the microtubule-organizing center. HSP27 and αB-crystallin can both be recruited to aggresomes when proteasomes are inhibited [248]. Recently, it was suggested that aggresomes are cytoprotective [249]. We have suggested that also the phenomenon we described could be beneficial to cells. We found the actin-localized aggregates only in myoblast-derived cell types. Therefore, it is possible that aggregates co-localizing with actin are found in these cell types in response to proteasomal inhibition, while aggresomes are formed in others.

THE (COMPLETE) FAMILY OF MAMMALIAN SMALL HEAT SHOCK PROTEINS

To study sHSPs, one can compare for example their cellular behavior in normal and stress situations as described above. However, in order to understand the unique and overlapping functions of sHSPs it is a prerequisite to first know the actual number of small heat shock proteins that are present within a human being. Up until 1994, only three members of the sHSP family were known. Over the past few years, four other members were discovered, some as result of the increased amount of data in databases. The publication of cvHSP [22], identified by computational search of tissue-selective expression of expressed sequence tags (ESTs), prompted us to search the EST databases for more, until then, unknown small heat shock proteins. This search resulted in the identification of HSPB8 and HSPB9 (Chapter 3). While exploring the human genome, we found yet another member of the human sHSP family, HSPB10 [13]. The use of exhaustive search procedures did not yield more than ten human sHSP genes and it seems thus unlikely that additional sHSPs will still be detected in the human genome.

The ten mammalian sHSPs can be subdivided based on, amongst others, their sequence, tissue distribution, developmental expression and behavior in stress situations. Since they are highly divergent in sequence (see Fig. 2, Chapter 1), it is difficult to resolve their gene phylogeny. Consistent support can only be found for the grouping of αA-, αB-crystallin and HSP20 [13] as the most closely related sHSPs. Based on their tissue distribution [13,22,27,29-31] (see also below), human sHSPs can be divided into three groups: αA-crystallin, HSPB9 and HSPB10 are expressed exclusively in a single tissue (αA-crystallin in eye lens; HSPB9 and HSPB10 in testis), HSPB3 and cvHSP are predominantly expressed in heart and muscle, while HSP27, αB-crystallin, HSP20, HSPB2 and HSPB8 are more ubiquitously expressed, but highly in heart and muscle. Concerning the comparison of developmental expression and stress behavior of sHSPs, we focused on HSPB8 and compared this sHSP to other family members.

MAMMALIAN SMALL HEAT SHOCK PROTEIN HSPB8

In Chapter 3 we described the identification of the novel sHSP HSPB8. While this study was performed, HSPB8

appeared in literature under several names (H11 kinase, E2IG1 and HSP22), and intriguingly was reportedly to have kinase activity, to be estrogen inducible, and to mediate cell growth. Nevertheless, the basic features of HSPB8 as a heat shock protein, such as expression patterns, stress behavior and complex formation, were not yet characterized. We therefore compared HSPB8 with other sHSPs, notably HSP27, HSP20 and αB-crystallin (Chapter 4). We show that HSPB8 is not upregulated during differentiation, only slightly after heat shock, and markedly after arsenite treatment. Regulation seems to be primarily at the level of transcription like for other sHSPs. Interestingly, even though HSPB8 is regulated by estrogen at the mRNA level in the human breast cancer cell line MCF-7, there is no effect at the protein level, suggesting translation regulation. Thus HSPB8 regulation seems to take place both at the transcriptional and translational level.

Stress-induced phosphorylation of HSPB8 is cell type-dependent, indicating that the kinase(s) responsible for its phosphorylation is not ubiquitously expressed or activated. This is in contrast to HSP27 phosphorylation, which seems to be cell type-independent. *In vitro*, HSPB8 can be phosphorylated by protein kinase C and by p44 mitogen-activated protein kinase, but not by MAPKAPK-2 [24], while the latter is the major kinase responsible for the phosphorylation of HSP27 [56]. We therefore conclude that phosphorylation of HSPB8 and Hps27 is mediated by different kinases.

In the yeast two-hybrid assay, HSPB8 specifically interacts with HSP27, αB-crystallin and HSP20, but not with αA-crystallin and HSPB2. It has previously been reported that two types of sHSP heteromeric complexes exist in muscle [30]: one complex consists of HSP27, αB-crystallin and HSP20, and the other of HSPB2 and HSPB3. Our yeast two hybrid data suggest that HSPB8 might be present is a complex with the former three sHSPs in muscle. Glycerol density gradient centrifugation, however, shows that HSPB8 forms complexes with a size very similar to HSP27 and HSP20, but different from αB-crystallin. Phosphorylation of HSP27 reduces its complex size, and HSPB8 cofractionates with the smaller HSP27 complexes, suggesting that HSPB8 prefers to interact with phosphorylated HSP27 as was shown by Benndorf *et al.* [24]. It is possible that also the interaction of HSPB8 with αB-crystallin is regulated by posttranslational modifications.

sHSP expression is developmentally regulated [211] and it has therefore been speculated that they have specific developmental functions. In Chapter 5 we have investigated the tissue distribution and developmental expression pattern of HSPB8 in pigs and compared them to HSP20, HSPB2 and cvHSP. We found a ubiquitous expression of HSP20 and HSPB8 as earlier reported for HSP27 and αB-crystallin. In contrast, cvHSP and HSPB2 expression was essentially restricted to heart and muscle. These expression patterns fit well with what has been reported in other mammals (see above). During development, we specifically focused on the expression patterns in the first few hours and days after birth, since the physiological circumstances of the different organs change dramatically during this period (e.g., lungs). We found that sHSP expression can be constant, (temporarily) increased, (temporarily) decreased or variable during development (see Fig. 6, Chapter 5). Each tissue has thus a unique profile of sHSP expression, which may reflect the need of a particular tissue to maintain at all stages an optimal chaperoning machinery to protect against physiological stress.

We conclude that HSPB8 is a unique stress responsive protein with a combination of features sometimes very similar, but sometimes also different from other sHSPs.

TESTIS-SPECIFIC HUMAN SMALL HEAT SHOCK PROTEIN HSPB9

In Chapter 3 we described the identification of the novel sHSP HSPB9. Northern blot and database analyses showed that expression of this new sHSP was restricted to testis. Interestingly, also HSPB9 ESTs were found originating from tumor tissues. These results prompted us to further analyze HSPB9 expression with a more sensitive assay in a much broader range of tissues, including tumor tissues. As shown in Chapter 6, we confirmed that expression of HSPB9 is indeed restricted to testis and tumors and that HSPB9 therefore belongs to the family of cancer/testis associated genes (CTAs; reviewed in [250]).

The unrelated members of this family are of particular interest because of their potential use in immunotherapy of tumors. Antigens expressed by tumors can be used as vaccines to generate a specific anti-tumor response by triggering the immune system. CTAs are normally expressed only in male germ cells, which do not express MHC molecules and therefore can not present peptides from these molecules to T lymphocytes. Tumor cells show widespread abnormalities of gene expression, including the activation of these genes and thus the presentation of these proteins to T cells, which will respond to them as though they were foreign proteins. However, the potential use of HSPB9 in immunotherapy of tumors is still questionable, since it remains to be proven whether it really is a cancer/testis antigen rather than just a cancer/testis associated gene. Furthermore, it will be interesting to know whether HSPB9 tumor expression contributes to the malignant behavior of cancer cells or is an epiphenomenon.

It is of equal interest to understand the role of HSPB9 in normal tissue. We found, both on mRNA and protein level, that HSPB9 expression within testis is restricted to developing sperm cells, suggesting a role in spermatogenesis. As already described above, one of the strategies in unraveling the function(s) of proteins, is to identify interacting proteins with possible known functions. One of the HSPB9 interacting proteins, identified in a yeast two-hybrid screen, turned out to be TCTEL1. TCTEL1 is a component of the tubulin motor complex, named dynein, which functions in the transport of proteins and protein complexes within a cell.

Even though we could confirm the HSPB9-TCTEL1 interaction in another assay, it is crucial that they are able to encounter each other *in situ*. TCTEL1 is found in many cell types, amongst which are the developing sperm cells. However, TCTEL1 is detected in the cytoplasm of these cells, while HSPB9 protein is found in the nucleus. One could thus question the functionality of the interaction, but since TCTEL1 could be responsible for the transport of HSPB9, the interaction may therefore be only temporarily and no colocalization is detected by immunohistochemistry.

What then is the function of HSPB9 in the nucleus of developing sperm cells? Up till now, we have no clear idea. However, it is interesting to mention that one of the other HSPB9 interacting proteins identified in our yeast two-hybrid screen is CCCTC-binding factor (CTCF). CTCF is an evolutionarily conserved 11-zinc finger DNA-binding nuclear phosphoprotein involved in multiple aspects of normal gene

regulation, including transcriptional repression and activation, gene silencing, chromatin insulation, and regulation of imprinted sites (reviewed in [246]). So far, we have not been able to confirm this interaction in another system, but one can speculate that a true interaction suggests that HSPB9 may be involved in imprinting. Further studies will be needed to test this hypothesis and to possibly reveal other functions of HSPB9.

In summary, sHSPs members were compared on basis of their stress behavior, tissue distribution and expression patterns. New sHSP family members were identified and characterized. Extrapolation of some of the findings reported in this thesis should be done with great care, since several of our results were obtained using cell lines, which can be very different from fully differentiated tissues. And even though the results presented in this thesis have not elucidated the exact function(s) of small heat shock proteins, they have increased our insight.

8

References

1. **Anfinsen CB.** (1973) Principles that govern the folding of protein chains. *Science* **181:** 223-230.
2. **Ellis RJ.** (2001) Macromolecular crowding: an important but neglected aspect of the intracellular environment. *Curr. Opin. Struct. Biol.* **11:** 114-119.
3. **Walter S and Buchner J.** (2002) Molecular chaperones-cellular machines for protein folding. *Angew. Chem. Int. Ed. Engl.* **41:** 1098-1113.
4. **Ehrnsperger M, Graber S, Gaestel M and Buchner J.** (1997) Binding of non-native protein to HSP25 during heat shock creates a reservoir of folding intermediates for reactivation. *EMBO J.* **16:** 221-229.
5. **Haslbeck M and Buchner J.** (2002) Chaperone function of sHSPs. *Prog. Mol. Subcell. Biol.* **28:** 37-59.
6. **de Jong WW, Caspers GJ and Leunissen JA.** (1998) Genealogy of the α-crystallin-small heat-shock protein superfamily. *Int. J. Biol. Macromol.* **22:** 151-162.
7. **Kim KK, Kim R and Kim SH.** (1998) Crystal structure of a small heat-shock protein. *Nature* **394:** 595-599.
8. **van Montfort RL, Basha E, Friedrich KL, Slingsby C and Vierling E.** (2001) Crystal structure and assembly of a eukaryotic small heat shock protein. *Nat. Struct. Biol.* **8:** 1025-1030.
9. **Giese KC and Vierling E.** (2002) Changes in oligomerization are essential for the chaperone activity of a small heat shock protein in vivo and in vitro. *J. Biol. Chem.* **277:** 46310-46318.
10. **Kokke BP, Leroux MR, Candido EP, Boelens WC and de Jong WW.** (1998) Caenorhabditis elegans small heat-shock proteins HSP12.2 and HSP12.3 form tetramers and have no chaperone-like activity. *FEBS Lett.* **433:** 228-232.
11. **Kappé G, Leunissen JA and de Jong WW.** (2002) Evolution and diversity of prokaryotic small heat shock proteins. *Prog. Mol. Subcell. Biol.* **28:** 1-17.
12. **Narberhaus F.** (2002) α-crystallin-type heat shock proteins: socializing minichaperones in the context of a multichaperone network. *Microbiol. Mol. Biol. Rev.* **66:** 64-93.
13. **Kappé G, Franck E, Verschuure P, Boelens WC, Leunissen JAM and de Jong WW.** (2003) The human genome encodes ten α-crystallin-related small heat shock proteins: HSPB1-10. *Cell Stress Chaperones* **8:** 53-61.
14. **Litt M, Kramer P, LaMorticella DM, Murphey W, Lovrien EW and Weleber RG.** (1998) Autosomal dominant congenital cataract associated with a missense mutation in the human α-crystallin gene CRYAA. *Hum. Mol. Genet.* **7:** 471-474.
15. **Iwaki T, Kume-Iwaki A, Liem RK and Goldman JE.** (1989) αB-crystallin is expressed in non-lenticular tissues and accumulates in Alexander's disease brain. *Cell* **57:** 71-78.
16. **Faucher C, Capdevielle J, Canal I, Ferrara P, Mazarguil H, McGuire WL and Darbon JM.** (1993) The 28-kDa protein whose phosphorylation is induced by protein kinase C activators in MCF-7 cells belongs to the family of low molecular mass heat shock proteins and is the estrogen-regulated 24-kDa protein. *J. Biol. Chem.* **268:** 15168-15173.
17. **Miron T, Vancompernolle K, Vandekerckhove J, Wilchek M and Geiger B.** (1991) A 25-kD inhibitor of actin polymerization is a low molecular mass heat shock protein. *J. Cell Biol.* **114:** 255-261.
18. **Kato K, Goto S, Inaguma Y, Hasegawa K, Morishita R and Asano T.** (1994) Purification and characterization of a 20-kDa protein that is highly homologous to αB crystallin. *J. Biol. Chem.* **269:** 15302-15309.
19. **Suzuki A, Sugiyama Y, Hayashi Y, Nyu-i N, Yoshida M, Nonaka I, Ishiura S, Arahata K and Ohno S.** (1998) MKBP, a novel member of the small heat shock protein family, binds and activates the myotonic dystrophy protein kinase. *J. Cell Biol.* **140:** 1113-1124.
20. **Lam WY, Wing Tsui SK, Law PT, Luk SC, Fung KP, Lee CY and Waye MM.** (1996) Isolation and characterization of a human heart cDNA encoding a new member of the small heat shock protein family-HSPL27. *Biochim. Biophys. Acta* **1314:** 120-124.
21. **Boelens WC, van Boekel MA and de Jong WW.** (1998) HSPB3, the most deviating of the six known human small heat shock proteins. *Biochim. Biophys. Acta* **1388:** 513-516.
22. **Krief S, Faivre JF, Robert P, Le Douarin B, Brument-Larignon N, Lefrere I, Bouzyk MM, Anderson KM, Greller LD, Tobin FL, Souchet M and Bril A.** (1999) Identification and characterization of cvHSP. A novel human small stress protein selectively expressed in cardiovascular and insulin-sensitive tissues. *J. Biol. Chem.* **274:** 36592-36600.
23. **Charpentier AH, Bednarek AK, Daniel RL, Hawkins KA, Laflin KJ, Gaddis S, MacLeod MC and Aldaz CM.** (2000) Effects of estrogen on global gene expression: identification of novel targets of estrogen action. *Cancer Res.* **60:** 5977-5983.
24. **Benndorf R, Sun X, Gilmont RR, Biederman KJ, Molloy MP, Goodmurphy CW, Cheng H, Andrews PC and Welsh MJ.** (2001) HSP22, a new member of the small heat shock protein superfamily, interacts with mimic of phosphorylated HSP27 ((3D)HSP27). *J. Biol. Chem.* **276:** 26753-26761.
25. **Smith CC, Yu YX, Kulka M and Aurelian L.** (2000) A novel human gene similar to the protein kinase (PK) coding domain of the large subunit of herpes simplex virus type 2 ribonucleotide reductase (ICP10) codes for a serine-threonine PK and is expressed in melanoma cells. *J. Biol. Chem.* **275:** 25690-25699.
26. **Kato K, Shinohara H, Goto S, Inaguma Y, Morishita R and Asano T.** (1992) Copurification of small heat shock protein with αB crystallin from human skeletal muscle. *J. Biol. Chem.* **267:** 7718-7725.
27. **Kappé G, Verschuure P, Philipsen RL, Staalduinen**

AA, Van de Boogaart P, Boelens WC and de Jong WW. (2001) Characterization of two novel human small heat shock proteins: protein kinase-related HSPB8 and testis-specific HSPB9. *Biochim. Biophys. Acta* **1520:** 1-6.

28. **Kato K, Shinohara H, Kurobe N, Inaguma Y, Shimizu K and Ohshima K.** (1991) Tissue distribution and developmental profiles of immunoreactive αB crystallin in the rat determined with a sensitive immunoassay system. *Biochim. Biophys. Acta* **1074:** 201-208.
29. **Yu YX, Heller A, Liehr T, Smith CC and Aurelian L.** (2001) Expression analysis and chromosome location of a novel gene (H11) associated with the growth of human melanoma cells. *Int. J. Oncol.* **18:** 905-911.
30. **Sugiyama Y, Suzuki A, Kishikawa M, Akutsu R, Hirose T, Waye MM, Tsui SK, Yoshida S and Ohno S.** (2000) Muscle develops a specific form of small heat shock protein complex composed of MKBP/HSPB2 and HSPB3 during myogenic differentiation. *J. Biol. Chem.* **275:** 1095-1104.
31. **Kato K, Shinohara H, Kurobe N, Goto S, Inaguma Y and Ohshima K.** (1991) Immunoreactive αA-crystallin in rat non-lenticular tissues detected with a sensitive immunoassay method. *Biochim. Biophys. Acta* **1080:** 173-180.
32. **Lutsch G, Vetter R, Offhauss U, Wieske M, Grone HJ, Klemenz R, Schimke I, Stahl J and Benndorf R.** (1997) Abundance and location of the small heat shock proteins HSP25 and αB-crystallin in rat and human heart. *Circulation* **96:** 3466-3476.
33. **Shama KM, Suzuki A, Harada K, Fujitani N, Kimura H, Ohno S and Yoshida K.** (1999) Transient up-regulation of myotonic dystrophy protein kinase-binding protein, MKBP, and HSP27 in the neonatal myocardium. *Cell Struct. Funct.* **24:** 1-4.
34. **Depre C, Hase M, Gaussin V, Zajac A, Wang L, Hittinger L, Ghaleb B, Yu X, Kudej RK, Wagner T, Sadoshima J and Vatner SF.** (2002) H11 kinase is a novel mediator of myocardial hypertrophy in vivo. *Circ. Res.* **91:** 1007-1014.
35. **Inaguma Y, Goto S, Shinohara H, Hasegawa K, Ohshima K and Kato K.** (1993) Physiological and pathological changes in levels of the two small stress proteins, HSP27 and αB-crystallin, in rat hindlimb muscles. *J. Biochem.* **114:** 378-384.
36. **Arrigo AP, Paul C, Ducasse C, Manero F, Kretz-Remy C, Virot S, Javouhey E, Mounier N and Diaz-Latoud C.** (2002) Small stress proteins: Novel negative modulators of apoptosis induced indepently of reactive oxygen species. *Prog. Mol. Subcell. Biol.* **28:** 185-204.
37. **Chaufour S, Mehlen P and Arrigo AP.** (1996) Transient accumulation, phosphorylation and changes in the oligomerization of HSP27 during retinoic acid-induced differentiation of HL-60 cells: possible role in the control of cellular growth and differentiation. *Cell Stress Chaperones* **1:** 225-235.
38. **Davidson SM and Morange M.** (2000) HSP25 and the p38 MAPK pathway are involved in differentiation of cardiomyocytes. *Dev. Biol.* **218:** 146-160.
39. **Kim M, Geum D, Khang I, Park YM, Kang BM, Lee KA and Kim K.** (2002) Expression pattern of HSP25 in mouse preimplantation embryo: heat shock responses during oocyte maturation. *Mol. Reprod. Dev.* **61:** 3-13.
40. **Hawse JR, Cumming JR, Oppermann B, Sheets NL, Reddy VN and Kantorow M.** (2003) Activation of Metallothioneins and α-Crystallin/sHSPs in Human Lens Epithelial Cells by Specific Metals and the Metal Content of Aging Clear Human Lenses. *Invest. Ophthalmol. Vis. Sci.* **44:** 672-679.
41. **Kato K, Ito H, Inaguma Y, Okamoto K,and Saga S.** (1996) Synthesis and accumulation of αB-crystallin in C6 glioma cells is induced by agents that promote the disassembly of microtubules. *J. Biol. Chem.* **271:** 26989-26994.
42. **Mitton KP, Tumminia SJ, Arora J, Zelenka P, Epstein DL and Russell P.** (1997) Transient loss of αB-crystallin: an early cellular response to mechanical stretch. *Biochem. Biophys. Res. Commun.* **235:** 69-73.
43. **Mao YW, Xiang H, Wang J, Korsmeyer S, Reddan J and Li DW.** (2001) Human bcl-2 gene attenuates the ability of rabbit lens epithelial cells against H_2O_2-induced apoptosis through down-regulation of the αB-crystallin gene. *J. Biol. Chem.* **276:** 43435-43445.
44. **Cvekl A, Kashanchi F, Sax CM, Brady JN and Piatigorsky J.** (1995) Transcriptional regulation of the mouse αA-crystallin gene: activation dependent on a cyclic AMP-responsive element (DE1/CRE) and a Pax-6-binding site. *Mol. Cell Biol.* **15:** 653-660.
45. **Sax CM, Cvekl A and Piatigorsky J.** (1997) Transcriptional regulation of the mouse αA-crystallin gene: binding of USF to the -7/+5 region. *Gene* **185:** 209-216.
46. **Gopal-Srivastava R and Piatigorsky J.** (1994) Identification of a lens-specific regulatory region (LSR) of the murine αB-crystallin gene. *Nucleic Acids Res.* **22:** 1281-1286.
47. **Gopal-Srivastava R, Kays WT and Piatigorsky J.** (2000) Enhancer-independent promoter activity of the mouse αB-crystallin/small heat shock protein gene in the lens and cornea of transgenic mice. *Mech. Dev.* **92:** 125-134.
48. **Andres V, Cervera M and Mahdavi V.** (1995) Determination of the consensus binding site for MEF2 expressed in muscle and brain reveals tissue-specific sequence constraints. *J. Biol. Chem.* **270:** 23246-23249.
49. **Oesterreich S, Lee AV, Sullivan TM, Samuel SK, Davie JR and Fuqua SA.** (1997) Novel nuclear matrix protein HET binds to and influences activity of the HSP27 promoter in human breast cancer cells.

J. Cell Biochem. **67:** 275-286.

50. **Iwaki A, Nagano T, Nakagawa M, Iwaki T and Fukumaki Y.** (1997) Identification and characterization of the gene encoding a new member of the α-crystallin/small HSP family, closely linked to the αB-crystallin gene in a head-to-head manner. *Genomics* **45:** 386-394.
51. **Swamynathan SK and Piatigorsky J.** (2002) Orientation-dependent Influence of an Intergenic Enhancer on the Promoter Activity of the Divergently Transcribed Mouse sHSP/αB-crystallin and Mkbp/HSPB2 Genes. *J. Biol. Chem.* **277:** 49700-49706.
52. **Morimoto RI.** (1998) Regulation of the heat shock transcriptional response: cross talk between a family of heat shock factors, molecular chaperones, and negative regulators. *Genes Dev.* **12:** 3788-3796.
53. **Sakamoto H, Mashima T, Yamamoto K and Tsuruo T.** (2002) Modulation of heat-shock protein 27 (HSP27) anti-apoptotic activity by methylglyoxal modification. *J. Biol. Chem.* **277:** 45770-45775.
54. **Eaton P, Fuller W and Shattock MJ.** (2002) S-thiolation of HSP27 regulates its multimeric aggregate size independently of phosphorylation. *J. Biol. Chem.* **277:** 21189-21196.
55. **Roquemore EP, Chevrier MR, Cotter RJ and Hart GW.** (1996) Dynamic O-GlcNAcylation of the small heat shock protein αB-crystallin. *Biochemistry* **35:** 3578-3586.
56. **Stokoe D, Engel K, Campbell DG, Cohen P and Gaestel M.** (1992) Identification of MAPKAP kinase 2 as a major enzyme responsible for the phosphorylation of the small mammalian heat shock proteins. *FEBS Lett.* **313:** 307-313.
57. **McLaughlin MM, Kumar S, McDonnell PC, Van Horn S, Lee JC, Livi GP and Young PR.** (1996) Identification of mitogen-activated protein (MAP) kinase-activated protein kinase-3, a novel substrate of CSBP p38 MAP kinase. *J. Biol. Chem.* **271:** 8488-8492.
58. **Maizels ET, Peters CA, Kline M, Cutler RE, Jr., Shanmugam M and Hunzicker-Dunn M.** (1998) Heat-shock protein-25/27 phosphorylation by the delta isoform of protein kinase C. *Biochem. J.* **332:** 703-712.
59. **Vietor I and Vilcek J.** (1994) Pathways of heat shock protein 28 phosphorylation by TNF in human fibroblasts. *Lymphokine Cytokine Res.* **13:** 315-323.
60. **Cairns J, Qin S, Philp R, Tan YH and Guy GR.** (1994) Dephosphorylation of the small heat shock protein HSP27 in vivo by protein phosphatase 2A. *J. Biol. Chem.* **269:** 9176-9183.
61. **Kantorow M and Piatigorsky J.** (1994) α-crystallin/small heat shock protein has autokinase activity. *Proc. Natl. Acad. Sci. USA* **91:** 3112-3116.
62. **Ito H, Kamei K, Iwamoto I, Inaguma Y, Nohara D and Kato K.** (2001) Phosphorylation-induced change of the oligomerization state of αB-crystallin. *J. Biol. Chem.* **276:** 5346-5352.
63. **Kato K, Ito H, Kamei K, Inaguma Y, Iwamoto I and Saga S.** (1998) Phosphorylation of αB-crystallin in mitotic cells and identification of enzymatic activities responsible for phosphorylation. *J. Biol. Chem.* **273:** 28346-28354.
64. **Moroni M and Garland D.** (2001) In vitro dephosphorylation of α-crystallin is dependent on the state of oligomerization. *Biochim. Biophys. Acta* **1546:** 282-290.
65. **Beall A, Bagwell D, Woodrum D, Stoming TA, Kato K, Suzuki A, Rasmussen H and Brophy CM.** (1999) The small heat shock-related protein, HSP20, is phosphorylated on serine 16 during cyclic nucleotide-dependent relaxation. *J. Biol. Chem.* **274:** 11344-11351.
66. **Brophy CM, Dickinson M and Woodrum D.** (1999) Phosphorylation of the small heat shock-related protein, HSP20, in vascular smooth muscles is associated with changes in the macromolecular associations of HSP20. *J. Biol. Chem.* **274:** 6324-6329.
67. **Fuchs LC, Giulumian AD, Knoepp L, Pipkin W, Dickinson M, Hayles C and Brophy C.** (2000) Stress causes decrease in vascular relaxation linked with altered phosphorylation of heat shock proteins. *Am. J. Physiol. Regul. Integr. Comp. Physiol.* **279:** R492-R498.
68. **Hoch B, Lutsch G, Schlegel WP, Stahl J, Wallukat G, Bartel S, Krause EG, Benndorf R and Karczewski P.** (1996) HSP25 in isolated perfused rat hearts: localization and response to hyperthermia. *Mol. Cell Biochem.* **160-161:** 231-239.
69. **van de Klundert FAJM, Gijsen ML, van den IJssel PR, Snoeckx LH and de Jong WW.** (1998) αB-crystallin and HSP25 in neonatal cardiac cells-differences in cellular localization under stress conditions. *Eur. J. Cell Biol.* **75:** 38-45.
70. **Yoshida K, Aki T, Harada K, Shama KM, Kamoda Y, Suzuki A and Ohno S.** (1999) Translocation of HSP27 and MKBP in ischemic heart. *Cell Struct. Funct.* **24:** 181-185.
71. **Atomi Y, Yamada S, Strohman R and Nonomura Y.** (1991) αB-crystallin in skeletal muscle: purification and localization. *J. Biochem.* **110:** 812-822.
72. **Bennardini F, Wrzosek A and Chiesi M.** (1992) αB-crystallin in cardiac tissue. Association with actin and desmin filaments. *Circ. Res.* **71:** 288-294.
73. **van de Klundert FAJM and de Jong WW.** (1999) The small heat shock proteins HSP20 and αB-crystallin in cultured cardiac myocytes: differences in cellular localization and solubilization after heat stress. *Eur. J. Cell Biol.* **78:** 567-572.
74. **FitzGerald PG and Graham D.** (1991) Ultrastructural localization of αA-crystallin to the bovine lens fiber cell cytoskeleton. *Curr. Eye Res.* **10:** 417-436.
75. **Welsh MJ, Wu W, Parvinen M and Gilmont RR.** (1996) Variation in expression of HSP27 messenger

ribonucleic acid during the cycle of the seminiferous epithelium and co-localization of HSP27 and microfilaments in Sertoli cells of the rat. *Biol. Reprod.* **55:** 141-151.

76. **Jonak C, Klosner G, Kokesch C, Fodinger D, Honigsmann H and Trautinger F.** (2002) Subcorneal colocalization of the small heat shock protein, HSP27, with keratins and proteins of the cornified cell envelope. *Br. J. Dermatol.* **147:** 13-19.
77. **Djabali K, de Nechaud B, Landon F and Portier MM.** (1997) αB-crystallin interacts with intermediate filaments in response to stress. *J. Cell Sci.* **110:** 2759-2769.
78. **Nakagawa M, Tsujimoto N, Nakagawa H, Iwaki T, Fukumaki Y and Iwaki A.** (2001) Association of HSPB2, a member of the small heat shock protein family, with mitochondria. *Exp. Cell Res.* **271:** 161-168.
79. **Paul C, Manero F, Gonin S, Kretz-Remy C, Virot S and Arrigo AP.** (2002) HSP27 as a negative regulator of cytochrome C release. *Mol. Cell Biol.* **22:** 816-834.
80. **Biggiogera M, Tanguay RM, Marin R, Wu Y, Martin TE and Fakan S.** (1996) Localization of heat shock proteins in mouse male germ cells: an immunoelectron microscopical study. *Exp. Cell Res.* **229:** 77-85.
81. **Cobb BA and Petrash JM.** (2000) Characterization of α-crystallin-plasma membrane binding. *J. Biol. Chem.* **275:** 6664-6672.
82. **Tsvetkova NM, Horvath I, Torok Z, Wolkers WF, Balogi Z, Shigapova N, Crowe LM, Tablin F, Vierling E, Crowe JH and Vigh L.** (2002) Small heat-shock proteins regulate membrane lipid polymorphism. *Proc. Natl. Acad. Sci. USA* **99:** 13504-13509.
83. **Negre-Aminou P, van Leeuwen RE, van Thiel GC, van den IJssel PRLA, de Jong WW, Quinlan RA and Cohen LH.** (2002) Differential effect of simvastatin on activation of Rac(1) vs. activation of the heat shock protein 27-mediated pathway upon oxidative stress, in human smooth muscle cells. *Biochem. Pharmacol.* **64:** 1483-1491.
84. **Brady JP, Garland D, Duglas-Tabor Y, Robison WG, Jr., Groome A and Wawrousek EF.** (1997) Targeted disruption of the mouse αA-crystallin gene induces cataract and cytoplasmic inclusion bodies containing the small heat shock protein αB-crystallin. *Proc. Natl. Acad. Sci. USA* **94:** 884-889.
85. **Clark JI and Muchowski PJ.** (2000) Small heat-shock proteins and their potential role in human disease. *Curr. Opin. Struct. Biol.* **10:** 52-59.
86. **Piotrowicz RS, Weber LA, Hickey E and Levin EG.** (1995) Accelerated growth and senescence of arterial endothelial cells expressing the small molecular weight heat-shock protein HSP27. *FASEB J.* **9:** 1079-1084.
87. **Cuesta R, Laroia G and Schneider RJ.** (2000) Chaperone HSP27 inhibits translation during heat shock by binding eIF4G and facilitating dissociation of cap-initiation complexes. *Genes Dev.* **14:** 1460-1470.
88. **den Engelsman J, Keijsers V, de Jong WW and Boelens WC.** (2003) The small heat-shock protein αB-crystallin promotes FBX4-dependent ubiquitination. *J. Biol. Chem.* **278:** 4699-4704.
89. **Brady JP, Garland DL, Green DE, Tamm ER, Giblin FJ and Wawrousek EF.** (2001) αB-crystallin in lens development and muscle integrity: a gene knockout approach. *Invest. Ophthalmol. Vis. Sci.* **42:** 2924-2934.
90. **Landry J, Chretien P, Lambert H, Hickey E and Weber LA.** (1989) Heat shock resistance conferred by expression of the human HSP27 gene in rodent cells. *J. Cell Biol.* **109:** 7-15.
91. **van den IJssel PRLA, Overkamp P, Knauf U, Gaestel M and de Jong WW.** (1994) αA-crystallin confers cellular thermoresistance. *FEBS Lett.* **355:** 54-56.
92. **Aoyama A, Frohli E, Schafer R and Klemenz R.** (1993) αB-crystallin expression in mouse NIH 3T3 fibroblasts: glucocorticoid responsiveness and involvement in thermal protection. *Mol. Cell Biol.* **13:** 1824-1835.
93. **van de Klundert FAJM, van den IJssel PRLA, Stege GJ and de Jong WW.** (1999) Rat HSP20 confers thermoresistance in a clonal survival assay, but fails to protect coexpressed luciferase in Chinese hamster ovary cells. *Biochem. Biophys. Res. Commun.* **254:** 164-168.
94. **Preville X, Salvemini F, Giraud S, Chaufour S, Paul C, Stepien G, Ursini MV and Arrigo AP.** (1999) Mammalian small stress proteins protect against oxidative stress through their ability to increase glucose-6-phosphate dehydrogenase activity and by maintaining optimal cellular detoxifying machinery. *Exp. Cell Res.* **247:** 61-78.
95. **Garrido C, Gurbuxani S, Ravagnan L and Kroemer G.** (2001) Heat shock proteins: endogenous modulators of apoptotic cell death. *Biochem. Biophys. Res. Commun.* **286:** 433-442.
96. **Beere HM.** (2001) Stressed to death: regulation of apoptotic signaling pathways by the heat shock proteins. *Sci. STKE* **2001:** RE1.
97. **Samali A, Cai J, Zhivotovsky B, Jones DP and Orrenius S.** (1999) Presence of a pre-apoptotic complex of pro-caspase-3, HSP60 and HSP10 in the mitochondrial fraction of jurkat cells. *EMBO J.* **18:** 2040-2048.
98. **Xanthoudakis S, Roy S, Rasper D, Hennessey T, Aubin Y, Cassady R, Tawa P, Ruel R, Rosen A and Nicholson DW.** (1999) HSP60 accelerates the maturation of pro-caspase-3 by upstream activator proteases during apoptosis. *EMBO J.* **18:** 2049-2056.
99. **Gupta S and Knowlton AA.** (2002) Cytosolic heat shock protein 60, hypoxia, and apoptosis. *Circulation* **106:** 2727-2733.
100. **Bruey JM, Ducasse C, Bonniaud P, Ravagnan L,**

Susin SA, Diaz-Latoud C, Gurbuxani S, Arrigo AP, Kroemer G, Solary E and Garrido C. (2000) HSP27 negatively regulates cell death by interacting with cytochrome c. *Nat. Cell Biol.* **2:** 645-652.

101. **Charette SJ, Lavoie JN, Lambert H and Landry J.** (2000) Inhibition of Daxx-mediated apoptosis by heat shock protein 27. *Mol. Cell Biol.* **20:** 7602-7612.
102. **Pandey P, Farber R, Nakazawa A, Kumar S, Bharti A, Nalin C, Weichselbaum R, Kufe D and Kharbanda S.** (2000) HSP27 functions as a negative regulator of cytochrome c-dependent activation of procaspase-3. *Oncogene* **19:** 1975-1981.
103. **Mehlen P, Hickey E, Weber LA and Arrigo AP.** (1997) Large unphosphorylated aggregates as the active form of HSP27 which controls intracellular reactive oxygen species and glutathione levels and generates a protection against TNFα in NIH-3T3-ras cells. *Biochem. Biophys. Res. Commun.* **241:** 187-192.
104. **Kamradt MC, Chen F, Sam S and Cryns VL.** (2002) The small heat shock protein αB-crystallin negatively regulates apoptosis during myogenic differentiation by inhibiting caspase-3 activation. *J. Biol. Chem.* **277:** 38731-38736.
105. **Kamradt MC, Chen F and Cryns VL.** (2001) The small heat shock protein αB-crystallin negatively regulates cytochrome c- and caspase-8-dependent activation of caspase-3 by inhibiting its autoproteolytic maturation. *J. Biol. Chem.* **276:** 16059-16063.
106. **Morrison LE, Hoover HE, Thuerauf DJ and Glembotski CC.** (2003) Mimicking phosphorylation of αB-crystallin on serine-59 is necessary and sufficient to provide maximal protection of cardiac myocytes from apoptosis. *Circ. Res.* **92:** 203-211.
107. **Andley UP, Song Z, Wawrousek EF, Fleming TP and Bassnett S.** (2000) Differential protective activity of αA- and αB-crystallin in lens epithelial cells. *J. Biol. Chem.* **275:** 36823-36831.
108. **Beresford PJ, Jaju M, Friedman RS, Yoon MJ and Lieberman J.** (1998) A role for heat shock protein 27 in CTL-mediated cell death. *J. Immunol.* **161:** 161-167.
109. **Mehlen P, Mehlen A, Godet J and Arrigo AP.** (1997) HSP27 as a switch between differentiation and apoptosis in murine embryonic stem cells. *J. Biol. Chem.* **272:** 31657-31665.
110. **Mehlen P, Coronas V, Ljubic-Thibal V, Ducasse C, Granger L, Jourdan F and Arrigo AP.** (1999) Small stress protein HSP27 accumulation during dopamine-mediated differentiation of rat olfactory neurons counteracts apoptosis. *Cell Death Differ.* **6:** 227-233.
111. **Miron T, Wilchek M and Geiger B.** (1988) Characterization of an inhibitor of actin polymerization in vinculin-rich fraction of turkey gizzard smooth muscle. *Eur. J. Biochem.* **178:** 543-553.
112. **Benndorf R, Hayess K, Ryazantsev S, Wieske M, Behlke J and Lutsch G.** (1994) Phosphorylation and supramolecular organization of murine small heat shock protein HSP25 abolish its actin polymerization-inhibiting activity. *J. Biol. Chem.* **269:** 20780-20784.
113. **Wieske M, Benndorf R, Behlke J, Dolling R, Grelle G, Bielka H and Lutsch G.** (2001) Defined sequence segments of the small heat shock proteins HSP25 and αB-crystallin inhibit actin polymerization. *Eur. J. Biochem.* **268:** 2083-2090.
114. **Wang K and Spector A.** (1996) α-crystallin stabilizes actin filaments and prevents cytochalasin-induced depolymerization in a phosphorylation-dependent manner. *Eur. J. Biochem.* **242:** 56-66.
115. **Iwaki T, Iwaki A, Tateishi J and Goldman JE.** (1994) Sense and antisense modification of glial αB-crystallin production results in alterations of stress fiber formation and thermoresistance. *J. Cell Biol.* **125:** 1385-1393.
116. **Brophy CM, Lamb S and Graham A.** (1999) The small heat shock-related protein-20 is an actin-associated protein. *J. Vasc. Surg.* **29:** 326-333.
117. **Rembold CM, Foster DB, Strauss JD, Wingard CJ and Eyk JE.** (2000) cGMP-mediated phosphorylation of heat shock protein 20 may cause smooth muscle relaxation without myosin light chain dephosphorylation in swine carotid artery. *J. Physiol.* **524 Pt 3:** 865-878.
118. **Stossel TP, Condeelis J, Cooley L, Hartwig JH, Noegel A, Schleicher M and Shapiro SS.** (2001) Filamins as integrators of cell mechanics and signalling. *Nat. Rev. Mol. Cell Biol.* **2:** 138-145.
119. **Nicholl ID and Quinlan RA.** (1994) Chaperone activity of α-crystallins modulates intermediate filament assembly. *EMBO J.* **13:** 945-953.
120. **Wisniewski T and Goldman JE.** (1998) αB-crystallin is associated with intermediate filaments in astrocytoma cells. *Neurochem. Res.* **23:** 385-392.
121. **Muchowski PJ, Valdez MM and Clark JI.** (1999) αB-crystallin selectively targets intermediate filament proteins during thermal stress. *Invest. Ophthalmol. Vis. Sci.* **40:** 951-958.
122. **Djabali K, Piron G, de Nechaud B and Portier MM.** (1999) αB-crystallin interacts with cytoplasmic intermediate filament bundles during mitosis. *Exp. Cell Res.* **253:** 649-662.
123. **Perng MD, Cairns L, van den IJssel PRLA, Prescott A, Hutcheson AM and Quinlan RA.** (1999) Intermediate filament interactions can be altered by HSP27 and αB-crystallin. *J. Cell Sci.* **112:** 2099-2112.
124. **Head MW, Hurwitz L, Kegel K and Goldman JE.** (2000) αB-crystallin regulates intermediate filament organization in situ. *Neuroreport* **11:** 361-365.
125. **Vicart P, Caron A, Guicheney P, Li Z, Prevost MC, Faure A, Chateau D, Chapon F, Tome F, Dupret JM, Paulin D and Fardeau M.** (1998) A missense mutation in the αB-crystallin chaperone gene causes a desmin-related myopathy. *Nat. Genet.* **20:** 92-95.
126. **Salvador-Silva M, Ricard CS, Agapova OA, Yang P and Hernandez MR.** (2001) Expression of small heat

shock proteins and intermediate filaments in the human optic nerve head astrocytes exposed to elevated hydrostatic pressure in vitro. *J. Neurosci. Res.* **66:** 59-73.

127. **Hino M, Kurogi K, Okubo MA, Murata-Hori M and Hosoya H.** (2000) Small heat shock protein 27 (HSP27) associates with tubulin/microtubules in HeLa cells. *Biochem. Biophys. Res. Commun.* **271:** 164-169.
128. **Bluhm WF, Martin JL, Mestril R and Dillmann WH.** (1998) Specific heat shock proteins protect microtubules during simulated ischemia in cardiac myocytes. *Am. J. Physiol.* **275:** H2243-H2249.
129. **Arai H and Atomi Y.** (1997) Chaperone activity of αB-crystallin suppresses tubulin aggregation through complex formation. *Cell Struct. Funct.* **22:** 539-544.
130. **Inaguma Y, Ito H, Iwamoto I, Saga S and Kato K.** (2001) αB-crystallin phosphorylated at Ser-59 is localized in centrosomes and midbodies during mitosis. *Eur. J. Cell Biol.* **80:** 741-748.
131. **Shinohara H, Inaguma Y, Goto S, Inagaki T and Kato K.** (1993) αB crystallin and HSP28 are enhanced in the cerebral cortex of patients with Alzheimer's disease. *J. Neurol. Sci.* **119:** 203-208.
132. **Renkawek K, Stege GJ and Bosman GJ.** (1999) Dementia, gliosis and expression of the small heat shock proteins HSP27 and αB-crystallin in Parkinson's disease. *Neuroreport* **10:** 2273-2276.
133. **Kato S, Hirano A, Umahara T, Llena JF, Herz F and Ohama E.** (1992) Ultrastructural and immunohistochemical studies on ballooned cortical neurons in Creutzfeldt-Jakob disease: expression of αB-crystallin, ubiquitin and stress-response protein 27. *Acta Neuropathol.* **84:** 443-448.
134. **Head MW, Corbin E and Goldman JE.** (1993) Overexpression and abnormal modification of the stress proteins αB-crystallin and HSP27 in Alexander disease. *Am. J. Pathol.* **143:** 1743-1753.
135. **Zabel C, Chamrad DC, Priller J, Woodman B, Meyer HE, Bates GP and Klose J.** (2002) Alterations in the mouse and human proteome caused by Huntington's disease. *Mol. Cell Proteomics* **1:** 366-375.
136. **Koyama Y and Goldman JE.** (1999) Formation of GFAP cytoplasmic inclusions in astrocytes and their disaggregation by αB-crystallin. *Am. J. Pathol.* **154:** 1563-1572.
137. **Wyttenbach A, Sauvageot O, Carmichael J, Diaz-Latoud C, Arrigo AP and Rubinsztein DC.** (2002) Heat shock protein 27 prevents cellular polyglutamine toxicity and suppresses the increase of reactive oxygen species caused by huntingtin. *Hum. Mol. Genet.* **11:** 1137-1151.
138. **Bova MP, Yaron O, Huang Q, Ding L, Haley DA, Stewart PL and Horwitz J.** (1999) Mutation R120G in αB-crystallin, which is linked to a desmin-related myopathy, results in an irregular structure and defective chaperone-like function. *Proc. Natl. Acad. Sci. USA* **96:** 6137-6142.
139. **Chang B, Hawes NL, Roderick TH, Smith RS, Heckenlively JR, Horwitz J and Davisson MT.** (1999) Identification of a missense mutation in the αA-crystallin gene of the lop18 mouse. *Mol. Vis.* **5:** 21.
140. **Ciocca DR and Vargas-Roig LM.** (2002) HSP27 as a prognostic and predictive factor in cancer. *Prog. Mol. Subcell. Biol.* **28:** 205-218.
141. **van Noort JM, van Sechel AC, Bajramovic JJ, el Ouagmiri M, Polman CH, Lassmann H and Ravid R.** (1995) The small heat-shock protein αB-crystallin as candidate autoantigen in multiple sclerosis. *Nature* **375:** 798-801.
142. **Agius MA, Kirvan CA, Schafer AL, Gudipati E and Zhu S.** (1999) High prevalence of anti-α-crystallin antibodies in multiple sclerosis: correlation with severity and activity of disease. *Acta Neurol. Scand.* **100:** 139-147.
143. **Tezel G, Seigel GM and Wax MB.** (1998) Autoantibodies to small heat shock proteins in glaucoma. *Invest. Ophthalmol. Vis. Sci.* **39:** 2277-2287.
144. **Elisei R, Weightman D, Kendall-Taylor P, Vassart G and Ludgate M.** (1993) Muscle autoantigens in thyroid associated ophthalmopathy: the limits of molecular genetics. *J. Endocrinol. Invest.* **16:** 533-540.
145. **Flickinger CJ, Rao J, Bush LA, Sherman NE, Oko RJ, Jayes FC and Herr JC.** (2001) Outer dense fiber proteins are dominant postobstruction autoantigens in adult Lewis rats. *Biol. Reprod.* **64:** 1451-1459.
146. **Mehlen P, Schulze-Osthoff K and Arrigo AP.** (1996) Small stress proteins as novel regulators of apoptosis. Heat shock protein 27 blocks Fas/APO-1- and staurosporine-induced cell death. *J. Biol. Chem.* **271:** 16510-16514.
147. **Wagner BJ and Margolis JW.** (1995) Age-dependent association of isolated bovine lens multicatalytic proteinase complex (proteasome) with heat-shock protein 90, an endogenous inhibitor. *Arch. Biochem. Biophys.* **323:** 455-462.
148. **Conconi M, Petropoulos I, Emod I, Turlin E, Biville F and Friguet B.** (1998) Protection from oxidative inactivation of the 20S proteasome by heat-shock protein 90. *Biochem. J.* **333:** 407-415.
149. **Boelens WC, Croes Y and de Jong WW.** (2001) Interaction between αB-crystallin and the human 20S proteasomal subunit C8/α7. *Biochim. Biophys. Acta* **1544:** 311-319.
150. **Ciechanover A.** (1998) The ubiquitin-proteasome pathway: on protein death and cell life. *EMBO J.* **17:** 7151-7160.
151. **Goldberg AL, Akopian TN, Kisselev AF, Lee DH and Rohrwild M.** (1997) New insights into the mechanisms and importance of the proteasome in intracellular protein degradation. *Biol. Chem.* **378:** 131-140.
152. **Johnston JA, Ward CL and Kopito RR.** (1998) Aggresomes: a cellular response to misfolded

proteins. *J. Cell Biol.* **143:** 1883-1898.

153. **Meriin AB, Gabai VL, Yaglom J, Shifrin VI and Sherman MY.** (1998) Proteasome inhibitors activate stress kinases and induce HSP72. Diverse effects on apoptosis. *J. Biol. Chem.* **273:** 6373-6379.
154. **Kawazoe Y, Nakai A, Tanabe M and Nagata K.** (1998) Proteasome inhibition leads to the activation of all members of the heat-shock-factor family. *Eur. J. Biochem.* **255:** 356-362.
155. **Orlowski RZ.** (1999) The role of the ubiquitin-proteasome pathway in apoptosis. *Cell Death Differ.* **6:** 303-313.
156. **Muchowski PJ, Bassuk JA, Lubsen NH and Clark JI.** (1997) Human αB-crystallin. Small heat shock protein and molecular chaperone. *J. Biol. Chem.* **272:** 2578-2582.
157. **Muchowski PJ, Wu GJ, Liang JJ, Adman ET and Clark JI.** (1999) Site-directed mutations within the core "α-crystallin" domain of the small heat-shock protein, human αB-crystallin, decrease molecular chaperone functions. *J. Mol. Biol.* **289:** 397-411.
158. **Smulders RH, van Geel IG, Gerards WL, Bloemendal H and de Jong WW.** (1995) Reduced chaperone-like activity of αA(ins)-crystallin, an alternative splicing product containing a large insert peptide. *J. Biol. Chem.* **270:** 13916-13924.
159. **van Kuppeveld FJ, Galama JM, Zoll J and Melchers WJ.** (1995) Genetic analysis of a hydrophobic domain of coxsackie B3 virus protein 2B: a moderate degree of hydrophobicity is required for a cis-acting function in viral RNA synthesis. *J. Virol.* **69:** 7782-7790.
160. **Klemenz R, Frohli E, Steiger RH, Schafer R and Aoyama A.** (1991) αB-crystallin is a small heat shock protein. *Proc. Natl. Acad. Sci. USA* **88:** 3652-3656.
161. **Voorter CE, Wintjes L, Bloemendal H and de Jong WW.** (1992) Relocalization of αB-crystallin by heat shock in ovarian carcinoma cells. *FEBS Lett.* **309:** 111-114.
162. **Kim D, Kim SH and Li GC.** (1999) Proteasome inhibitors MG132 and lactacystin hyper-phosphorylate HSF1 and induce HSP70 and HSP27 expression. *Biochem. Biophys. Res. Commun.* **254:** 264-268.
163. **Zantema A, Verlaan-De Vries M, Maasdam D, Bol S and van der Eb A.** (1992) Heat shock protein 27 and αB-crystallin can form a complex, which dissociates by heat shock. *J. Biol. Chem.* **267:** 12936-12941.
164. **Merck KB, Groenen PJ, Voorter CE, Haard-Hoekman WA, Horwitz J, Bloemendal H and de Jong WW.** (1993) Structural and functional similarities of bovine α-crystallin and mouse small heat-shock protein. A family of chaperones. *J. Biol. Chem.* **268:** 1046-1052.
165. **Sakamoto K, Urushidani T and Nagao T.** (1998) Translocation of HSP27 to cytoskeleton by repetitive hypoxia-reoxygenation in the rat myoblast cell line, H9c2. *Biochem. Biophys. Res. Commun.* **251:** 576-579.
166. **Armstrong SC, Delacey M and Ganote CE.** (1999) Phosphorylation state of HSP27 and p38 MAPK during preconditioning and protein phosphatase inhibitor protection of rabbit cardiomyocytes. *J. Mol. Cell. Cardiol.* **31:** 555-567.
167. **Golenhofen N, Htun P, Ness W, Koob R, Schaper W and Drenckhahn D.** (1999) Binding of the stress protein αB-crystallin to cardiac myofibrils correlates with the degree of myocardial damage during ischemia/reperfusion in vivo. *J. Mol. Cell. Cardiol.* **31:** 569-580.
168. **Iwaki T, Iwaki A, Tateishi J, Sakaki Y and Goldman JE.** (1993) αB-crystallin and 27-kd heat shock protein are regulated by stress conditions in the central nervous system and accumulate in Rosenthal fibers. *Am. J. Pathol.* **143:** 487-495.
169. **Kato K, Inaguma Y, Ito H, Iida K, Iwamoto I, Kamei K, Ochi N, Ohta H and Kishikawa M.** (2001) Ser-59 is the major phosphorylation site in αB-crystallin accumulated in the brains of patients with Alexander's disease. *J. Neurochem.* **76:** 730-736.
170. **Mountain I, Waelkens E, Missiaen L and van Driessche W.** (1998) Changes in actin cytoskeleton during volume regulation in C6 glial cells. *Eur. J. Cell Biol.* **77:** 196-204.
171. **MacRae TH.** (2000) Structure and function of small heat shock/α-crystallin proteins: established concepts and emerging ideas. *Cell. Mol. Life Sci.* **57:** 899-913.
172. **Koteiche HA and McHaourab HS.** (1999) Folding pattern of the α-crystallin domain in αA-crystallin determined by site-directed spin labeling. *J. Mol. Biol.* **294:** 561-577.
173. **Carver JA.** (1999) Probing the structure and interactions of crystallin proteins by NMR spectroscopy. *Prog. Retinal Eye Res.* **18:** 431-462.
174. **Sun TX and Liang JJ.** (1998) Intermolecular exchange and stabilization of recombinant human αA- and αB-crystallin. *J. Biol. Chem.* **273:** 286-290.
175. **Bova MP, McHaourab HS, Han Y and Fung BK.** (2000) Subunit exchange of small heat shock proteins. Analysis of oligomer formation of αA-crystallin and HSP27 by fluorescence resonance energy transfer and site-directed truncations. *J. Biol. Chem.* **275:** 1035-1042.
176. **Haley DA, Bova MP, Huang QL, McHaourab HS and Stewart PL.** (2000) Small heat-shock protein structures reveal a continuum from symmetric to variable assemblies. *J. Mol. Biol.* **298:** 261-272.
177. **Horwitz J.** (1992) α-Crystallin can function as a molecular chaperone. *Proc. Natl. Acad. Sci. USA* **89:** 10449-10453.
178. **Veinger L, Diamant S, Buchner J and Goloubinoff P.** (1998) The small heat-shock protein IbpB from Escherichia coli stabilizes stress-denatured proteins for subsequent refolding by a multichaperone network. *J. Biol. Chem.* **273:** 11032-11037.

179. **Lee GJ and Vierling E.** (2000) A small heat shock protein cooperates with heat shock protein 70 systems to reactivate a heat-denatured protein. *Plant Physiol.* **122:** 189-198.
180. **Inaguma Y, Hasegawa K, Goto S, Ito H and Kato K.** (1995) Induction of the synthesis of HSP27 and αB crystallin in tissues of heat-stressed rats and its suppression by ethanol or an α1-adrenergic antagonist. *J. Biochem.* **117:** 1238-1243.
181. **Hickey E, Brandon SE, Potter R, Stein G, Stein J and Weber LA.** (1986) Sequence and organization of genes encoding the human 27 kDa heat shock protein. *Nucleic Acids Res.* **14:** 4127-4145.
182. **van den IJssel PRLA, Norman DG and Quinlan RA.** (1999) Molecular chaperones: small heat shock proteins in the limelight. *Curr. Biol.* **9:** R103-R105.
183. **Russell LD, Ettlin RA, Sinhahikim AP and Clegg ED.** (1990) Histological and Histopathalogical Evaluation of the Testis, 1st ed., Cache River Press, Clearwater.
184. **Wakayama T and Iseki S.** (1999) Specific expression of the mRNA for 25 kDA heat-shock protein in the spermatocytes of mouse seminiferous tubules. *Anat. Embryol.* **199:** 419-425.
185. **Sharma KK, Kumar RS, Kumar GS and Quinn PT.** (2000) Synthesis and characterization of a peptide identified as a functional element in αA-crystallin. *J. Biol. Chem.* **275:** 3767-3771.
186. **Civetta A and Singh RS.** (1998) Sex-related genes, directional sexual selection, and speciation. *Mol. Biol. Evol.* **15:** 901-909.
187. **Tsaur SC, Ting CT and Wu CI.** (1998) Positive selection driving the evolution of a gene of male reproduction, Acp26Aa, of Drosophila: II. Divergence versus polymorphism. *Mol. Biol. Evol.* **15:** 1040-1046.
188. **Munchbach M, Nocker A and Narberhaus F.** (1999) Multiple small heat shock proteins in rhizobia. *J. Bacteriol.* **181:** 83-90.
189. **Ding L and Candido EP.** (2000) HSP25, a small heat shock protein associated with dense bodies and M-lines of body wall muscle in Caenorhabditis elegans. *J. Biol. Chem.* **275:** 9510-9517.
190. **Tam Y and Heikkila JJ.** (1995) Identification of members of the HSP30 small heat shock protein family and characterization of their developmental regulation in heat-shocked Xenopus laevis embryos. *Dev. Genet.* **17:** 331-339.
191. **Waters ER.** (1995) The molecular evolution of the small heat-shock proteins in plants. *Genetics* **141:** 785-795.
192. **Van Montfort R, Slingsby C and Vierling E.** (2001) Structure and function of the small heat shock protein/α-crystallin family of molecular chaperones. *Adv. Protein Chem.* **59:** 105-156.
193. **Arrigo AP and Müller WEG.** (2002) Small Stress Proteins, Springer Verlag, Berlin.
194. **Gastmann O, Burfeind P, Gunther E, Hameister H, Szpirer C and Hoyer-Fender S.** (1993) Sequence, expression, and chromosomal assignment of a human sperm outer dense fiber gene. *Mol. Reprod. Dev.* **36:** 407-418.
195. **Hofferbert S, Burfeind P, Hoyer-Fender S, Lange R, Haidl G and Engel W.** (1993) A homozygous deletion of 27 basepairs in the coding region of the human outer dense fiber protein gene does not result in a pathologic phenotype. *Hum. Mol. Genet.* **2:** 2167-2170.
196. **Verschuure P, Croes Y, van den IJssel PRLA, Quinlan RA, de Jong WW and Boelens WC.** (2002) Translocation of small heat shock proteins to the actin cytoskeleton upon proteasomal inhibition. *J. Mol. Cell. Cardiol.* **34:** 117-128.
197. **Bollag DM, Rozycki MD and Edelstein SJ.** (1996) Isoelectric Focussing and Two-Dimensional Gel Electrophoresis. *In* "Protein Methods", 2nd ed., Wiley-Liss, New York, NY.
198. **van de Klundert FAJM, Smulders RH, Gijsen ML, Lindner RA, Jaenicke R, Carver JA and de Jong WW.** (1998) The mammalian small heat-shock protein HSP20 forms dimers and is a poor chaperone. *Eur. J. Biochem.* **258:** 1014-1021.
199. **Mehlen P, Preville X, Chareyron P, Briolay J, Klemenz R and Arrigo AP.** (1995) Constitutive expression of human HSP27, Drosophila HSP27, or human αB-crystallin confers resistance to TNF- and oxidative stress-induced cytotoxicity in stably transfected murine L929 fibroblasts. *J. Immunol.* **154:** 363-374.
200. **Goldbaum O and Richter-Landsberg C.** (2001) Stress proteins in oligodendrocytes: differential effects of heat shock and oxidative stress. *J. Neurochem.* **78:** 1233-1242.
201. **Berthois Y, Katzenellenbogen JA and Katzenellenbogen BS.** (1986) Phenol red in tissue culture media is a weak estrogen: implications concerning the study of estrogen-responsive cells in culture. *Proc. Natl. Acad. Sci. USA* **83:** 2496-2500.
202. **Quinlan R.** (2002) Cytoskeletal competence requires protein chaperones. *Prog. Mol. Subcell. Biol.* **28:** 219-233.
203. **Groenen PJ, Merck KB, de Jong WW and Bloemendal H.** (1994) Structure and modifications of the junior chaperone α-crystallin. From lens transparency to molecular pathology. *Eur. J. Biochem.* **225:** 1-19.
204. **Edwards DP, Adams DJ, Savage N and McGuire WL.** (1980) Estrogen induced synthesis of specific proteins in human breast cancer cells. *Biochem. Biophys. Res. Commun.* **93:** 804-812.
205. **Edwards DP, Adams DJ and McGuire WL.** (1981) Estradiol stimulates synthesis of a major intracellular protein in a human breast cancer cell line (MCF-7). *Breast Cancer Res. Treat.* **1:** 209-223.
206. **Sheikh MS, Shao ZM, Hussain A, Chen JC, Roberts CT, LeRoith D and Fontana JA.** (1993)

Retinoic acid and estrogen modulation of insulin-like growth factor binding protein-4 gene expression and the estrogen receptor status of human breast carcinoma cells. *Biochem. Biophys. Res. Commun.* **193:** 1232-1238.

207. **Mark PJ, Ward BK, Kumar P, Lahooti H, Minchin RF and Ratajczak T.** (2001) Human cyclophilin 40 is a heat shock protein that exhibits altered intracellular localization following heat shock. *Cell Stress Chaperones* **6:** 59-70.
208. **Kato K, Hasegawa K, Goto S and Inaguma Y.** (1994) Dissociation as a result of phosphorylation of an aggregated form of the small stress protein, HSP27. *J. Biol. Chem.* **269:** 11274-11278.
209. **Gaestel M.** (2002) sHSP-phosphorylation: enzymes, signaling pathways and functional implications. *Prog. Mol. Subcell. Biol.* **28:** 151-169.
210. **Tallot P, Grongnet JF and David JC.** (2003) Dual perinatal and developmental expression of the small heat shock proteins αB-crystallin and HSP27 in different tissues of the developing piglet. *Biol. Neonate* **83:** 281-288.
211. **Davidson SM, Loones MT, Duverger O and Morange M.** (2002) The developmental expression of small HSP. *Prog. Mol. Subcell. Biol.* **28:** 103-128.
212. **David JC, Landry J and Grongnet JF.** (2000) Perinatal expression of heat-shock protein 27 in brain regions and nonneural tissues of the piglet. *J. Mol. Neurosci.* **15:** 109-120.
213. **David JC, Tanguay RM and Grongnet JF.** (2001) Perinatal expression of heat shock proteins HSC 70 and HSP 70 in neural and non neural tissues of the piglet. *Brain Res. Dev. Brain Res.* **128:** 91-99.
214. **David JC and Grongnet JF.** (2001) Perinatal expression of heat-shock protein 90 in different regions of the brain and in non-neural tissues of the piglet. *Biol. Neonate* **79:** 131-139.
215. **Lowry OH, Rosebrough NJ, Farr AL and Randall RJ.** (1951) Protein measurements with the folin phenol reagent. *J. Biol. Chem.* **193:** 265-275.
216. **Joanisse DR, Michaud S, Inaguma Y and Tanguay RM.** (1998) Small heat shock proteins of *Drosophila*: Developmental expression and functions. *J. Biosci.* **23:** 369-376.
217. **Linder B, Jin Z, Freedman JH and Rubin CS.** (1996) Molecular characterization of a novel, developmentally regulated small embryonic chaperone from *Caenorhabditis elegans*. *J. Biol. Chem.* **271:** 30158-30166.
218. **Ohan NW, Tam Y, Fernando P and Heikkila JJ.** (1998) Characterization of a novel group of basic small heat shock proteins in *Xenopus laevis* A6 kidney epithelial cells. *Biochem. Cell Biol.* **76:** 665-671.
219. **Kurtz S, Rossi J, Petko L and Lindquist S.** (1986) An ancient developmental induction: heat-shock proteins induced in sporulation and oogenesis. *Science* **231:** 1154-1157.
220. **Oertel MF, May CA, Bloemendal H and Lutjen-Drecoll E.** (2000) αB-crystallin expression in tissues derived from different species in different age groups. *Ophthalmologica* **214:** 13-23.
221. **Horman S, Fokan D, Mosselmans R, Mairesse N and Galand P.** (1999) Anti-sense inhibition of small-heat-shock-protein (HSP27) expression in MCF-7 mammary-carcinoma cells induces their spontaneous acquisition of a secretory phenotype. *Int. J. Cancer* **82:** 574-582.
222. **De Plaen E, Arden K, Traversari C, Gaforio JJ, Szikora JP, De Smet C, Brasseur F, van der Bruggen P, Lethe B and Lurquin C.** (1994) Structure, chromosomal localization, and expression of 12 genes of the MAGE family. *Immunogenetics* **40:** 360-369.
223. **van den Eynde B, Peeters O, de Backer O, Gaugler B, Lucas S and Boon T.** (1995) A new family of genes coding for an antigen recognized by autologous cytolytic T lymphocytes on a human melanoma. *J. Exp. Med.* **182:** 689-698.
224. **Gure AO, Tureci O, Sahin U, Tsang S, Scanlan MJ, Jager E, Knuth A, Pfreundschuh M, Old LJ and Chen YT.** (1997) SSX: a multigene family with several members transcribed in normal testis and human cancer. *Int. J. Cancer* **72:** 965-971.
225. **Chen YT, Scanlan MJ, Sahin U, Tureci O, Gure AO, Tsang S, Williamson B, Stockert E, Pfreundschuh M and Old LJ.** (1997) A testicular antigen aberrantly expressed in human cancers detected by autologous antibody screening. *Proc. Natl. Acad. Sci. USA* **94:** 1914-1918.
226. **Liu XF, Helman LJ, Yeung C, Bera TK, Lee B and Pastan I.** (2000) XAGE-1, a new gene that is frequently expressed in Ewing's sarcoma. *Cancer Res.* **60:** 4752-4755.
227. **Zendman AJ, Van Kraats AA, Weidle UH, Ruiter DJ and van Muijen GN.** (2002) The XAGE family of cancer/testis-associated genes: alignment and expression profile in normal tissues, melanoma lesions and Ewing's sarcoma. *Int. J. Cancer* **99:** 361-369.
228. **Zendman AJ, Cornelissen IM, Weidle UH, Ruiter DJ and van Muijen GN.** (1999) CTp11, a novel member of the family of human cancer/testis antigens. *Cancer Res.* **59:** 6223-6229.
229. **de Wit NJ, Weidle UH, Ruiter DJ and van Muijen GN.** (2002) Expression profiling of MMA-1a and splice variant MMA-1b: new cancer/testis antigens identified in human melanoma. *Int. J. Cancer* **98:** 547-553.
230. **de Smet C, de Backer O, Faraoni I, Lurquin C, Brasseur F and Boon T.** (1996) The activation of human gene MAGE-1 in tumor cells is correlated with genome-wide demethylation. *Proc. Natl. Acad. Sci. USA* **93:** 7149-7153.
231. **Ono T, Kurashige T, Harada N, Noguchi Y, Saika T, Niikawa N, Aoe M, Nakamura S, Higashi T, Hiraki A, Wada H, Kumon H, Old LJ and Nakayama E.** (2001) Identification of proacrosin

binding protein sp32 precursor as a human cancer/testis antigen. *Proc. Natl. Acad. Sci. USA* **98:** 3282-3287.

232. **King SM, Dillman JF, III, Benashski SE, Lye RJ, Patel-King RS and Pfister KK.** (1996) The mouse t-complex-encoded protein Tctex-1 is a light chain of brain cytoplasmic dynein. *J. Biol. Chem.* **271:** 32281-32287.
233. **de Vries TJ, Verheijen JH, de Bart AC, Weidle UH, Ruiter DJ and van Muijen GN.** (1996) Decreased expression of both the low-density lipoprotein receptor-related protein/α(2)-macroglobulin receptor and its receptor-associated protein in late stages of cutaneous melanocytic tumor progression. *Cancer Res.* **56:** 1432-1439.
234. **Westphal JR, van 't Hullenaar RG, van der Laak JA, Cornelissen IM, Schalkwijk LJ, van Muijen GN, Wesseling P, de Wilde PC, Ruiter DJ and de Waal RM.** (1997) Vascular density in melanoma xenografts correlates with vascular permeability factor expression but not with metastatic potential. *Br. J. Cancer* **76:** 561-570.
235. **van den Berg A, Draaijers TG, Kok K, Timmer T, van der Veen AY, Veldhuis PM, de Leij L, Gerhartz CD, Naylor SL, Smith DI and Buys CH.** (1997) Normal FHIT transcripts in renal cell cancer- and lung cancer-derived cell lines, including a cell line with a homozygous deletion in the FRA3B region. *Genes Chromosomes Cancer* **19:** 220-227.
236. **Maas IW, Boven E, Pinedo HM, Schluper HM and Haisma HJ.** (1991) The effects of gamma-interferon combined with 5-fluorouracil or 5-fluoro-2'-deoxyuridine on proliferation and antigen expression in a panel of human colorectal cancer cell lines. *Int. J. Cancer* **48:** 749-756.
237. **Kreis TE.** (1986) Microinjected antibodies against the cytoplasmic domain of vesicular stomatitis virus glycoprotein block its transport to the cell surface. *EMBO J.* **5:** 931-941.
238. **Gyuris J, Golemis E, Chertkov H and Brent R.** (1993) Cdi1, a human G1 and S phase protein phosphatase that associates with Cdk2. *Cell* **75:** 791-803.
239. **Junqueira LC, Carneiro J and Kelly RO.** (1992) Basic Histology, 7th ed., Appleton & Lange, East Norwalk, Connecticut.
240. **Takahashi K, Shichijo S, Noguchi M, Hirohata M and Itoh K.** (1995) Identification of MAGE-1 and MAGE-4 proteins in spermatogonia and primary spermatocytes of testis. *Cancer Res.* **55:** 3478-3482.
241. **Jungbluth AA, Busam KJ, Kolb D, Iversen K, Coplan K, Chen YT, Spagnoli GC and Old LJ.** (2000) Expression of MAGE-antigens in normal tissues and cancer. *Int. J. Cancer* **85:** 460-465.
242. **Lader E, Ha HS, O'Neill M, Artzt K and Bennett D.** (1989) tctex-1: a candidate gene family for a mouse t complex sterility locus. *Cell* **58:** 969-979.
243. **Gibbons IR.** (1996) The role of dynein in microtubule-based motility. *Cell Struct. Funct.* **21:** 331-342.
244. **Harrison A, Olds-Clarke P and King SM.** (1998) Identification of the t complex-encoded cytoplasmic dynein light chain tctex1 in inner arm I1 supports the involvement of flagellar dyneins in meiotic drive. *J. Cell Biol.* **140:** 1137-1147.
245. **Kamal A and Goldstein LS.** (2002) Principles of cargo attachment to cytoplasmic motor proteins. *Curr. Opin. Cell Biol.* **14:** 63-68.
246. **Ohlsson R, Renkawitz R and Lobanenkov V.** (2001) CTCF is a uniquely versatile transcription regulator linked to epigenetics and disease. *Trends Genet.* **17:** 520-527.
247. **Sussman MA.** (2002) Cellular indigestion: chaperones head to the cytoskeleton. *J. Mol. Cell. Cardiol.* **34:** 83-85.
248. **Ito H, Kamei K, Iwamoto I, Inaguma Y, Garcia-Mata R, Sztul E and Kato K.** (2002) Inhibition of proteasomes induces accumulation, phosphorylation and recruitment of HSP27 and αB-crystallin to aggresomes. *J. Biochem.* **131:** 593-603.
249. **Taylor JP, Tanaka F, Robitschek J, Sandoval CM, Taye A, Markovic-Plese S and Fischbeck KH.** (2003) Aggresomes protect cells by enhancing the degradation of toxic polyglutamine-containing protein. *Hum. Mol. Genet.* **12:** 749-757.
250. **Zendman AJ, Ruiter DJ and van Muijen GN.** (2003) Cancer/testis-associated genes: identification, expression profile and putative function. *J. Cell Physiol.* **194:** 272-288.
251. **Rost B and Sander C.** (1994) Combining evolutionary information and neural networks to predict protein secondary structure. *Proteins* **19:** 55-72.
252. **Aurelian L, Smith CC, Winchurch R, Kulka M, Gyotoku T, Zaccaro L, Chrest FJ and Burnett JW.** (2001) A novel gene expressed in human keratinocytes with long-term in vitro growth potential is required for cell growth. *J. Invest. Dermatol.* **116:** 286-295.

SAMENVATTING

De kleine heat shock eiwitten vormen een familie van moleculaire chaperonnes, die aanwezig zijn in bijna alle organismen. Ze bevatten een geconserveerd C-uiteinde, het α-crystalline domein, terwijl het N-uiteinde variabel is. Ze hebben een massa tussen 16 en 25 kDa, maar kunnen grotere complexen vormen die uit één en dezelfde of uit verschillende kleine heat shock eiwitten bestaan.

Onze kennis over de structuur en functie van deze kleine heat shock eiwitten is beperkt. Recentelijk zijn twee eukaryotische kleine heat shock eiwitten gekristalliseerd, waardoor (een deel van) hun structuur is opgehelderd, maar over hun precieze functie is nog steeds niet veel bekend. Ze kunnen ontvouwen eiwitten binden *in vitro* en hen overdragen aan andere heat shock eiwitten zodat ze hervouwen kunnen worden. *In vivo* kunnen ze cellen thermotolerant maken door overexpressie, ze beschermen cellen tegen apoptose, zijn betrokken bij de organisatie van het cytoskelet en spelen een rol bij vele ziekten.

In de inleiding van dit proefschrift (Hoofdstuk 1) worden de kleine heat shock eiwitten in meer detail beschreven. Aangezien niet alle kleine heat shock eiwitten de bovengenoemde eigenschappen hebben, ligt er een grote uitdaging in het ontrafelen van de exacte functie(s) van elk klein heat shock eiwit. Dit proefschrift beschrijft de verkenning van eigenschappen en functies van de kleine heat shock eiwitten van zoogdieren onder zowel normale fysiologische omstandigheden als in stress situaties.

Eiwitten hebben een bepaalde drie-dimensionale structuur nodig om goed te kunnen functioneren. Op verschillende manieren kan die structuur veranderen, waardoor de eiwitten nutteloos en soms zelfs schadelijk worden voor een cel en afgebroken moeten worden door bijvoorbeeld de proteasomen, de 'afbraakfabriekjes' van een cel. In hoofdstuk 2 hebben we gekeken wat er gebeurt als slecht gevouwen eiwitten in een cel niet meer afgebroken kunnen worden. We weten dat de kleine heat shock eiwitten deze ontvouwen eiwitten kunnen binden. We hebben gevonden dat de kleine heat shock eiwitten, die normaal als vrije eiwitten in de cel aanwezig zijn, als klonten aan het skelet van de cel gaan zitten. We hebben gesuggereerd dat deze herverdeling een mogelijk mechanisme is waardoor cellen beschermd worden tegen beschadigde eiwitten door ze te bewaren op het cytoskelet.

Om meer te weten te komen over de unieke en overlappende functies van de kleine heat shock eiwitten is het allereerst nodig om precies te weten hoeveel er aanwezig zijn in de mens. Tot 1994 waren er maar drie familieleden bekend en er zijn daarna nog eens vier bijgekomen. De beschrijving van één van hen, ontdekt door in databanken te zoeken naar *expressed sequence tags* (ESTs) die selectief in hart voorkomen, zette ons aan tot het zoeken van andere, tot dan toe onbekende, kleine heat shock eiwitten. Deze zoektocht in EST databanken resulteerde in de identificatie van twee nieuwe kleine heat shock eiwitten, HSPB8 en HSPB9 (Hoofdstuk 3).

Terwijl we bezig waren met deze zoektocht, verscheen HSPB8 al in de literatuur onder verschillende namen. Er werden verschillende interessante eigen-

schappen van HSPB8 als heat shock eiwit, zoals expressiepatronen, stressgedrag en de vorming van complexen, werden niet beschreven. Wij hebben deze eigenschappen wel onderzocht en ze vergeleken met enkele andere kleine heat shock eiwitten (Hoofstuk 4). We laten zien dat HSPB8 expressie niet verhoogd wordt tijdens celdifferentiatie, maar een klein beetje bij een verhoogde temperatuur en aanzienlijk na het toedienen van arseniet. De regulering van expressie lijkt voornamelijk plaats te vinden op het niveau van transcriptie, maar na oestradiol behandeling lijkt de regulatie translationeel te zijn. Verder hebben we laten zien, dat HSPB8 gefosforyleerd kan worden als reactie op stress. Aangezien de kleine heat shock eiwitten met elkaar in een complex kunnen zitten, hebben we bestudeerd aan welke andere familieleden HSPB8 kan binden. In het gist twee-hybriden systeem, bindt HSPB8 specifiek aan HSP27, αB-crystalline en HSP20, maar niet aan αA-crystalline en HSPB2. Door middel van glyceroldichtheidsgradiënt centrifugatie laten we echter zien, dat, in ieder geval in cellen, HSPB8 in een ander complex lijkt te zitten dan αB-crystalline.

De expressie van vele kleine heat shock eiwitten wordt gereguleerd tijdens de ontwikkeling van organismen. In hoofdstuk 5 hebben wij de weefseldistributie van HSPB8 en diens expressiepatroon tijdens de ontwikkeling bekeken in varkens en hebben dat vergeleken met de andere kleine heat shock eiwitten HSP20, HSPB2 en cvHSP. We vonden een alomtegenwoordige expressie van HSPB8 en HSP20, zoals al eerder was gevonden voor HSP27 en αB-crystalline, terwijl cvHSP en HSPB2 alleen in hart en spier voorkomen. Verder vonden we dat de expressie tijdens de ontwikkeling constant was, (tijdelijk) vermeerderde, (tijdelijk) verminderde of variabel was. Hierdoor heeft elk weefsel een uniek profiel van kleine heat shock eiwitten, dat waarschijnlijk nodig is om dat weefsel optimaal te beschermen tegen fysiologische stress.

In hoofdstuk 6 hebben we het andere nieuwe kleine heat shock eiwit, HSPB9, verder bestudeerd. Uit de resultaten van hoofdstuk 3 bleek al dat HSPB9 alleen in testis voorkomt, maar we vonden ook ESTs afkomstig van tumoren. In dit hoofdstuk hebben we dit verder bestudeerd door met een gevoeligere methode in veel meer weefsels, waaronder tumorweefsels, te kijken. We bevestigen, dat HSPB9 inderdaad alleen aanwezig is in testis (specifiek in de zich ontwikkelende spermacellen) en in tumoren en concluderen dat het dus een kanker/testis eiwit is. Dergelijke eiwitten zijn interessant vanwege hun potentieel gebruik in de immunotherapeutische behandeling van kanker. Verder hebben we laten zien dat HSPB9 kan binden aan TCTEL1, een onderdeel van dyneïne, dat zorgt voor transport binnen in een cel. Er is meer onderzoek nodig om uit te zoeken wat dit precies betekent.

De resultaten die beschreven staan in dit proefschrift hebben dan wel niet de exacte functie(s) van de kleine heat shock eiwitten opgehelderd, ze hebben wel ons inzicht vergroot. Vervolgonderzoek zal nodig zijn om deze eiwitten precies te begrijpen.

LIST OF PUBLICATIONS

- **Stege GJ, Renkawek K, Overkamp PS, Verschuure P, van Rijk AF, Reijnen-Aalbers A, Boelens WC, Bosman GJ and de Jong WW**. (1999) The molecular chaperone αB-crystallin enhances amyloid β neurotoxicity. *Biochem. Biophys. Res. Commun.* **262**: 152-156.
- **Kappé G, Verschuure P, Philipsen RL, Staalduinen AA, van de Boogaart P, Boelens WC and de Jong WW**. (2001) Characterization of two novel human small heat shock proteins: protein kinase-related HSPB8 and testis-specific HSPB9. *Biochim. Biophys. Acta* **1520**: 1-6.
- **Verschuure P, Croes Y, van den IJssel PR, Quinlan RA, de Jong WW and Boelens WC**. (2002) Translocation of small heat shock proteins to the actin cytoskeleton upon proteasomal inhibition. *J. Mol. Cell. Cardiol.* **34**: 117-128.
- **Kappé G, Franck E, Verschuure P, Boelens WC, Leunissen JAM and de Jong WW**. (2003) The human genome encodes ten α-crystallin-related small heat shock proteins: HSPB1-10. *Cell Stress Chaperones* **8**: 53-61.
- **Verschuure P, Wunderink LU, Heuts DPHM, de Jong WW and Boelens WC**. (2003) Expression and stress response of the mammalian small heat shock protein HSPB8. *(manuscript in preparation)*
- **Verschuure P, Tatard C, Boelens WC, Grongnet JF and David JC**. (2003) Expression of small heat shock proteins HSPB2, HSPB8, HSP20 and cvHSP in different tissues of the perinatal developing pig. *Eur. J. Cell Biol.* (in press)
- **Verschuure P, de Wit NJW, Kappé G, King SM, de Jong WW, Boelens WC and van Muijen GNP**. (2003) Testis-specific human small heat shock protein HSPB9 is a novel cancer/testis associated gene, and interacts with the dynein subunit TCTEL1. *(submitted for publication)*
- **Jira PE, Verschuure P, de Jong J, Rommerts FF, Sengers RCA, Smeitink JAM, Wolthers BG and Wevers RA**. (2003) Identification of 3β-hydroxy-5,7-pregnandien-20-one (7-dehydropregnenolone) in Leydig cells inhibited by BM 15.766. A Smith-Lemli-Opitz syndrome model. *(manuscript in preparation)*

CURRICULUM VITAE

Pauline Verschuure werd geboren op 10 juni 1974 te Delfzijl. Zij begon haar VWO opleiding aan het Geert Groote College te Deventer, verhuisde na vier jaar en behaalde het diploma Gymnasium β in 1992 aan het Liemers College te Zevenaar. Vervolgens ging zij voor een jaar naar de Verenigde Staten. Zij verbleef daar in een gastgezin en studeerde Scheikunde aan het Tacoma Community College te Tacoma, WA.

Bij terugkomst in Nederland begon zij aan haar studie Scheikunde aan de Katholieke Universiteit Nijmegen. Het doctoraal examen werd in augustus 1998 afgesloten met als hoofdrichting Biochemie (Prof. Dr. W.W. de Jong) en als nevenrichting Klinische Chemie (Prof. Dr. R. A. Wevers, UMC St. Radboud).

Van september 1998 tot maart 2003 was zij als AiO (assistent in opleiding) werkzaam op de afdeling Biochemie FNWI van de Katholieke Universiteit Nijmegen. Gedurende die tijd heeft zij het in dit proefschrift beschreven onderzoek verricht.

Sinds 1 september 2003 is zij in opleiding tot klinisch chemicus onder supervisie van Dr. L.W.J.J.M. Westerhuis (St. Elisabeth Ziekenhuis te Tilburg)

DANKWOORD

Dit proefschrift mag dan wel mijn naam op de kaft dragen, het zou niet tot stand zijn gekomen zonder de hulp van vele mensen. Zonder iemand te kort te doen wil ik toch enkele mensen met name noemen.

Natuurlijk allereerst de beide 'Willies'. Wilbert ontzettend bedankt voor je begeleiding en de ruimte en vrijheid die ik op het lab heb gekregen. Ondanks dat ik vaak de dingen heb aangekaart, die mij niet bevielen, heb ik het ontzettend naar mijn zin gehad op het lab! Wilfried, heel erg bedankt voor de fijne tijd die ik op het lab heb gehad. Je corrigeerwerk was erg snel, nauwkeurig en leerzaam.

Het begeleiden van studenten is een heel leuk en leerzaam onderdeel van de AiO-tijd, zowel voor mij als de studenten. Henk-Jan, je was mijn eerste 'uitprobeersel'. Ik heb bewondering voor je doorzettingsvermogen, je harde werken en de manier waarop je het werk met je privé-leven combineert. Helaas is je werk niet in dit proefschrift terecht gekomen. Marjolijn, je was maar voor een korte tijd 'van mij'. Ik vond het bijzonder gezellig, maar jammer dat jouw werk niet een wat positiever resultaat opleverde. Dominic, ook jij hebt het niet makkelijk gekregen. Toch is uiteindelijk een deel van je werk in hoofdstuk 4 terecht gekomen en zal het een co-auteurschap opleveren.

Heel veel succes allemaal met jullie eigen promotie-onderzoek!!!

Een apart bedankje voor Lisa, die gedurende anderhalf jaar mijn analiste was. Wat een luxe zeg! Ik heb bijzonder genoten van onze samenwerking. Je hebt hard gewerkt en ondanks dat een deel van je werk (nog) niet gepubliceerd gaat worden, staat een ander deel in hoofdstuk 4 en 6. Als dank voor al je werk sta je vandaag naast mij als paranimf (sta je er toch eerder dan Sander!).

Wouter, Bas, Guido en Marjon. Jullie waren mijn vriendjes zowel op het lab als daarbuiten. Wouter, het was voor mij niet altijd makkelijk om te zien hoe moeilijk je het op het lab had. Je hebt een dappere beslissing genomen. Veel succes in het Groningse land! Bas, veel gekker kan het niet worden. Bedankt voor alle steun op het lab en de vele lekkere etentjes daarbuiten! Guido, je zult het wel lekker rustig hebben nu ik niet steeds bij je kom (Guido, de computer doet het niet...). Heel erg bedankt voor al je computer- en andere hulp en initiatieven om weer eens een filmpje te gaan kijken. Marjon, het was vooral erg gezellig. Eerst deelden we een tafel en toen stond er opeens een muur tussen. Je zit nu helemaal in Breda, maar wie weet worden we nog wel buurtjes...

Ik hoop dat we nog lang vrienden zullen blijven!

Ook alle ander mensen van het lab wil ik bedanken voor de fijne tijd. Met name noem ik mijn 'U-genoot' Ole en natuurlijk Carla. Ole, je hebt een bijzondere kijk op de wereld. Carla, heel erg bedankt voor alle dingen die je voor mij gedaan hebt. Ik heb nu een heleboel mensen niet bij naam genoemd (collega's en oud-collega's), maar jullie waren net zo goed verantwoordelijk voor de fijne tijd die ik op het lab heb gehad.

Ook wil ik de collega's van de VRT bedanken. We werden gescheiden na de verhuizing, maar gelukkig kon ik altijd aankloppen voor tips, technieken en een gezellig praatje.

Natuurlijk leverde de verhuizing ook nieuwe contacten op. Moleculaire Biologie, het was kort maar gezellig!

Els, met jou heb ik heel wat problemen besproken, maar ook gezellig gekletst. Je liet me inzien, dat het lab soms een gekkenhuis was waardoor ik misschien toch niet zo misplaatst was als ik dacht. Heel erg bedankt voor je belangstelling, wijze woorden en luisterend oor.

Nicole en Goos, ik vond het een bijzondere ervaring om samen met jullie aan een artikel te werken. Het resultaat mag er zijn! Nicole, ik wist niet dat het schrijven van een artikel zo gezellig kon zijn. Heel veel succes in je verdere carrière.

Mijn ouders wil ik graag bedanken voor de gelegenheid en vrijheid die ze me hebben geboden dit te bereiken. Dankzij jullie ben ik zover gekomen. Bedankt voor jullie belangstelling, ennuh, ik zal wel altijd blijven studeren!

Ten slotte wil ik Maurice, mijn mannetje, bedanken. Ondanks dat ik vaak op je zit te mopperen, ben je mijn grote steun geweest. Dank je wel voor al het geduld dat je met mij hebt gehad. Ik hou van je!

COLOUR PLATES

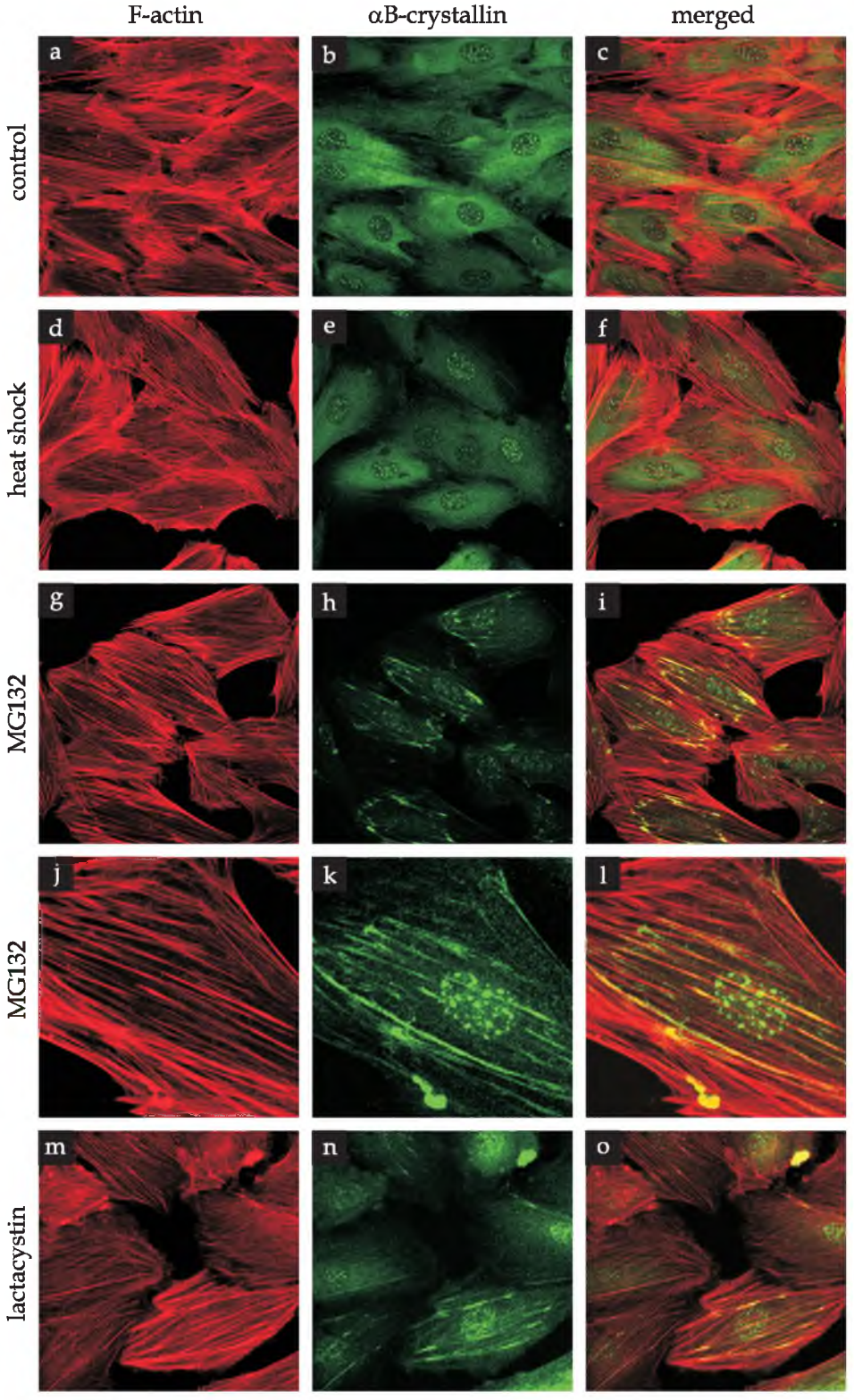

Chapter 2, figure 3, page 28

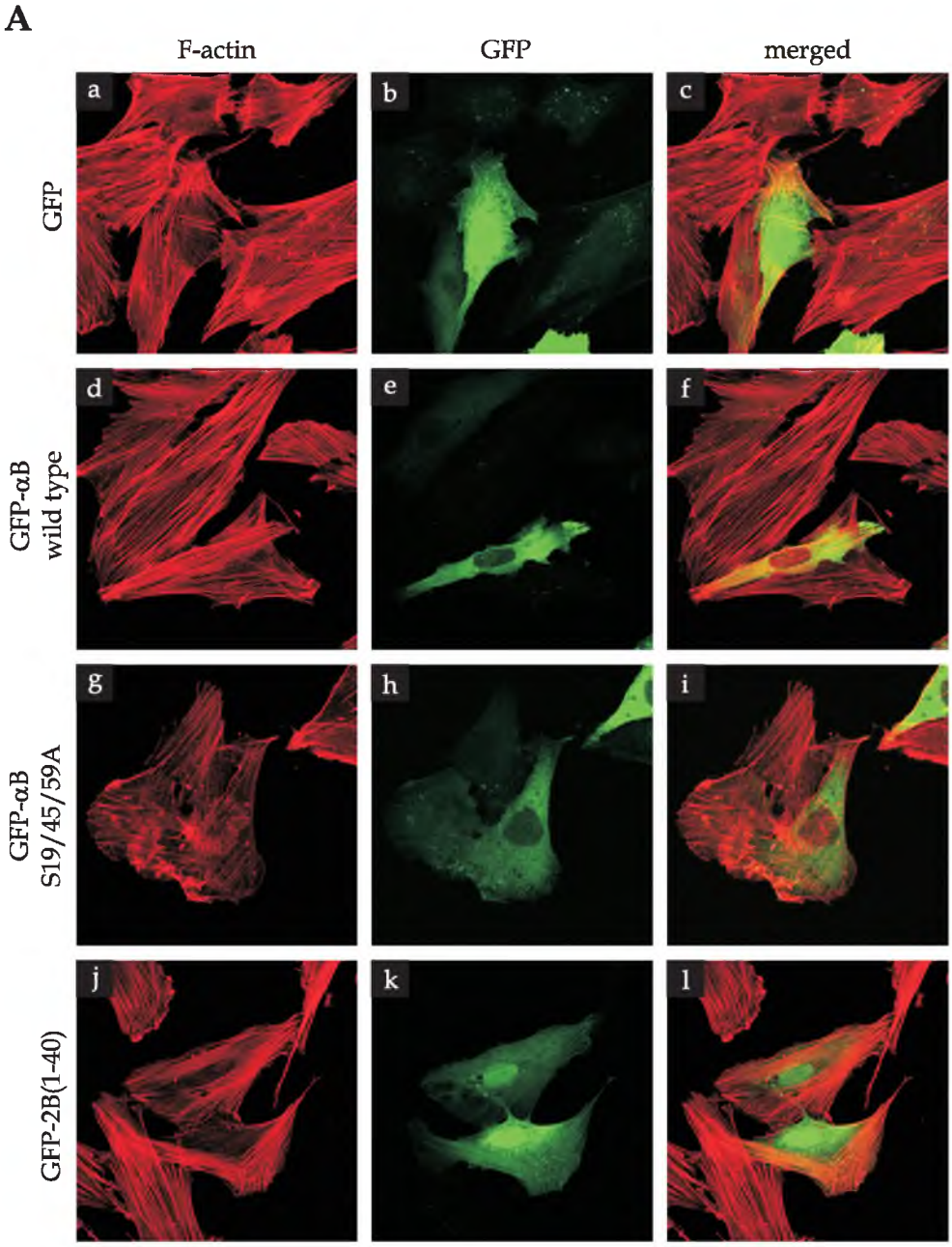

Chapter 2, figure 4A, page 30

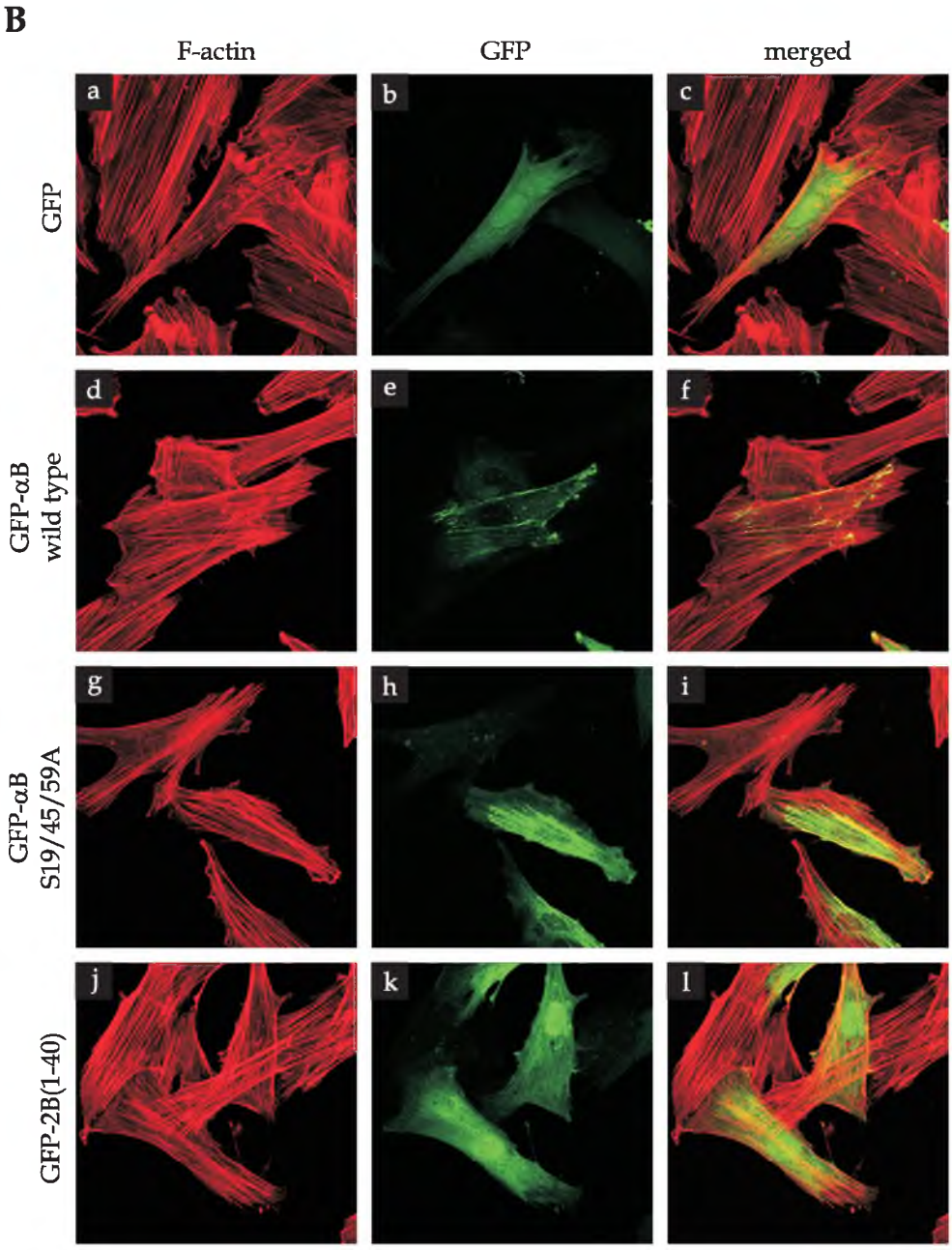

Chapter 2, figure 4B, page 31

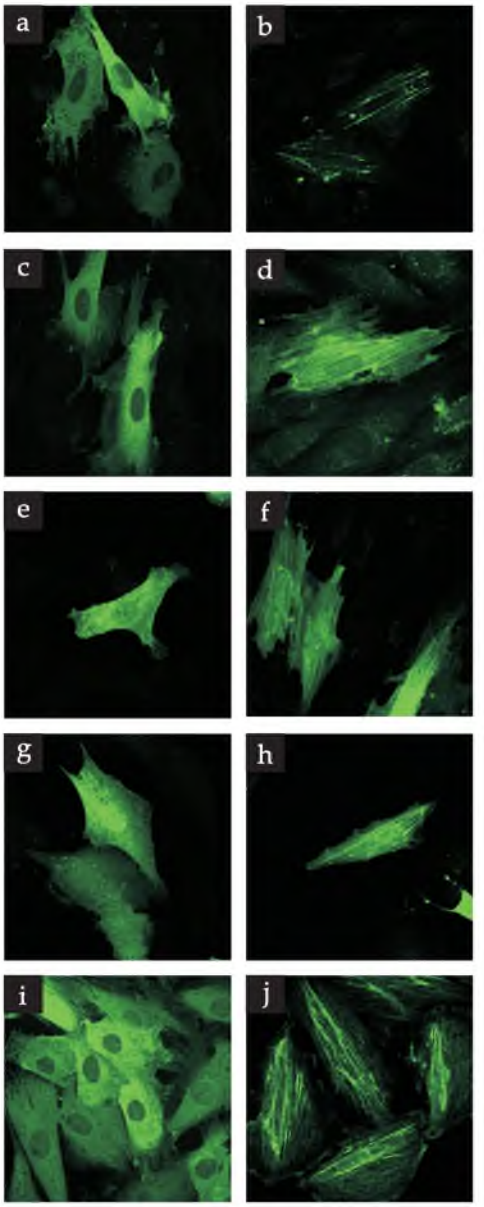

Chapter 2, figure 5, page 32

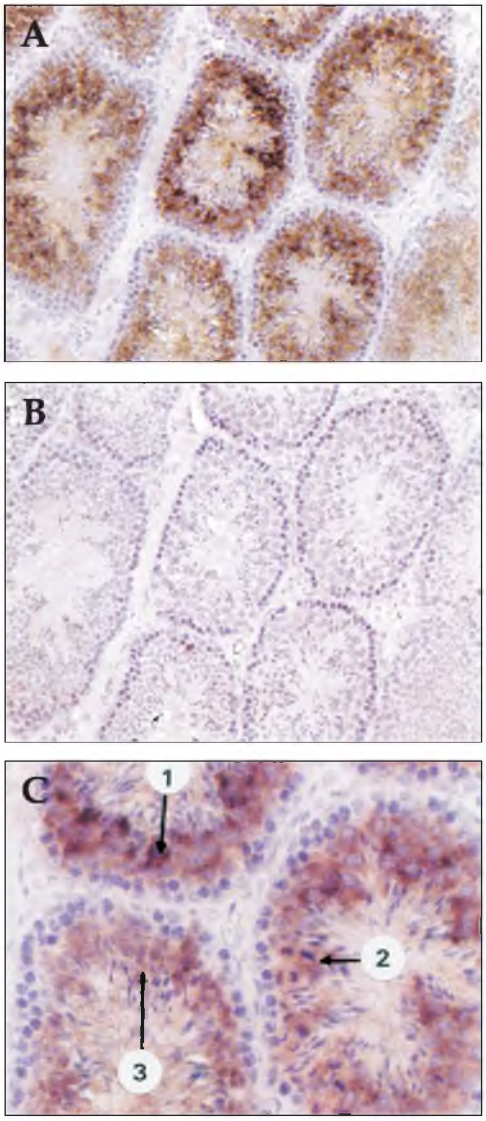

Chapter 3, figure 3, page 42

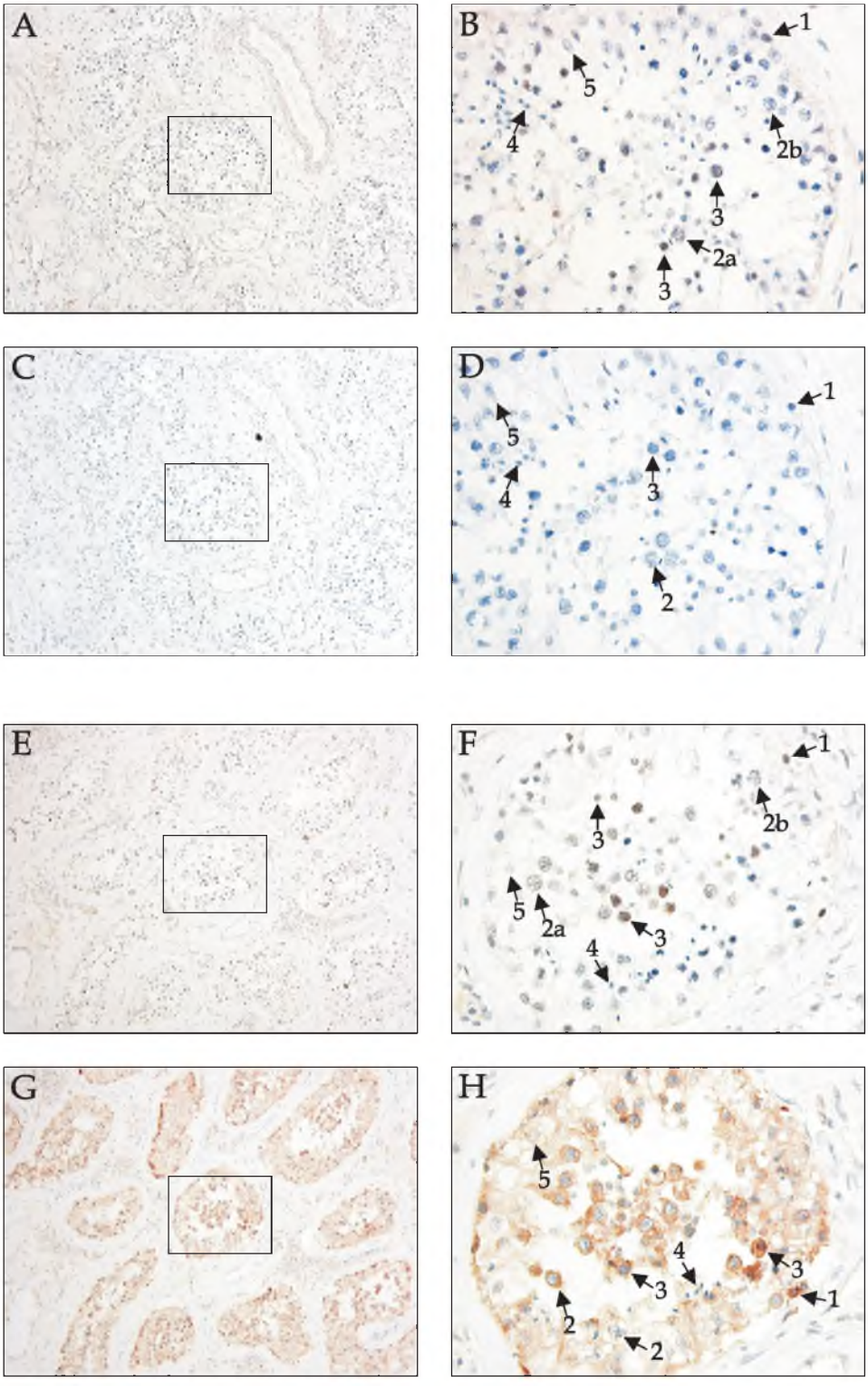

Chapter 6, figure 4, page 84